UNIVERSITY OF CALIFORNIA,
IRVINE

Cytochrome P450: Nature's Aircraft Carrier

DISSERTATION

submitted in partial satisfaction of the requirements
for the degree of

DOCTOR OF PHILOSOPHY

in Chemistry

by

Alec Hoffman Follmer

Dissertation Committee:
Professor Thomas L. Poulos, Chair
Professor Andrew S. Borovik
Professor Michael T. Green

2019

DEDICATION

To my parents, for everything.

A Psalm of life
-Henry Wadsworth Longfellow

"Tell me not, in mournful numbers,
"Life is but an empty dream!"
For the soul is dead that slumbers,
And things are not what they seem.

Life is real! Life is earnest!
And the grave is not its goal;
"Dust thou art, to dust returnest,"
Was not spoken of the soul.

Not enjoyment, and not sorrow,
Is our destined end or way;
But to act, that each to-morrow
Finds us farther than to-day.

Art is long, and Time is fleeting,
And our hearts, though stout and brave,
Still, like muffled drums, are beating
Funeral marches to the grave.

In the world's broad field of battle,
In the bivouac of Life,
Be not like dumb, driven cattle!
Be a hero in the strife!

Trust no Future, howe'er pleasant!
Let the dead Past bury its dead!
Act,--act in the living Present!
Heart within, and God o'erhead!

Lives of great men all remind us
We can make our lives sublime,
And, departing, leave behind us
Footprints on the sands of time;

Footprints, that perhaps another,
Sailing o'er life's solemn main,
A forlorn and shipwrecked brother,
Seeing, shall take heart again.

Let us, then, be up and doing,
With a heart for any fate;
Still achieving, still pursuing
Learn to labor and to wait."

TABLE OF CONTENTS

LIST OF FIGURES

LIST OF TABLES

LIST OF EQUATIONS

ACKNOWLEDGMENTS

I would like to first and foremost thank my advisor, Professor Thomas L. Poulos. TP, like many of your graduate students, I joined your lab under unconventional circumstances. The offer to rotate in your group changed the trajectory of my life forever and I am deeply grateful for that. Within your group, you provided an environment that I could thrive in and possess pure intellectual freedom, which is not as common as you would hope it would be these days. You allowed me to be an essentially unencumbered academic and to take on whatever challenges I desired, even if it meant another year of classes or working with another group on an unrelated project. At the end of the day, you really do a wonderful job of making the PhD about the success of the student and I am grateful to have been given the chance to work with you. Additionally, not many graduate students have the ability to say that we are motivated by our professors to stay in shape, but the fear of being out-lifted by my advisor every morning is something I hope to one day instill into students of my own. Just as a reminder…here are some of my favorite TP gym quotes..."I need a sewing machine because I'm ripped"…"Let me know when you start lifting real weight, then I can work in."…"Why are you working out alone…were the others too weak?"

I would like to thank my committee members, Profs. Andy S. Borovik and Michael T. Green, with whom I've been blessed to have developed wonderful relationships with during my time at UCI.

Andy, I basically invaded your group and for that you can thank one of your former graduate students. I started attending your group meetings when I transferred into the chemistry department with the desire to develop a better understanding of inorganic chemistry. By my first meeting, I knew I was hooked. Although, I never expected I would be quite the FOBG that I am today. Working with your group has pushed me to be a better scientist in the way that I learn, teach, and think. Thank you for everything. You have been essentially a second advisor to me and your encouragement and support mean so much. Thank you for taking the time to talk with me about chemistry, mentorship, and my future.

Mike, I am deeply indebted to you for a number of reasons. First, bringing my appreciation for P450 chemistry to another depth. When you arrived at UCI, I had just joined the Poulos lab. I was fortunate enough to meet you and Tim and be a part of the initial experiments conducted here, which fundamentally changed the way I thought about bioinorganic chemistry. Coupled to that was the opportunity to take classes from and teach classes with you. Your style as a professor was one that finally made perfect sense to me. Whether purely intellectual or getting your hands dirty, your do-it-yourself attitude towards tackling a problem head-on provided me with a self confidence that I needed to be successful here. Thank you for pushing and supporting me and for your guidance.

Drs. Irina Sevrioukova and Huiying Li, I am grateful to you both for so many reasons. Irina, for teaching me priceless lab techniques, the value of being direct and to the point, and imparting so much wisdom on me about science and life. Huiying, for your invaluable help with X-ray crystallography, but also for teaching me how to fix and maintain all of the lab

equipment especially the Rigaku. Thank you for your patience and taking the time to show me how to troubleshoot and fix things myself.

I must also thank my advancement committee. Profs. Andrej Luptak, Jenny Yang, Rachel Martin, and Celia Goulding. A special thank you to Rachel Martin, who encouraged and facilitated my transfer to the Chemistry Department when I felt my work and passions were moving in a new direction. Celia Goulding, who has been an absolute pleasure to talk to and work around. Thank you for your support and being candid with me about many aspects of being in academia.

Finally, I must thank Profs. Melanie Cocco and Alex McPherson. Melanie, you helped me through a challenging time in my graduate career and your continued guidance during my PhD is invaluable. Alex, I am lucky enough to have known you, let alone teach and work with you. Your passion and knowledge of crystallography have influenced me in more ways than you will ever know.

I also have a long list of people to thank that I have had the opportunity to work, work-out, and hang-out with, but can only mention a few.

Bronte, I mean what can I say. You have become one of my best friends. Thank you for everything you have done for me. For being my sense of reason. Thank you for letting me be me; letting me rant about science and life and being an outlet for my ridiculousness. -Haymitch Swanson.

Victoria, I have already told you how much you influenced my graduate experience, but it's always worth mentioning one more time. Thank you for all you have done for me and I will never forget our "dark" times. Okurrrrr…

Georges, I know I annoyed you into talking to me, but eventually you were won over. You were the first person to tell me to switch programs and, for that, I can't thank you enough. Your friendship and our lunches got me through a lot here. But don't worry, we will have them again soon.

Sam, Bro. Thanks for being exactly that. Sometimes that's just what you need.

Kelsey, I never thought I would care as much about Precious as you do. And I don't, no one will (ok, maybe Andy), I mean you are ridiculous about her. But that's what great about you and thank you for including me in your projects. Your excitement and commitment to your science rubs off on people and your uninhibited attitude, while **a lot** at times, is fun to be around. Thanks for being a good friend and homie.

Andrew, thank you for lifting, drinking, and teaching me when to be disciplined and when to stop giving a… May the clown story never die.

Tim, thank you for mentoring me. You were one of the few people during my time that actually showed me how to do anything hands-on. Your patience and support allowed me to convince myself that I could do experiments.

Jessica, Ehh... ok… soo… from quantum dynamics to team dynamics, thank you for making everything more enjoyable from classes to football (which I still don't understand).

Wyeth, thank you for being a nerd. It is weird to be called a nerd in graduate school, but it's a good thing. I proudly share this title with you. Thanks for being opinionated and

always willing to go down any rabbit hole discussion with me and making me constantly question myself.

Sarah, often I would think to myself, "is this really happening…?" And you were always a person I could look to for a reasonable opinion. Also, thanks for being a part of AGS and making me not feel so crazy.

Thank you to the other members of the Poulos lab past and present. Marie True, a truly spectacular master's student, who I had the pleasure of mentoring, thank you for all your hard work. Also, Matt Lewis, Scott Hollingsworth, Jessica Gable, Vidhi Murararka, Dipa Batabyal and José Amaya.

Outside of lab, Neal, Gwen, Frenchy, Eric, Melissa, James, and Sara, thank you for keeping me sane.

I thank the Associated Graduate Students of UCI for allowing me to serve as a representative for three years. I am also thankful to the UCI Women's and Men's Club teams, who I had the pleasure of coaching for nearly four years of my graduate career. You have all taught me so much about being a better coach, mentor, and friend, which truly transformed the way I work with people in lab or in the classroom.

And of course, my mother and father. Without your endless love and support, there is no way I would be here. Thank you for always treating me like an adult and letting me find my own way. I know that by no means did I make it easy, but I think it eventually paid off. And Claire, I definitely did not make your life easy growing up, but thank you for being such a loving sister, even though I know I can be an absolute pain in the ass.

I would also like to acknowledge the American Chemical Society for giving me the permission to include portions of my published works in chapters 2 and 3 in my dissertation, as well as collaborators Drs. John Stegeman and David Lamb for permission to include portions of a manuscript under revision in chapter 5. Financial support was provided by NIH grant GM57353 (T.L.P.). Finally, I would like to thank the staff at the San Diego Supercomputing Cluster's (SDSC) TSCC, Stanford Synchrotron Radiation Lightsource (SSRL) and at Berkeley's Advanced Light Source (ALS), who have provided excellent facilities and resources to carry out crystallographic experiments.

CURRICULUM VITAE

EDUCATION

Ph.D., Biophysical Chemistry — University of California, Irvine
Research Advisor: Professor Thomas L. Poulos — **2014-2019**

B.S., Biochemistry, *cum laude* — University of the Pacific
Research Advisor: Professor Jianhua Ren — **2011-2014**

AWARDS & HONORS

National Science Foundation Graduate Research Fellowship Honorable Mention **2016**

National Science Foundation Graduate Research Fellowship Honorable Mention **2015**

University of the Pacific Outstanding Graduating Senior in Biochemistry **2014**

University of the Pacific Hoefer Prize Grant for Student-Faculty Research **2014**

Alpha Chi Sigma District Counselor Citation for Impressive Leadership **2014**

Univ. of the Pacific Paul Gross Award Outstanding Achievement in Organic Chemistry **2013**

ORAL PRESENTATIONS

(1) "The Dynamic States of Cytochrome P450"
- West Coast Structural Biology Workshop, Asilomar, CA, **2019**

(2) "Dynamics and Allostery of Cytochrome P450cam"
- Southern California Bioinorganic Meeting, Pasadena, CA, **2018**

(3) "Phosphopantetheine: Development of a Non-Standard Force Field Library for Molecular Dynamics of Biosynthetic Enzymes"
- Iterative Polyketide Synthase Conference, Banff, Canada, **2015**

(4) "Computational Studies of the Gas-Phase Acidity and Basicity of Organic Molecules"
- National Conference for Undergraduate Research, Lexington, KY, **2014**
- American Chemical Society Undergraduate Research Conference, San Francisco, CA, **2014**
- Pacific Undergraduate Research Conference, Stockton, CA, **2014**

POSTER PRESENTATIONS

(1) "Redox Partner Selectivity of P450terp and the Effector Role of Tdx"
- 20th International Conference on Cytochrome P450, Dusseldorf, Germany, **2017**
- Southern California Bioinorganic Meeting, Irvine, CA, **2017**

(2) "Effects of Range and Frequency on DIDSON Measurement Accuracy"
- Pacific Undergraduate Research Conference, Stockton, CA, **2012**
-

PUBLICATIONS

Follmer, A.H., Tripathi, S., Poulos, T.L. "Ligand and Redox Partner Binding Generates a New Conformational State in Cytochrome P450cam (CYP101A1) *J. Am. Chem. Soc.* **2019**, 141(6) 2678-2683.

Follmer, A.H., Mahomed, M., Goodin, D.B., Poulos, T.L., Substrate Dependent Allosteric Regulation in Cytochrome P450cam (CYP101A1) *J. Am. Chem. Soc.* **2018**, 140(47) 16222-16228.

Lamb, D.C.*, **Follmer, A.H.***, Goldstone, J.V.*, Nelson, D.R., Warrilow, A.G., Price, C.L., True, M.Y., Kelly, S.L., Poulos, T.L., Stegeman, J.J. "On the Occurrence of Cytochromes P450 in Viruses" *PNAS* (submitted) *co-first authors

Greene, D.[*]; Botello-Smith, W. M.[*]; **Follmer, A.,** Xiao, L.; Lambros, E.; Luo, R., Modeling Membrane Protein–Ligand Binding Interactions: The Human Purinergic Platelet Receptor. *J. Phys. Chem. B* **2016**, *120*, 12293–12304.

MANUSCRIPTS IN PREPARATION

Follmer A.H., Gable J., Green. M.T., Poulos, T.L. "Redox Partner Specificity in *Pseudomonad* P450s"

Schaub, A.J., Truong, H.V., **Follmer, A.H.**, Milligan, J.C., Tsai, S.-C., Luo, R., "Fatty Acid and Natural Product Biosynthesis Force Field for Investigation of Conformational Dynamics"

TEACHING

High-Resolution Structures: NMR and X-ray — University of California, Irvine
Teaching Assistant — Spring **2018**
Instructors: Alexander McPherson,
Melanie Cocco

Graduate Inorganic Chemistry — University of California, Irvine
Teaching Assistant — Fall **2018**
Instructor: Michael T. Green

General Chemistry 1 — University of California, Irvine
Teaching Assistant — Fall **2017**
Instructor: Ramesh Arasasingham

Biochemistry Lab — University of California, Irvine
Teaching Assistant — Spring **2016**
Instructor: Pavan Kandandale

Molecular Biology — University of California, Irvine
Teaching Assistant — Spring **2016**
Instructors: Olga Razorenova,
Donald Senear

General Chemistry Lab — University of the Pacific
Teaching Assistant — Spring **2014**
Instructor: Balint Sztarzay

MEMBERSHIPS

Associated Graduate Students of UCI — **2014-2018**
- Representative for School of Physical Sciences
- AGS Representative for Academic Senate
  Council on Research, Computing, and
  Libraries (CORCL)

Alpha Chi Sigma – Professional Chemistry Fraternity — **2012-2019**
- Beta Pi Chapter President **2014**

ABSTRACT OF THE DISSERTATION

Cytochrome P450: Nature's Aircraft Carrier

By

Alec Hoffman Follmer

Doctor of Philosophy in Chemistry

University of California, Irvine, 2019

Professor Thomas L. Poulos, Chair

Cytochromes P450 are heme-containing enzymes that utilize O_2 for C–H bond activation and play essential roles in drug detoxification and biosynthesis of steroids and a variety of natural products. A number of P450s now have been shown to adopt both an open and closed conformational state. In the open state, the active site is solvent exposed. Upon substrate binding, the P450 shifts to the closed state and sequesters the active site from bulk solvent. Since its discovery, cytochrome P450cam has served as a paradigm for mechanistic and structure-function studies. Over many years of investigation, a wealth of data has suggested that P450cam may possess two camphor binding sites, the active site pocket and an additional site that shifts P450cam toward the open state. However, location of this secondary site was never determined. Here, molecular dynamics simulations were performed that revealed the location of a secondary site on the surface of P450cam. Binding to this allosteric site assists in the opening of both the primary and new secondary active site access channel. Related to these observations is the recent finding that the binding of

P450cam's redox partner, Pdx, favors the open conformation. This shift towards the open state has led to the hypothesis that in order to provide the proton relay network required for O_2 activation, P450cam must undergo a structural rearrangement from the closed form. Here, we present the X-ray crystal structure of P450cam complexed with its redox partner, Pdx, substrate, and cyanide as a mimic of a critical intermediate of the catalytic cycle, the "oxy-complex". The structure of P450cam undergoes ordered changes proposed originally by NMR but never observed crystallographically. These changes provide a channel for water entry and product egress in agreement with the channel formation hypothesized by our simulations. These redox partner interactions studies are extended to a homologue of P450cam, P450terp, which exhibits a less stringent selectivity for its native redox partner Tdx, whose binding may still induce a conformational change in P450terp. Finally, a new P450, CYP102L1, was classified and characterized from *Mycobacterium phage Adler* and its potential role in viruses is discussed.

Chapter 1

Introduction to Cytochrome P450

Introduction

The cytochrome P450 superfamily (P450s or CYPs) is a broad class of heme-containing enzymes united by their rare heme thiolate ligation (Figure 1-1A) and conserved fold (Figure 1-2). P450s are ubiquitous throughout the biosphere and are involved in a number of essential biological transformations that are of interest to scientists across a wide range of disciplines, the most well-known of which is their role in drug metabolism.[1] First isolated and identified in the early 1950's, the importance of these enzymes in mammalian systems was immediately clear in

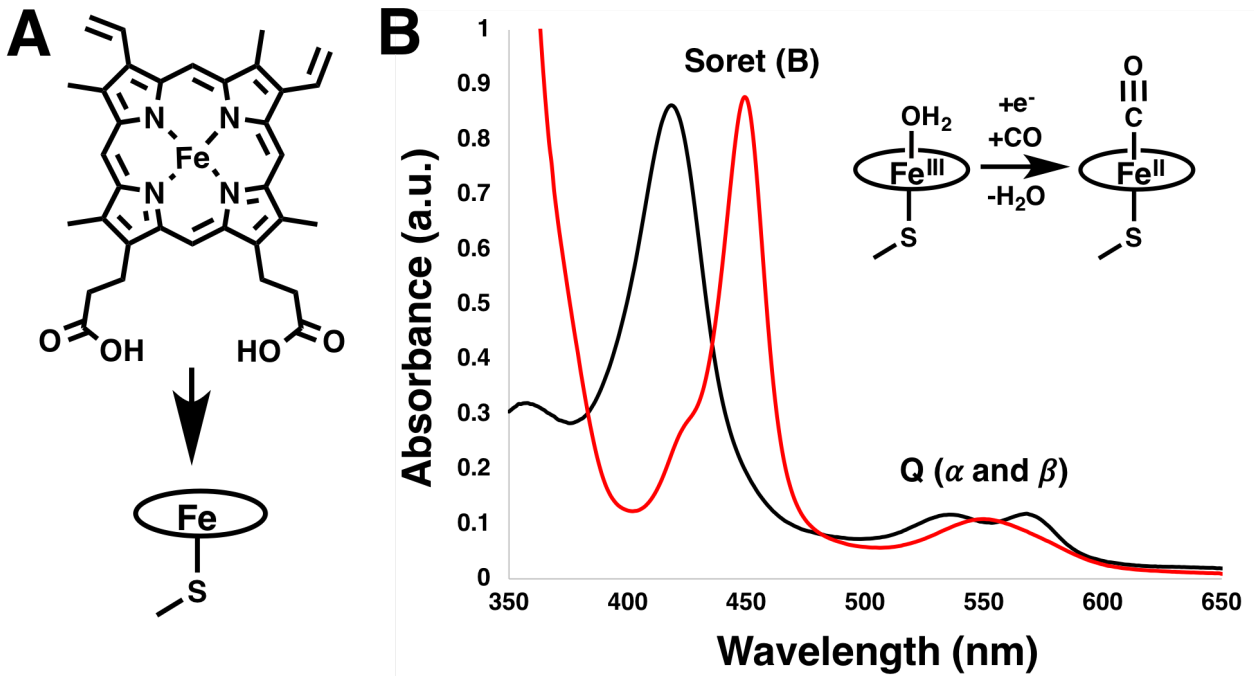

Figure 1-1. (A) Iron protoporphyrin IX or heme B represented as a circle bound to a cysteine-based thiolate in cytochrome P450. **(B)** UV-vis spectra of low-spin ferric resting state (black) and signature reduced CO-bound state (red).

the role of detoxification of drugs and other hydrophobic molecules by the incorporation of one atom of atmospheric dioxygen.[2-3] These initial findings began a crusade to understand the mechanism of these metalloenzymes and despite nearly 65 years of investigation, aspects of this protein's mechanism still remain unclear.

The initial discovery of cytochromes P450 as metabolic enzymes by Axelrod and Brodie in 1955 demonstrated that an enzyme system in liver microsomes was capable of oxidizing foreign drugs and chemical compounds (xenobiotics) using NADPH as a reductant.[2] The identification and isolation followed soon after from the independent studies by Klingenberg, Omura and Sato, and Estabrook.[3-6] The name "P450" is derived from the electronic absorption spectrum that appears upon reduction of the enzyme's active site heme cofactor followed by the incubation and binding of carbon monoxide (CO) (Figure 1-1B).[3] This absorption spectrum was unique with respect to

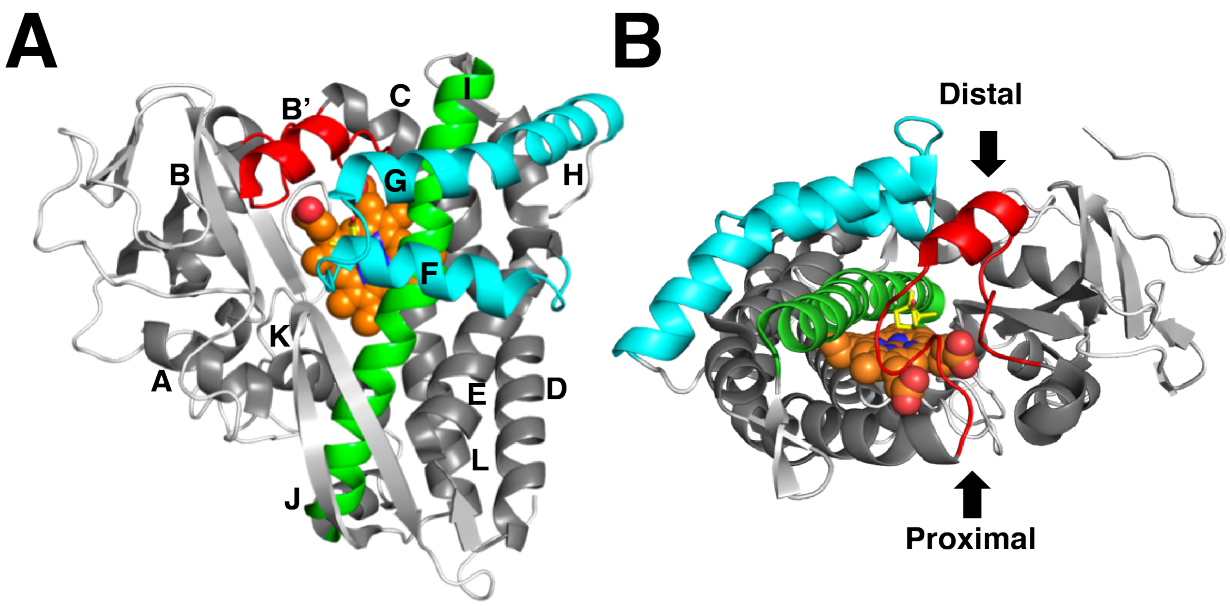

Figure 1-2. Overview of P450 structure with from proximal face **(A)** and side-on **(B)**. (PDB ID: 2CPP)

other cytochromes as it displayed an intense absorbance maximum that underwent a bathochromic shift (red shift) from 420 nm to 450 nm, which did not occur in other heme proteins studied at the time, thus providing the basis for the name "pigment 450" or cytochrome P450.[6]

Briefly, the electronic absorption spectra of porphyrin containing systems (e.g. heme), possess common spectral features consisting of 2 major bands: the Soret or B band (~400 nm) and Q band (a weak transition ~550 nm), which is often split into α and β bands.[7] These bands arise from the strong π-π^* transition that can be split and change in energy depending on a number of factors including the metal ion bound to the porphyrin, spin and/or oxidation state of the metal ion, and nature of additional coordinating ligands in the metal's axial positions and are thus a sensitive probe of the state of the enzyme (*vide infra*).

Nomenclature

With over 55,000 P450 genes named to date from all kingdoms of life, development of a nomenclature system was necessary to keep track and identify their origin and function as annotated by sequence similarity.[8] First, CYP for **CY**tochrome **P**450 precedes all named genes followed by an alphanumeric code that serves to describe the origin of the gene. The code is CYPxyz, where 'x' is a numeric code that indicates the enzyme's family, 'y' is a letter denoting the subfamily, ending with a number, 'z', that indicates the member number.[9] Maintained by David R. Nelson, a database of these P450s is available at:

drnelson.uthsc.edu/CytochromeP450.html

According to the current naming convention: CYP1-50, CYP301-499 and CYP3001-4999 are of animal origin, CYP51-70, CYP501-699 and CYP5001-6999 are reserved for lower eukaryotes, while CYP71-100, CYP701-999 and CYP7001-9999 are given to plants and CYP101-299 and CYP1001-2999 to prokaryotes. CYP101A1, for example, describes a bacterial P450 from *Pseudomonas putida* that has a narrow substrate scope and serves as a model system for P450 structure-function relationship and will serve as the major focus of this thesis.[9-10] 101 indicates that this is the first bacterial P450 with a particular known function or substrate to be identified, while A1 designates this as the first isoform identified with 101's functionality. Within the P450

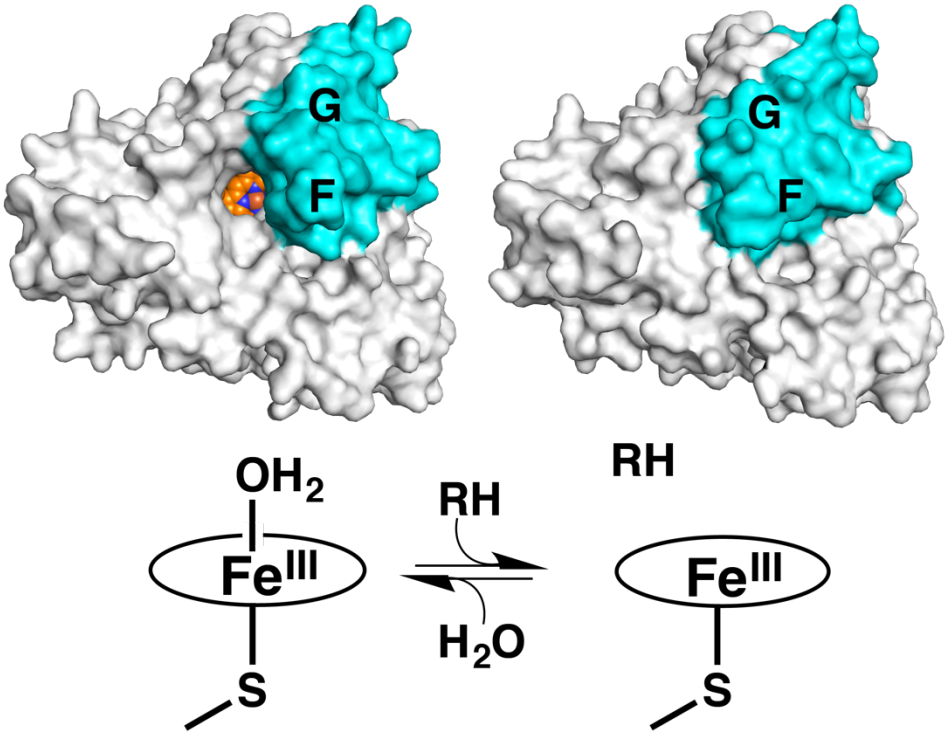

Figure 1-3. Surface and ChemDraw representations of the conformational and coordination changes that occur upon substrate binding, which shifts the P450 from open (left) to closed (right). (PDB ID: 4JX1, 2CPP)

community, this enzyme is commonly referred to as P450cam, where 'cam' is an abbreviation of the enzyme's natural substrate, camphor, a small terpenoid that can serve as the *P. putida*'s sole carbon source.[11] For comparison, one of the most intensively studied mammalian examples is CYP3A4, a membrane bound P450 expressed in the liver, which is responsible for the metabolism of a majority of xenobiotics ingested by humans.[12]

Cytochrome P450 Structure

With a significant number of P450 structures deposited in the protein databank (PDB) extending over a large range of organisms and functions, it is safe to conclude the P450 fold remains highly conserved despite large sequence diversity and substrate scope. One notable exception is the presence of an N-terminal tail that anchors insoluble (mitochondrial and hepatic) P450s to the membrane, although its removal does not seem to affect the overall structure.[1] Viewed from a plane parallel to the heme and normal to the axial H_2O-Fe-S-Cys bonds (deemed the distal side of the heme), P450s exhibit a largely alpha-helical, triangular fold (Figure 1-2A). This conserved structure lends itself to a useful alphabetical naming convention that is used to describe various regions of the protein as seen in Figure 1-2.[13] Of particular note and importance to this discussion are the B', F, G, I, and L helices. The B' helix and associated B-C loop is one of the most flexible and important parts of any P450 fold.[14-15] Its motion and structure are intricately tied to the F and G helices movement, which govern substrate access. The collective size and movement of these regions is the major factor in determination of substrate accommodation as well as regio- and stereo- selectivity of these enzymes and are often referred to collectively as the substrate recognition site (SRS).[16-19] In particular, the F/G helices act as a lid to the active site

and determine what were traditionally referred to as the “open” or “closed” states of the enzyme (Figure 1-3). Contacts between the F/G helices and I helix are important in the regulation of the mechanism of P450.[20-22] When the F/G helices move from the open to closed conformation, they introduce a kink in the I helix near the active site heme positioning a conserved threonine residue for a hydrogen bond network that is essential for O_2 activation.[22-24]

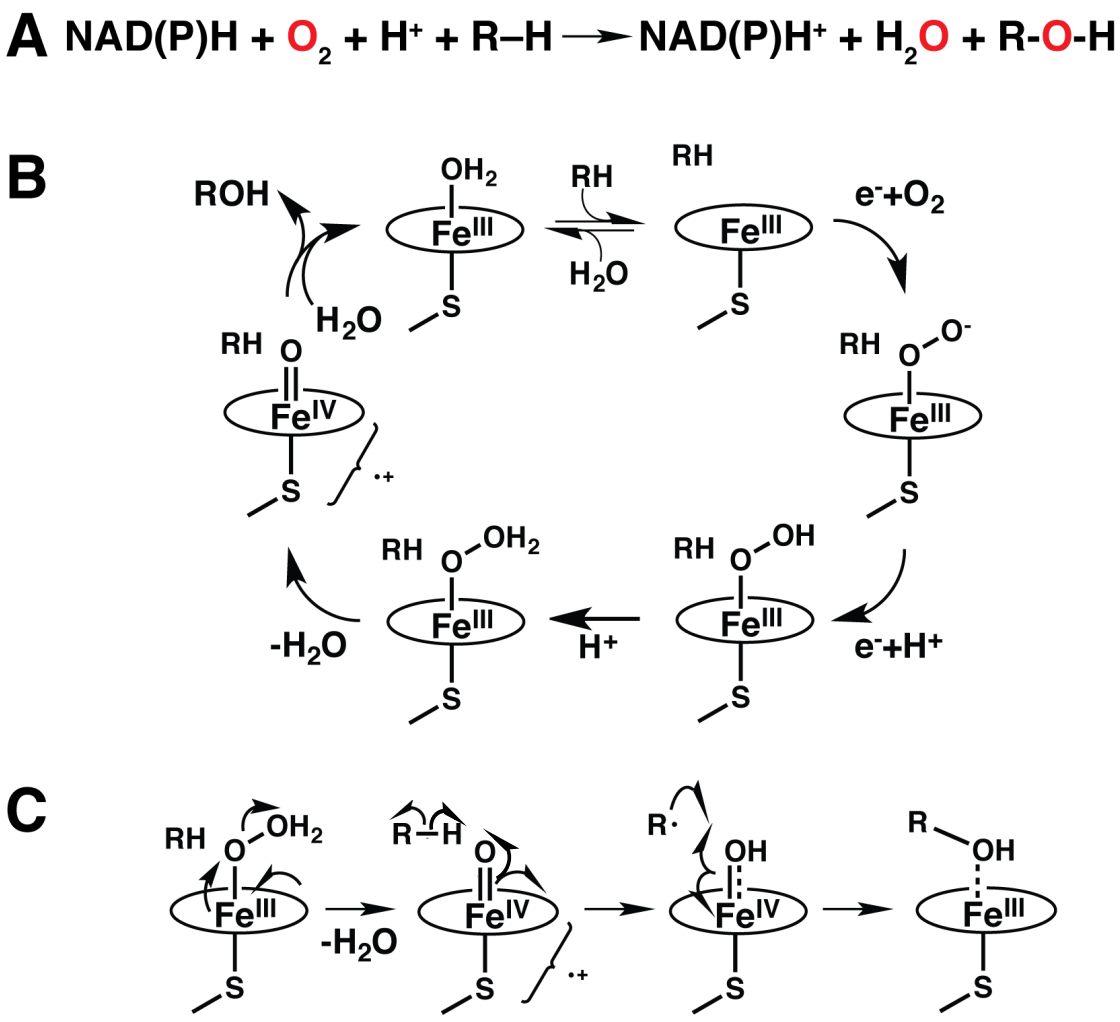

Figure 1-4. (A) Cytochrome P450 net reaction. **(B)** Catalytic cycle. **(C)** Mechanism of hydroxylation.

On the proximal side of the heme, near the beginning of the L-helix is the axially ligating cysteine that is largely responsible for P450s unique reactivity. Around this residue is a conserved loop geometry that tunes the sulfur's electron donating character.[25-27]

Cytochrome P450 Mechanism

The mechanism of cytochrome P450 is complex, but logical and highly regulated. In this section, we will take a detailed look at the generalized active site mechanism of P450s to lay a foundation for the following discussion of how protein dynamics regulate this process. One of the unifying properties of the P450 family is the thiolate ligation that attaches a molecule of heme B, iron-protoporphyrin IX, to the protein scaffold, the porphyrin ring will be represented by the circle that encapsulates the iron, as in Figure 1-1A.

We begin with the resting state of the enzyme, where an aquo- ligand occupies the sixth site in the axial position of the iron. The resting state has been probed by nearly every spectroscopic methodology and exhibits a ferric, six-coordinate, low-spin signal (S=1/2), that has been corroborated by X-ray crystallography.[28-29] This substrate-free form has been shown to be in the "open" conformation to allow for access of substrate to the active site.[29] Under these conditions, the redox potential is too low (-300 mV vs NHE) to abstract an electron from its native electron transfer (ET) partner protein.[30-32] However, the role of substrate binding (RH) is twofold; it closes the protein active site from solvent by a conformational change of the F/G helices and hydrophobic substrate displaces the axial water providing a pentacoordinate system with a vacant site for O_2 to bind (Figure 1-3). This change from six to five coordinate changes the ligand field such that the iron undergoes a spin-state change from low (S=1/2) to high-spin (S=5/2),

effectively increasing the redox potential of the complex.[33] A ~130 mV (vs NHE) increase in redox potential to -170 mV (vs NHE) is sufficient to allow for reduction by its redox partner, which, for the purpose of this work, will predominately be putidaredoxin (Pdx) that has a redox potential of -230 mV (vs NHE).[31, 34-35] This is the rate limiting step in the catalytic cycle.[36]

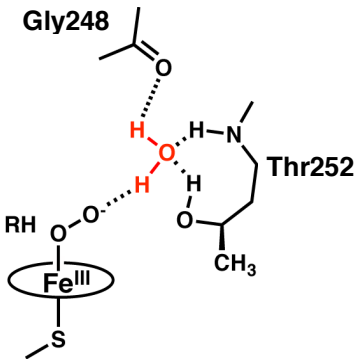

Figure 1-5. Probable active site hydrogen bonding network of the oxy complex.

The oxidation state change from ferric to ferrous allows for the binding of dioxygen. Formally, there are two ways to describe the oxygen bound intermediate, often designated as the "oxy-complex". One is ferrous-dioxygen; the other, ferric-superoxide.[37] In P450s, this intermediate has been demonstrated to exist predominately as the ferric superoxide species by Mössbauer spectroscopy.[38] Additionally, the oxy complex is the origin of the auto-oxidation shunt, where the O_2 unit is released as superoxide and the enzyme returns to its ferric resting state without completing the catalytic cycle.[39-40] The stability of this intermediate varies from P450 to P450 and gives rise to an unproductive turnover otherwise known as "uncoupling" of electron transfer (ET) and substrate hydroxylation. Measuring the degree of uncoupling is

typically done by comparing the ratio of NAD(P)H consumed to product formed, which in a perfectly coupled system is 1:1.[41]

The ordering of the next steps in the catalytic cycle is still debated, but is generally accepted to be a proton coupled electron transfer (PCET) where the ET step occurs first forming ferric peroxide and is then coupled to a proton transfer where a solvent derived proton is abstracted to form the hydroxyperoxide complex, Compound 0.[28] A second proton transfer occurs and the dihydroxoperoxy complex O–O bond undergoes a heterolytic cleavage and loss of a molecule of water, most likely driven by hydrogen bonding the distal oxygen.[42-44]

As a result of this heterolytic cleavage, the oxygen oxidizes the Fe(III) center and forms a formal Fe(V). However, this complex is highly oxidizing and thus removes an electron from the π system of the redox active porphyrin and forms iron(IV)-oxo (Fe(IV)=O) coupled to a delocalized ligand radical, known as Compound I (Cpd-I).[26-27, 45-50] This initiates a hydrogen atom abstraction (HAT) from substrate and forms Compound II (Cpd-II), an iron-(IV)-hydroxo and a carbon-based substrate radical.[51] A radical rebound mechanism, originally proposed by Groves, is allows for recombination of the substrate radical with the oxygen of Cpd-II.[44, 52] Following product formation, the iron returns to low-spin Fe(III) state as product egresses from the active site and water rebinds the vacant coordination site.

Cytochrome P450: Nature's Aircraft Carrier

Cytochrome P450 has been referred to as "Nature's blowtorch" because of its ability to oxidize strong C–H bonds in a regio- and stereo- selective manner.[48, 53] However, I would like to take this opportunity to extend the P450 metaphor to that of "Nature's aircraft carrier".

The launch mechanism of a fighter jet from an aircraft carrier is comprised of the tow bar attached to the plane's nose gear through a slot in the deck and the hold back bar attached to the rear wheels to keep the jet in place. The catapult officer, or "shooter", prepares the catapults that will generate the necessary lift for takeoff. When the plane is prepared, the officer opens valves that fill the cylinders with high-pressure steam from the ship's reactors, which will be the driving force that propels the pistons at high speed and throw the fighter jet into the air. The engines are fully engaged, the holdback bars release the back wheels, and shuttle throws the plane to the end of the runway and the tow bar is released from the shuttle. Too much pressure, and the nose gear will be ripped off, too little and the plane will be thrown into the ocean. This system takes a 45,000-pound plane from 0 to 165 miles per hour in two seconds! Needless to say, any mistake in this process could be disastrous.[54]

Figure 1-6. (Left) "Low Resolution" snapshot of fighter jet taking off from an aircraft carrier. **(Right)** "High Resolution" on the flight deck.

Let us begin with the fighter jet, the competent oxidant, the reactive intermediate that is responsible for the chemistry, the infamous Compound I. This powerful intermediate draws its power from the primary coordination sphere; in particular, a thiolate ligation and redox active

heme. It has a very specific mission that it must carry out effectively and with precision. In particular, its mission of C–H bond activation is thermodynamically demanding ($E^{\circ\prime}_{CH/C\bullet}$ = 1.5 V vs NHE), but Compound I carries out this oxidation without destroying its protein environment.[26, 48] Given the wrong conditions and the wrong instructions, the fighter jet, Compound I, could do some serious damage to the external scaffold, its own ship, the protein matrix. The fighter jet is hard to capture once it is on its mission, and in order to study it, it must be trapped within its native environment before leaving the runway.

This brings us to the ship and some interesting facts about aircraft carriers. First, why an aircraft carrier? Given broad environmental conditions (i.e solvent, temperature, time), it is possible to get a fighter jet into the air from an airport runway, just as synthetic chemists can make general catalysts for C–H bond activation. The real question is, given the thermodynamics of C–H bond activation, how do you launch a 45,000 lbs fighter jet in 300 feet surrounded by a sea of water (aqueous environment) when traditional airport runways are 6000 to 8000 feet with 2300 feet needed for takeoff alone?

From a bird's eye view, or low resolution, one would be hard-pressed to define the exact mechanism of fighter jet launch. While one may be able to define some larger features of the carrier, such as the jet blast deflectors, runway lines, or the watchtower, it would be nearly impossible to provide an accurate picture of their dynamics. It is not until we go to high spatial and temporal resolution of someone standing on the flight deck that we clearly see the intricate regulatory processes required for take-off. Here, we can see the jet's engines are fully engaged before take-off and excess energy is dissipated by the jet blast deflectors (Tyr/Trp channels)[55-56],

the hold back bar is keeping the plane in place (Cys-loop)[27, 57-58], the hydraulic catapult is fully pressurized (thiolate)[59], and finally, the long-range communication that occurs between the tower and those on deck signals the jet for take-off (long range mechanical coupling)[60] (Figure 1-6).

With high spatial and temporal resolution, we would see all of the pieces necessary to accomplish this complex task and why tight regulation is required if a process is efficient. But without this level of resolution, it would be impossible to understand how the structure of the carrier assists the fighter jet through a series of catapults that are initiated through long range networks from the tower to the deck.

As biochemists, we examine the active sites of the protein and test residues local to the activity and observe effects on rates or examine the overall fold. Again, at a modest resolution, we could probably identify the jet blast deflectors behind the planes and infer that they may have a role in redirecting or dissipating some of the jet's energy before takeoff, providing a clue that jet engines may be fully engaged while the plane is in place. By removing them, what happens to the structure and function? From the overall structure, we could determine the tarmac and directionality providing a sense for which way takeoff should occur. Finally, we would observe the tower, perhaps indicating some form of long-range communication.

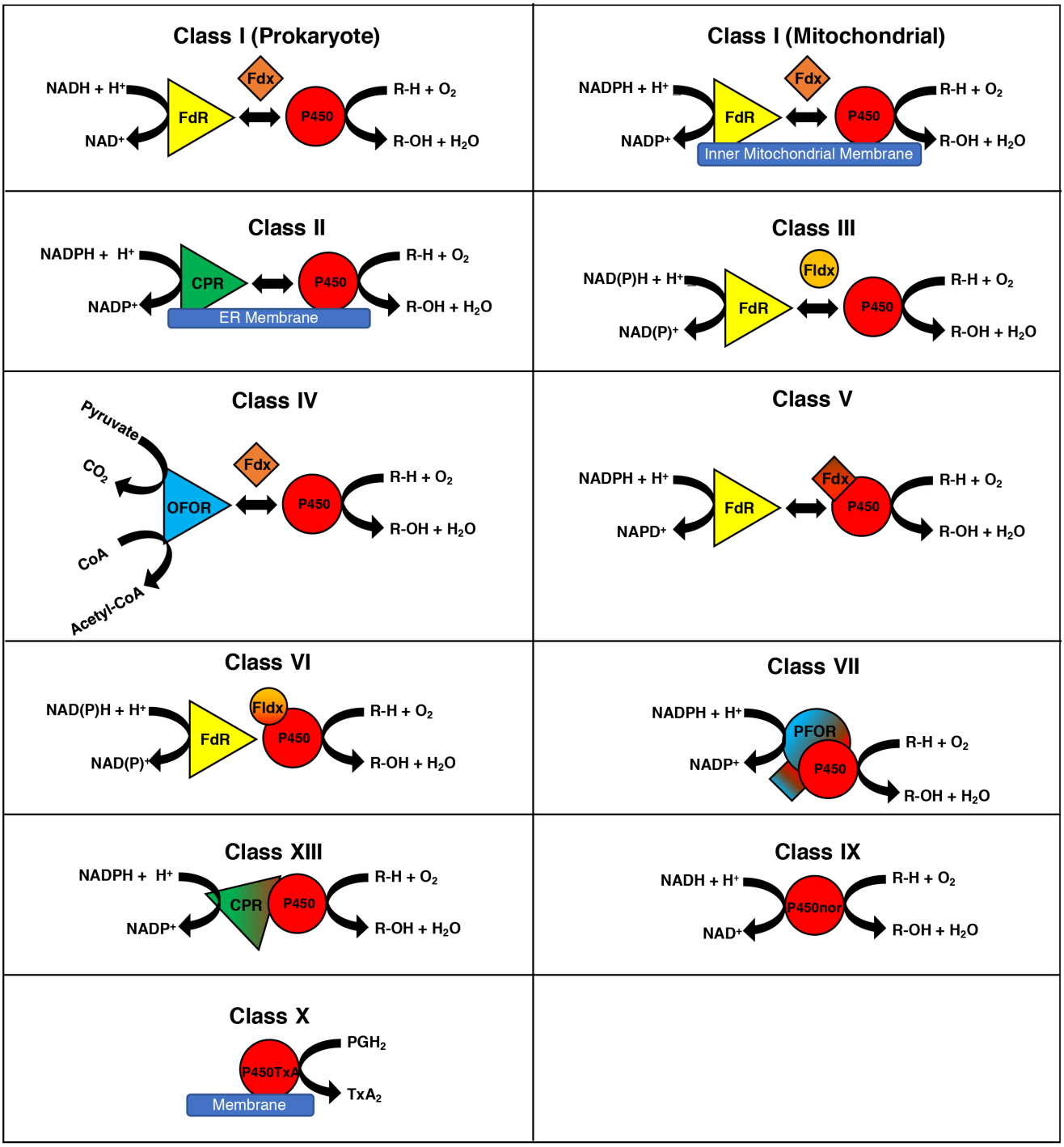

Figure 1-7. Classes of Cytochromes P450. FdR – Ferredoxin Reductase. Fdx – Ferredoxin. CPR – Cytochrome P450 Reductase. Fldx – Flavodoxin. OFOR – Oxoacid:Ferredoxin Oxidoreductase. PFOR – Phthalate Family Oxygenase Reductase. PGH_2 – Prostaglandin H_2. TxA_2 – Thromboxane A

As inorganic chemists, we probe the jet. How much power does the jet possess? What are the minimum qualities a jet must possess to be able to do what the fighter jet does? We build our own jets to see how an increase in the size of the wings or flap material affects the jet's precision. We gather significant insight this way, by stripping away the aircraft carrier and looking at the fine details from the bottom up.

As physical chemists, we use a combination of spectroscopic and computational tools to probe changes as a function of some perturbation and try to simulate their behavior and thus make a model carrier and jet mathematically and use it to predict the fighter's behavior.

The point of describing these different approaches is to emphasize the necessity to continually integrate them to create a more complete picture of bioinorganic chemistry. We must integrate these processes to show how structure and function are related through dynamics that occur over a broad range of timescales and in complex environments. While they are necessarily disentangled by our distinct approaches, the natural systems are necessarily entangled for the purpose of efficiency. Nature does not have the leeway to be wasteful.

Classes of Cytochromes P450

CYPs possess an immense diversity of function such as metabolism of xenobiotics, biosynthesis of natural products, and fatty acid decarboxylation and while the naming convention helps to distinguish P450s from one another, it is also helpful to be able to generalize about classes of P450 systems.[61] In order to more easily discuss cytochrome P450 diversity, the enzymes are segregated by the most differential part of their mechanism, their electron donors or "redox partners".[62] Nearly all P450s require two sequential electron transfers from an electron donor.

The nature of this electron donor partner separates P450s into distinct classes. To date, there are greater than 10 classes of P450 (Figure 1-7). However, the two major classes, Class 1 and Class 2, tend to dominate the discussion and account for 90% of known CYPs.[62] The majority of the focus of this work is on Class I systems.

Class I systems are comprised of three proteins: an FAD-containing reductase, a Fe_2S_2-containing redoxin, and the P450.[62] Overall, the FAD containing reductase binds NADH which undergoes a hydride transfer to the FAD cofactor. Two electron equivalents are subsequently passed one at a time from the reductase to the redoxin, which are then passed to the P450 in two sequential steps. This class of P450 is typically found in bacteria or attached to the mitochondrial membrane.

Class II P450s are two component enzymes usually associated with liver microsomes.[62] In Class II systems, a flavin mononucleotide (FMN)-containing reductase removes a hydride from NADPH and passes the electrons from FAD to FMN to P450.

While the number of P450s in a eukaryotic organism far outnumber those present in a prokaryote, the sheer number of prokaryotic genomes provide unpresented diversity in terms of CYP function. All of this reactivity is tied to the ability for P450 to activate strong C–H bonds (~101 kcal/mol) through the activation of atmospheric dioxygen. However, the diversity of reactivity that is possible by these enzymes is much broader. While most notable P450's hydroxylate or epoxidate their substrates, they are also capable of N-, O- and S-dealkylations, sulphoxidations, deaminations, desulfurations, dehalogenations, peroxidations, and N-oxide reductions.[63-64]

Cytochrome P450cam (CYP101A1)

The first official report of P450cam was in 1968 when Katagiri *et al.* reported an NADH-dependent P450 in *Pseudomonas putida*.[11] As a Class I system, hydroxylation of the physiological substrate D-camphor to 5-*exo*-hydroxycamphor requires three soluble components: a flavin adenine dinucleotide (FAD) dependent reductuase, putidaredoxin reductase (PdR), a Fe_2S_2-containing depended redoxin, putidaredoxin (Pdx), and the cytochrome P450 (P450cam) (Figure 1-8). These are expressed under the control of a polycistronic operon which is regulated by CamR, a camphor-dependent repressor. The solubility of this system made it much simpler to dissect the structure-function relationship and mechanism of hydroxylation. P450cam was the first cytochrome P450 to be successfully crystallized and its crystal structure was determined in 1985 by Poulos *et al.*[65] P450cam is an average size P450 comprised of 414 amino acid residues and a molecular weight of 46.6 kDa. In total, P450cam is composed of thirteen alpha-helices (A-L and

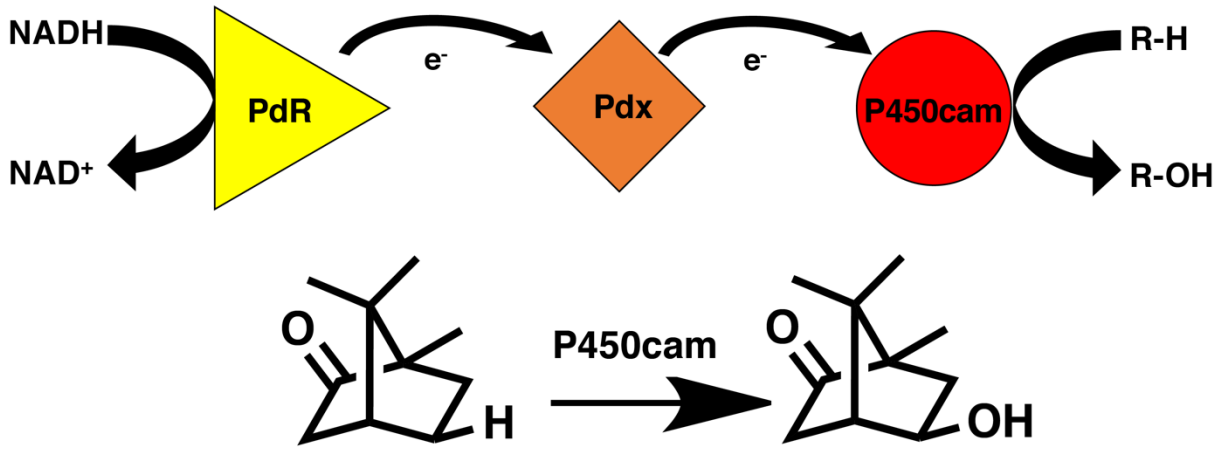

Figure 1-8. (Top) P450cam redox components. **(Bottom)** Hydroxylation of d-camphor to 5-exo-hydroxycamphor.

B') and 5 beta sheets (ß1-5) (Figure 1-2A). Since this time, P450cam has served as the paradigm for structure-function relationships and mechanistic conclusions as the conserved features of the superfamily make it possible to generalize across both prokaryotic and eukaryotic P450s.[66] Thus, here, we can expand on some of the specifics of the O_2 and C–H activation mechanisms through the lens of P450cam (*vide supra)*.

Cys357 coordinates the heme b iron in the axial position. Substrate access occurs on the distal side of the enzyme while Pdx binds to the proximal side. As the first structure of P450cam was solved in the presence of substrate, the enzyme was found in the closed form with no obvious access channel for substrate to enter. This led to a significant effort to identify the access channel. While advanced molecular dynamics techniques provided arguments for probable access channels,[16-17, 19] it was not until decades later, in 2002, that Dunn *et al.*[67] utilized ruthenium linked substrate mimics to crystallize the open conformation. Nearly a decade later still, Lee *et al.* solved the crystal structure of the substrate free form which revealed the same channel that was found in the 2002 study.[29]

With structures of the "open" and "closed" closed structures solved, it was possible to see how the B', F, G, and I helices work together to change conformations for accommodating substrate. This was believed to complete the crystallographic characterization of the catalytic cycle as a series of intermediates such as the oxy complex had been previously characterized.[53] Prior to the solution of these structures, P450cam had demonstrated a strong sensitivity to concentrations of potassium by spectroscopy that was believed to affect substrate binding.[68-71] Through these crystal structures, a K^+ binding site was revealed and further NMR studies by the

Pochapsky group corroborated the specificity and relative location of this site located on the B-C loop.[72] Pochapsky also examined the active site mobility as a function of the potassium concentration and found that the B' helix was significantly more mobile than previously thought. The potassium ion is coordinated by the backbone carbonyls of Glu84, Gly93, Glu94, and Y96 and stabilizes the secondary structure of the B' helix, and thus stabilizes the closed conformation of the protein. Spectroscopically, addition of K^+ in the presence of substrate increases the high spin fraction.[68] Chapters 2 and 3 will discuss the critical role of the B' helix in the mechanism of P450cam in detail. Pochapsky demonstrated not only the importance of potassium but also the role of proline isomerization, a concept that had not been previously observed in P450s.[73]

Combining these results led to the hypothesis that the opening of these helices and movement of I helix is essential in freeing an aspartate residue (D251), adjacent to the active site threonine residue (Thr252), from a strong ion pair with an arginine located on the F helix near the F/G loop and that this aspartate residue (D251) plays an important role in the proton delivery mechanism of P450cam during the second ET step.[21, 24] Specifically, in the crystal structures of the resting state, the hydroxyl group of the Thr252 sidechain forms a hydrogen bond with Gly248 carbonyl that breaks upon O_2 (or CN) binding.[53, 74-75] The breaking of this bond and the widening of the I helix groove allows water to move into the active site and the backbone of Asp251 moves into a normal hydrogen bonding configuration. With this Thr252-G248 H-bond broken, there are now two H-bond acceptors poised within 3 Å of the distal oxygen atom which are suggested to assist in the protonation of the hydoxyperoxo complex and heterolytic cleavage mechanism to form Compound I (Figure 1-5). As previously mentioned, Asp251 is locked up in ion pairs with

K178 and R186 in the resting state, but, upon reorientation of the I helix and shifting to the open state, was hypothesized to assist in the shuttling protons to form and cleave the dihydroxyperoxo complex. Support for this hypothesis came from mutagenesis studies[22, 44, 74] and was further corroborated by the X-ray crystal structure of the P450cam-Pdx complex where Asp251 is rotated toward the active site and in the open conformation.[24]

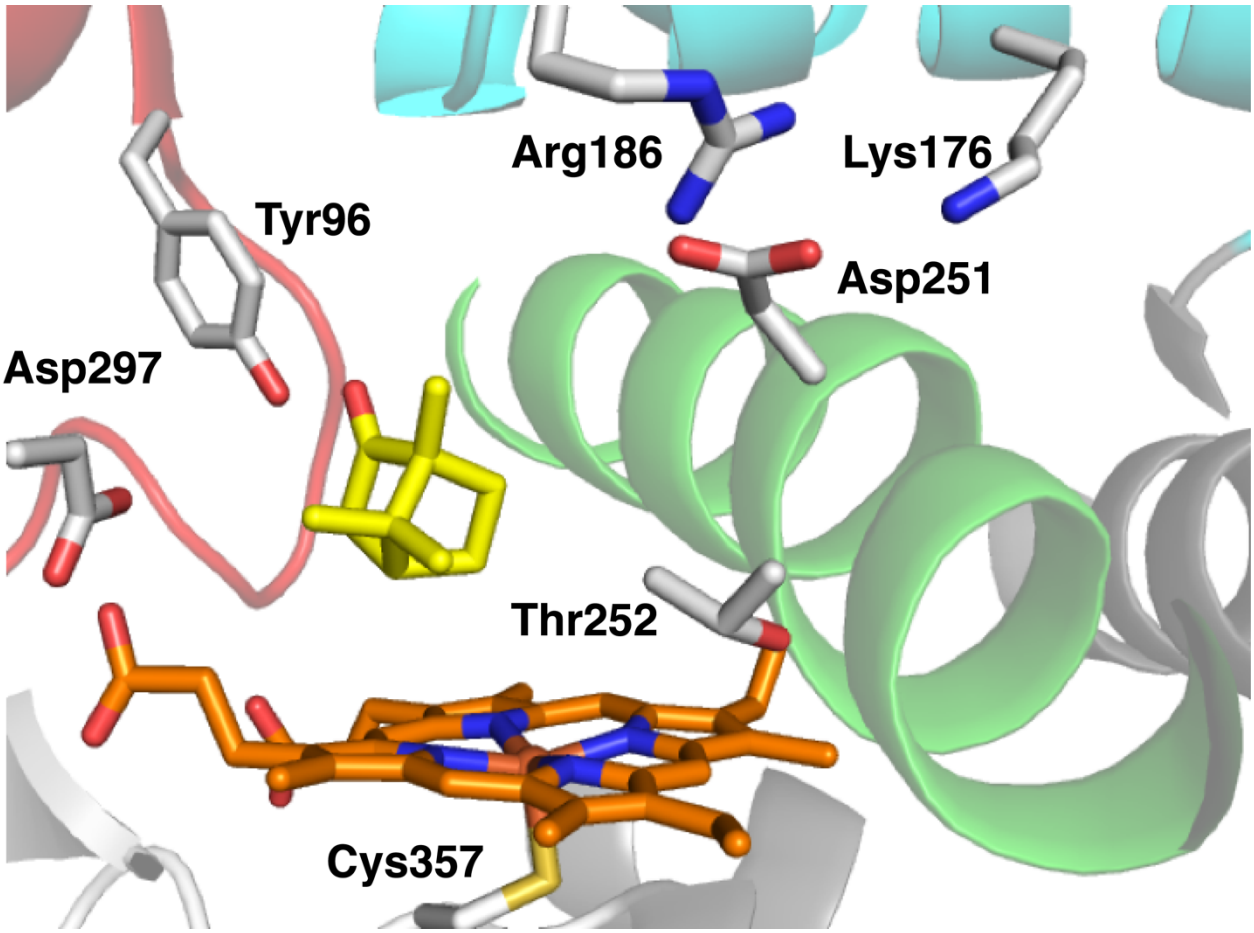

Figure 1-9. Active site of closed substrate bound resting state structure of P450cam. (PDB: 2CPP)

Putidaredoxin and the P450cam-Pdx Complex

Within the catalytic cycle of cytochrome P450, there are two unique electron transfer events. The first of which promotes the binding of dioxygen and the second drives the protonation and subsequent loss of water to form the active oxidizing species, Compound I.

In P450cam, both of these electron transfers are from putidaredoxin, Pdx. Pdx is a 2-iron-2-sulfur containing ferredoxin that is comprised of 106 amino acids (11.6 kDa) capable of carrying out one electron redox processes with a redox potential ~-230 mV vs NHE.[34] The amino acid composition of these ferredoxins is highly acidic with pIs ~3-4. Early on, it was shown that the two ET events between Pdx and P450cam were distinct.[76-78] In particular, it was shown that the first ET could be carried out by any reductant of the appropriate potential including non-endogenous ferredoxins or cytochromes, while the second ET is specific and can only be carried out by Pdx. This stands in direct contrast to many other P450s where redox partner selectivity is more promiscuous and redox partners can serve a multitude of P450s or metalloenzymes. As the investigation of this specificity progressed, it was demonstrated that there was a conformational and allosteric role to this P450cam-Pdx interaction, deemed the "effector" role of Pdx and has been the subject of intense investigation.[35, 79-81] Within this context, early mutagenesis studies identified Trp106, the terminal residue of Pdx, as a major contributor to this selectivity (Figure 1-10B).[82]

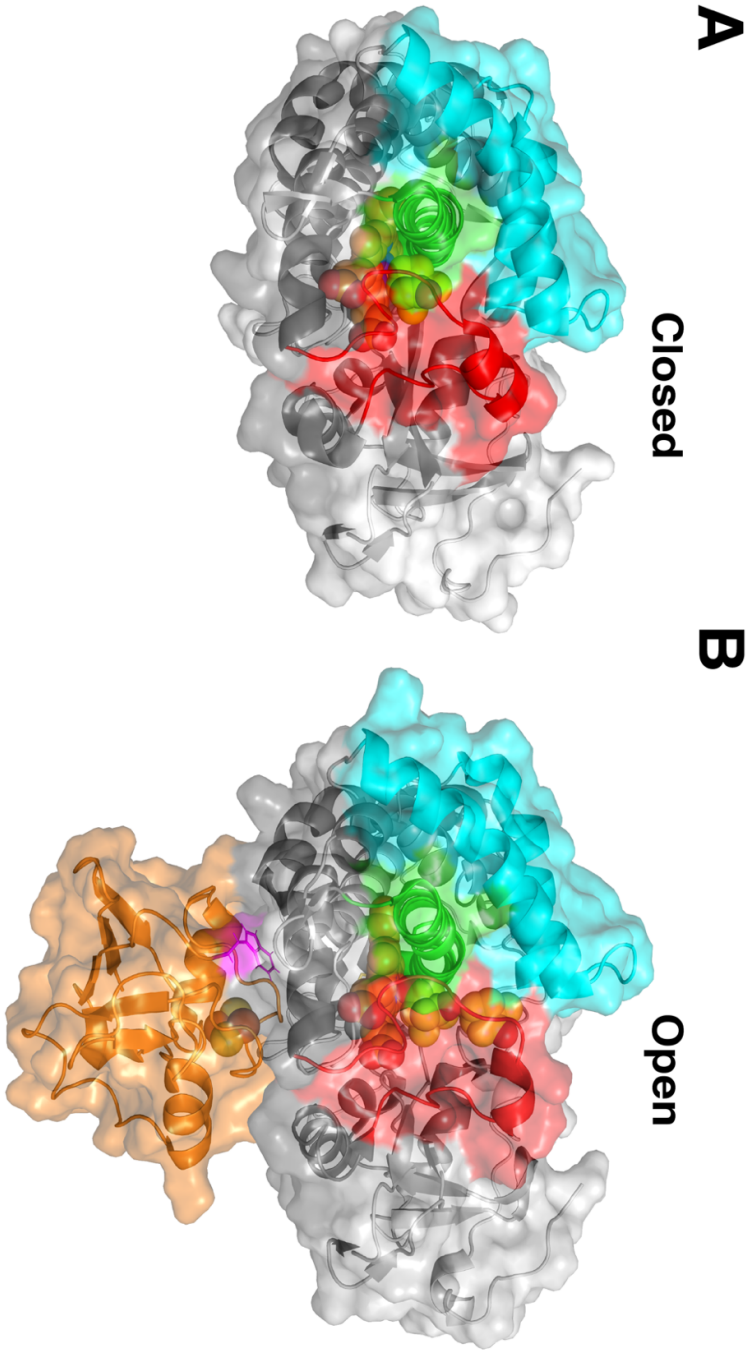

Figure 1-10. (A) Substrate bound closed structure of P450cam. **(B)** Open structure of P450cam-Pdx complex (PDB: 2CPP, 4JWU) B-C loop and B' helix (red). F/G helices (cyan). I helix (green). Pdx (orange) Trp106 (magneta).

However, determination of the structure of Pdx alone was a challenge. By NMR, the structure determination was hampered by paramagnetic broadening stemming from the two high-spin iron sites, a feat eventually overcome by the substitution of iron with gallium, however this change still induced deviations from wild-type (WT).[83-87] By X-ray crystallography, it was not until 2003, where the substitution of two surface exposed cysteines (C73 and C85) for serines allowed for its crystallization and eventual solution.[88]

With the structures of both components in hand, a number of computational and mutagenesis studies sought to unravel the nature of this intriguing specificity. It was not until a decade later, that in our lab, Tripathi *et al.* was able to solve the crystal structure of the two proteins, P450cam and Pdx, complexed together in both the oxidized and reduced form.[24] Shortly after, publication of the corroborative structures of the non-covalently linked structures by NMR and X-ray crystallography were published by the Ubbink group.[89]

These structures clarify the wealth of spectral and mutagenesis data and illustrate how critical residues and domains such as Trp106 of Pdx and the C helix of P450cam couple their motion to ensure a tight interface. Both crystal structures of the complex (oxidized and reduced) revealed the open conformation of the enzyme, supporting spectroscopic studies in which Pdx binding shifts P450cam to the low-spin form.[35, 90-91] However, the structure of the dithionite reduced complex revealed product in the active site indicating ET, O_2 activation, and substrate hydroxylation occurred within the crystal during data collection.[24] In support of this active complex, is the breaking of the Asp251 ion pairs, which would free the side chain to participate in the proton relay network.

Later, double electron-electron resonance (DEER) studies by Goodin indicated the conformational states accessible to P450cam are dependent on the oxidation state of Pdx and supported the binding oxidized Pdx to the open state.[92]

Putidaredoxin Reductase

The final component of the P450cam system is Putidaredoxin reductase or PdR, a 45.6 kDa FAD-containing reductase. PdR removes a hydride from NADH and passes the two reducing equivalents to FAD then to Pdx. The PdR structure has been solved in addition to the PdR-Pdx complex.[93-94]

From a comparison of the P450cam-Pdx and PdR-Pdx complexes, an intriguing question arises about the nature of activity. While interfaces that Pdx makes with its partner proteins are relatively similar in both complexes, the PdR complex remains active in solution, while the P450cam complex is inactive. How and why are there differential activity between these complexes?

Summary of Dissertation

The remaining chapters will focus primarily on Class 1 cytochromes P450, in particular P450cam, and the interactions that occur between their substrates and their redox partners. In particular, Chapters 2 and 3 will focus on the model P450, P450cam. Chapters 2 and 3 open completely new territory in regard to the P450 mechanism. Chapter 2 will first examine the, to date, unknown cooperativity that occurs between an allosteric second substrate binding site and the formation of an egress channel. Chapter 3 will reveal how diatomic and redox partner binding can induce conformational changes that are predicted by molecular dynamics and controlled by

conformational changes never before crystallographically observed in a P450. Chapters 4 lays the ground work for understanding these redox partner interactions through other bacterial Class 1 P450s. Chapter 5 examines the proposed roles of viral P450 through structure and bioinformatics. Chapter 6 unites and concludes the discussions within this work.

References

1. Poulos, T. L., Heme enzyme structure and function. *Chem Rev* **2014,** *114* (7), 3919-62.
2. Brodie, B. B.; Axelrod, J.; Cooper, J. R.; Gaudette, L.; La Du, B. N.; Mitoma, C.; Udenfriend, S., Detoxication of drugs and other foreign compounds by liver microsomes. *Science* **1955,** *121* (3147), 603-4.
3. Klingenberg, M., Pigments of rat liver microsomes. *Arch Biochem Biophys* **1958,** *75* (2), 376-86.
4. Omura, T.; Sato, R., The Carbon Monoxide-Binding Pigment of Liver Microsomes. Ii. Solubilization, Purification, and Properties. *J Biol Chem* **1964,** *239*, 2379-85.
5. Estabrook, R. W.; Cooper, D. Y.; Rosenthal, O., The Light Reversible Carbon Monoxide Inhibition of the Steroid C21-Hydroxylase System of the Adrenal Cortex. *Biochem Z* **1963,** *338*, 741-55.
6. Omura, T.; Sato, R., A new cytochrome in liver microsomes. *J Biol Chem* **1962,** *237*, 1375-6.
7. Gouterman, M., Spectra of Porphyrins. *Journal of Molecular Spectroscopy* **1961,** *6* (1), 138-&.
8. Nelson, D. R., Cytochrome P450 diversity in the tree of life. *Biochim Biophys Acta Proteins Proteom* **2018,** *1866* (1), 141-154.
9. Nelson, D. R., Cytochrome P450 Nomenclature, 2004. In *Cytochrome P450 Protocols*, Phillips, I. R.; Shephard, E. A., Eds. Humana Press: Totowa, NJ, 2006; pp 1-10.
10. Nelson, D. R.; Koymans, L.; Kamataki, T.; Stegeman, J. J.; Feyereisen, R.; Waxman, D. J.; Waterman, M. R.; Gotoh, O.; Coon, M. J.; Estabrook, R. W.; Gunsalus, I. C.; Nebert, D. W., P450 superfamily: update on new sequences, gene mapping, accession numbers and nomenclature. *Pharmacogenetics* **1996,** *6* (1), 1-42.
11. Katagiri, M.; Ganguli, B. N.; Gunsalus, I. C., A soluble cytochrome P-450 functional in methylene hydroxylation. *J Biol Chem* **1968,** *243* (12), 3543-6.
12. Shimada, T.; Yamazaki, H.; Mimura, M.; Inui, Y.; Guengerich, F. P., Interindividual variations in human liver cytochrome P-450 enzymes involved in the oxidation of drugs, carcinogens and toxic chemicals: studies with liver microsomes of 30 Japanese and 30 Caucasians. *J Pharmacol Exp Ther* **1994,** *270* (1), 414-23.
13. Poulos, T. L.; Finzel, B. C.; Howard, A. J., High-resolution crystal structure of cytochrome P450cam. *J Mol Biol* **1987,** *195* (3), 687-700.
14. Poulos, T. L., Cytochrome P450 flexibility. *Proceedings of the National Academy of Sciences* **2003,** *100* (23), 13121-13122.

15. Di Gleria, K.; Nickerson, D. P.; Hill, H. A. O.; Wong, L.-L.; Fülöp, V., Covalent Attachment of an Electroactive Sulfydryl Reagent in the Active Site of Cytochrome P450cam as Revealed by the Crystal Structure of the Modified Protein. *Journal of the American Chemical Society* **1998,** *120* (1), 46-52.
16. Ludemann, S. K.; Lounnas, V.; Wade, R. C., How do substrates enter and products exit the buried active site of cytochrome P450cam? 2. Steered molecular dynamics and adiabatic mapping of substrate pathways. *J Mol Biol* **2000,** *303* (5), 813-30.
17. Ludemann, S. K.; Lounnas, V.; Wade, R. C., How do substrates enter and products exit the buried active site of cytochrome P450cam? 1. Random expulsion molecular dynamics investigation of ligand access channels and mechanisms. *J Mol Biol* **2000,** *303* (5), 797-811.
18. Winn, P. J.; Ludemann, S. K.; Gauges, R.; Lounnas, V.; Wade, R. C., Comparison of the dynamics of substrate access channels in three cytochrome P450s reveals different opening mechanisms and a novel functional role for a buried arginine. *Proc Natl Acad Sci U S A* **2002,** *99* (8), 5361-6.
19. Cojocaru, V.; Winn, P. J.; Wade, R. C., The ins and outs of cytochrome P450s. *Biochim Biophys Acta* **2007,** *1770* (3), 390-401.
20. Benson, D. E.; Suslick, K. S.; Sligar, S. G., Reduced oxy intermediate observed in D251N cytochrome P450cam. *Biochemistry* **1997,** *36* (17), 5104-7.
21. Vidakovic, M.; Sligar, S. G.; Li, H.; Poulos, T. L., Understanding the role of the essential Asp251 in cytochrome p450cam using site-directed mutagenesis, crystallography, and kinetic solvent isotope effect. *Biochemistry* **1998,** *37* (26), 9211-9.
22. Deng, T.; Macdonald, I. D.; Simianu, M. C.; Sykora, M.; Kincaid, J. R.; Sligar, S. G., Hydrogen-bonding interactions in the active sites of cytochrome P450cam and its site-directed mutants. *J Am Chem Soc* **2001,** *123* (2), 269-78.
23. Follmer, A. H.; Tripathi, S.; Poulos, T. L., Ligand and Redox Partner Binding Generates a New Conformational State in Cytochrome P450cam (CYP101A1). *J Am Chem Soc* **2019**.
24. Tripathi, S.; Li, H.; Poulos, T. L., Structural basis for effector control and redox partner recognition in cytochrome P450. *Science* **2013,** *340* (6137), 1227-30.
25. Behan, R. K.; Hoffart, L. M.; Stone, K. L.; Krebs, C.; Green, M. T., Evidence for basic ferryls in cytochromes P450. *J Am Chem Soc* **2006,** *128* (35), 11471-4.
26. Green, M. T., C-H bond activation in heme proteins: the role of thiolate ligation in cytochrome P450. *Curr Opin Chem Biol* **2009,** *13* (1), 84-8.
27. Krest, C. M.; Silakov, A.; Rittle, J.; Yosca, T. H.; Onderko, E. L.; Calixto, J. C.; Green, M. T., Significantly shorter Fe-S bond in cytochrome P450-I is consistent with greater reactivity relative to chloroperoxidase. *Nat Chem* **2015,** *7* (9), 696-702.
28. Luthra, A.; Denisov, I. G.; Sligar, S. G., Spectroscopic features of cytochrome P450 reaction intermediates. *Arch Biochem Biophys* **2011,** *507* (1), 26-35.
29. Lee, Y. T.; Wilson, R. F.; Rupniewski, I.; Goodin, D. B., P450cam visits an open conformation in the absence of substrate. *Biochemistry* **2010,** *49* (16), 3412-9.

30. Fisher, M. T.; Sligar, S. G., Control of heme protein redox potential and reduction rate: linear free energy relation between potential and ferric spin state equilibrium. *Journal of the American Chemical Society* **1985,** *107* (17), 5018-5019.
31. Davies, M. D.; Qin, L.; Beck, J. L.; Suslick, K. S.; Koga, H.; Horiuchi, T.; Sligar, S. G., Putidaredoxin reduction of cytochrome P-450cam: dependence of electron transfer on the identity of putidaredoxin's C-terminal amino acid. *Journal of the American Chemical Society* **1990,** *112* (20), 7396-7398.
32. Martinis, S. A.; Blanke, S. R.; Hager, L. P.; Sligar, S. G.; Hoa, G. H.; Rux, J. J.; Dawson, J. H., Probing the heme iron coordination structure of pressure-induced cytochrome P420cam. *Biochemistry* **1996,** *35* (46), 14530-6.
33. Lipscomb, J. D., Electron paramagnetic resonance detectable states of cytochrome P-450cam. *Biochemistry* **1980,** *19* (15), 3590-3599.
34. Wilson, G. S.; Tsibris, J. C. M.; Gunsalus, I. C., Electrochemical studies of putidaredoxin and its selenium analog. *Journal of Biological Chemistry* **1973,** *248* (17), 6059-6061.
35. Gunsalus, I. C.; Lipscomb, J. D.; Meeks, J. R., Cytochrome P-450cam Substrate And Effector Interactions. *Annals of the New York Academy of Sciences* **1973,** *212* (1), 107-121.
36. Brewer, C. B.; Peterson, J. A., Single turnover kinetics of the reaction between oxycytochrome P-450(cam) and reduced putidaredoxin. *Journal of Biological Chemistry* **1988,** *263* (2), 791-798.
37. Momenteau, M.; Reed, C. A., Synthetic Heme Dioxygen Complexes. *Chemical Reviews* **1994,** *94* (3), 659-698.
38. Sharrock, M.; Debrunner, P. G.; Schulz, C.; Lipscomb, J. D.; Marshall, V.; Gunsalus, I. C., Cytochrome P450cam and its complexes, Mo¨ssbauer parameters of the heme iron. *Biochimica et Biophysica Acta (BBA) - Protein Structure* **1976,** *420* (1), 8-26.
39. Kuthan, H.; Ullrich, V., Oxidase and Oxygenase Function of the Microsomal Cytochrome P450 Monooxygenase System. *European Journal of Biochemistry* **1982,** *126* (3), 583-588.
40. Ost, T. W. B.; Clark, J.; Mowat, C. G.; Miles, C. S.; Walkinshaw, M. D.; Reid, G. A.; Chapman, S. K.; Daff, S., Oxygen Activation and Electron Transfer in Flavocytochrome P450 BM3. *Journal of the American Chemical Society* **2003,** *125* (49), 15010-15020.
41. Loida, P. J.; Sligar, S. G., Molecular recognition in cytochrome P-450: Mechanism for the control of uncoupling reactions. *Biochemistry* **1993,** *32* (43), 11530-11538.
42. Davydov, R.; Kappl, R.; Huttermann, J.; Peterson, J. A., EPR-spectroscopy of reduced oxyferrous-P450cam. *FEBS Lett* **1991,** *295* (1-3), 113-5.
43. Davydov, R. M.; Smieja, J.; Dikanov, S. A.; Zang, Y.; Que, L., Jr.; Bowman, M. K., EPR properties of mixed-valent mu-oxo and mu-hydroxo dinuclear iron complexes produced by radiolytic reduction at 77 K. *J Biol Inorg Chem* **1999,** *4* (3), 292-301.
44. Davydov, R.; Makris, T. M.; Kofman, V.; Werst, D. E.; Sligar, S. G.; Hoffman, B. M., Hydroxylation of camphor by reduced oxy-cytochrome P450cam: mechanistic implications of EPR and ENDOR studies of catalytic intermediates in native and mutant enzymes. *J Am Chem Soc* **2001,** *123* (7), 1403-15.

45. Dunford, H. B.; Stillman, J. S., On the function and mechanism of action of peroxidases. *Coordination Chemistry Reviews* **1976,** *19* (3), 187-251.
46. Green, M. T., Evidence for Sulfur-Based Radicals in Thiolate Compound I Intermediates. *Journal of the American Chemical Society* **1999,** *121* (34), 7939-7940.
47. Stone, K. L.; Behan, R. K.; Green, M. T., X-ray absorption spectroscopy of chloroperoxidase compound I: Insight into the reactive intermediate of P450 chemistry. *Proc Natl Acad Sci U S A* **2005,** *102* (46), 16563-5.
48. Rittle, J.; Green, M. T., Cytochrome P450 compound I: capture, characterization, and C-H bond activation kinetics. *Science* **2010,** *330* (6006), 933-7.
49. Rittle, J.; Younker, J. M.; Green, M. T., Cytochrome P450: the active oxidant and its spectrum. *Inorg Chem* **2010,** *49* (8), 3610-7.
50. Krest, C. M.; Onderko, E. L.; Yosca, T. H.; Calixto, J. C.; Karp, R. F.; Livada, J.; Rittle, J.; Green, M. T., Reactive intermediates in cytochrome p450 catalysis. *J Biol Chem* **2013,** *288* (24), 17074-81.
51. Yosca, T. H.; Rittle, J.; Krest, C. M.; Onderko, E. L.; Silakov, A.; Calixto, J. C.; Behan, R. K.; Green, M. T., Iron(IV)hydroxide pK(a) and the role of thiolate ligation in C-H bond activation by cytochrome P450. *Science* **2013,** *342* (6160), 825-9.
52. Groves, J. T., High-valent iron in chemical and biological oxidations. *Journal of Inorganic Biochemistry* **2006,** *100* (4), 434-447.
53. Schlichting, I.; Berendzen, J.; Chu, K.; Stock, A. M.; Maves, S. A.; Benson, D. E.; Sweet, R. M.; Ringe, D.; Petsko, G. A.; Sligar, S. G., The catalytic pathway of cytochrome p450cam at atomic resolution. *Science* **2000,** *287* (5458), 1615-22.
54. Harris, T. "How Aircraft Carriers Work". https://science.howstuffworks.com/aircraft-carrier.htm (accessed 11 February 2019).
55. Ener, M. E.; Gray, H. B.; Winkler, J. R., Hole Hopping through Tryptophan in Cytochrome P450. *Biochemistry* **2017,** *56* (28), 3531-3538.
56. Gray, H. B.; Winkler, J. R., Living with Oxygen. *Acc Chem Res* **2018,** *51* (8), 1850-1857.
57. Green, M. T.; Dawson, J. H.; Gray, H. B., Oxoiron(IV) in chloroperoxidase compound II is basic: implications for P450 chemistry. *Science* **2004,** *304* (5677), 1653-6.
58. Davydov, R.; Im, S.; Shanmugam, M.; Gunderson, W. A.; Pearl, N. M.; Hoffman, B. M.; Waskell, L., Role of the Proximal Cysteine Hydrogen Bonding Interaction in Cytochrome P450 2B4 Studied by Cryoreduction, Electron Paramagnetic Resonance, and Electron-Nuclear Double Resonance Spectroscopy. *Biochemistry* **2016,** *55* (6), 869-83.
59. Yosca, T. H.; Ledray, A. P.; Ngo, J.; Green, M. T., A new look at the role of thiolate ligation in cytochrome P450. *J Biol Inorg Chem* **2017,** *22* (2-3), 209-220.
60. Colthart, A. M.; Tietz, D. R.; Ni, Y.; Friedman, J. L.; Dang, M.; Pochapsky, T. C., Detection of substrate-dependent conformational changes in the P450 fold by nuclear magnetic resonance. *Sci Rep* **2016,** *6*, 22035.
61. Sono, M.; Roach, M. P.; Coulter, E. D.; Dawson, J. H., Heme-Containing Oxygenases. *Chem Rev* **1996,** *96* (7), 2841-2888.

62. Hannemann, F.; Bichet, A.; Ewen, K. M.; Bernhardt, R., Cytochrome P450 systems—biological variations of electron transport chains. *Biochimica et Biophysica Acta (BBA) - General Subjects* **2007,** *1770* (3), 330-344.
63. Werck-Reichhart, D.; Feyereisen, R., Cytochromes P450: a success story. *Genome Biol* **2000,** *1* (6), 3003.
64. Guengerich, F. P., Uncommon P450-catalyzed reactions. *Curr Drug Metab* **2001,** *2* (2), 93-115.
65. Poulos, T. L.; Finzel, B. C.; Gunsalus, I. C.; Wagner, G. C.; Kraut, J., The 2.6-A crystal structure of Pseudomonas putida cytochrome P-450. *J Biol Chem* **1985,** *260* (30), 16122-30.
66. Ortiz de Montellano, P. R., *Cytochrome P450: Structure, Mechanism, and Biochemistry*. 2015.
67. Dunn, A. R.; Hays, A. M.; Goodin, D. B.; Stout, C. D.; Chiu, R.; Winkler, J. R.; Gray, H. B., Fluorescent probes for cytochrome p450 structural characterization and inhibitor screening. *J Am Chem Soc* **2002,** *124* (35), 10254-5.
68. Lange, R.; Debey, P., Spin transition of camphor-bound cytochrome P-450. 1. local paH and electrostatic interactions. *Eur J Biochem* **1979,** *94* (2), 485-9.
69. Lange, R.; Hui Bon Hoa, G.; Debey, P.; Gunsalus, I. C., Spin transition of camphor-bound cytochrome P-450. 2. Kinetics following rapid changes of the local paH at sub-zero temperatures. *Eur J Biochem* **1979,** *94* (2), 491-6.
70. Lange, R.; Hui Bon Hoa, G.; Debey, P.; Gunsalus, I. C., A thermodynamic-kinetic analysis of the cytochrome P-450 heme pocket. *Acta Biol Med Ger* **1979,** *38* (2-3), 143-52.
71. Hui Bon Hoa, G.; Marden, M. C., The pressure dependence of the spin equilibrium in camphor-bound ferric cytochrome P-450. *Eur J Biochem* **1982,** *124* (2), 311-5.
72. OuYang, B.; Pochapsky, S. S.; Pagani, G. M.; Pochapsky, T. C., Specific effects of potassium ion binding on wild-type and L358P cytochrome P450cam. *Biochemistry* **2006,** *45* (48), 14379-88.
73. OuYang, B.; Pochapsky, S. S.; Dang, M.; Pochapsky, T. C., A functional proline switch in cytochrome P450cam. *Structure* **2008,** *16* (6), 916.
74. Nagano, S.; Poulos, T. L., Crystallographic study on the dioxygen complex of wild-type and mutant cytochrome P450cam. Implications for the dioxygen activation mechanism. *J Biol Chem* **2005,** *280* (36), 31659-63.
75. Raag, R.; Martinis, S. A.; Sligar, S. G.; Poulos, T. L., Crystal structure of the cytochrome P-450CAM active site mutant Thr252Ala. *Biochemistry* **1991,** *30* (48), 11420-9.
76. Tyson, C. A.; Lipscomb, J. D.; Gunsalus, I. C., The role of putidaredoxin and P450 cam in methylene hydroxylation. *J Biol Chem* **1972,** *247* (18), 5777-84.
77. Sligar, S. G.; Debrunner, P. G.; Lipscomb, J. D.; Namtvedt, M. J.; Gunsalus, I. C., A role of the putidaredoxin COOH-terminus in P-450cam (cytochrome m) hydroxylations. *Proc Natl Acad Sci U S A* **1974,** *71* (10), 3906-10.
78. Lipscomb, J. D.; Sligar, S. G.; Namtvedt, M. J.; Gunsalus, I. C., Autooxidation and hydroxylation reactions of oxygenated cytochrome P-450cam. *J Biol Chem* **1976,** *251* (4), 1116-24.
79. Kuznetsov, V. Y.; Poulos, T. L.; Sevrioukova, I. F., Putidaredoxin-to-cytochrome P450cam electron transfer: differences between the two reductive steps required for catalysis. *Biochemistry* **2006,** *45* (39), 11934-44.

80. Batabyal, D.; Lewis-Ballester, A.; Yeh, S. R.; Poulos, T. L., A Comparative Analysis of the Effector Role of Redox Partner Binding in Bacterial P450s. *Biochemistry* **2016,** *55* (47), 6517-6523.
81. Liou, S. H.; Mahomed, M.; Lee, Y. T.; Goodin, D. B., Effector Roles of Putidaredoxin on Cytochrome P450cam Conformational States. *J Am Chem Soc* **2016,** *138* (32), 10163-72.
82. Stayton, P. S.; Sligar, S. G., Structural microheterogeneity of a tryptophan residue required for efficient biological electron transfer between putidaredoxin and cytochrome P-450cam. *Biochemistry* **1991,** *30* (7), 1845-51.
83. Pochapsky, T. C.; Ratnaswamy, G.; Patera, A., Redox-dependent 1H NMR spectral features and tertiary structural constraints on the C-terminal region of putidaredoxin. *Biochemistry* **1994,** *33* (21), 6433-41.
84. Pochapsky, T. C.; Ye, X. M.; Ratnaswamy, G.; Lyons, T. A., An NMR-derived model for the solution structure of oxidized putidaredoxin, a 2-Fe, 2-S ferredoxin from Pseudomonas. *Biochemistry* **1994,** *33* (21), 6424-32.
85. Kazanis, S.; Pochapsky, T. C., Structural features of the metal binding site and dynamics of gallium putidaredoxin, a diamagnetic derivative of a Cys4Fe2S2 ferredoxin. *J Biomol NMR* **1997,** *9* (4), 337-46.
86. Pochapsky, T. C.; Kuti, M.; Kazanis, S., The solution structure of a gallium-substituted putidaredoxin mutant: GaPdx C85S. *J Biomol NMR* **1998,** *12* (3), 407-15.
87. Pochapsky, T. C.; Jain, N. U.; Kuti, M.; Lyons, T. A.; Heymont, J., A refined model for the solution structure of oxidized putidaredoxin. *Biochemistry* **1999,** *38* (15), 4681-90.
88. Sevrioukova, I. F.; Garcia, C.; Li, H.; Bhaskar, B.; Poulos, T. L., Crystal structure of putidaredoxin, the [2Fe-2S] component of the P450cam monooxygenase system from Pseudomonas putida. *J Mol Biol* **2003,** *333* (2), 377-92.
89. Hiruma, Y.; Hass, M. A.; Kikui, Y.; Liu, W. M.; Olmez, B.; Skinner, S. P.; Blok, A.; Kloosterman, A.; Koteishi, H.; Lohr, F.; Schwalbe, H.; Nojiri, M.; Ubbink, M., The structure of the cytochrome p450cam-putidaredoxin complex determined by paramagnetic NMR spectroscopy and crystallography. *J Mol Biol* **2013,** *425* (22), 4353-65.
90. Unno, M.; Christian, J. F.; Sjodin, T.; Benson, D. E.; Macdonald, I. D.; Sligar, S. G.; Champion, P. M., Complex formation of cytochrome P450cam with Putidaredoxin. Evidence for protein-specific interactions involving the proximal thiolate ligand. *J Biol Chem* **2002,** *277* (4), 2547-53.
91. Pochapsky, S. S.; Pochapsky, T. C.; Wei, J. W., A model for effector activity in a highly specific biological electron transfer complex: the cytochrome P450(cam)-putidaredoxin couple. *Biochemistry* **2003,** *42* (19), 5649-56.
92. Myers, W. K.; Lee, Y. T.; Britt, R. D.; Goodin, D. B., The conformation of P450cam in complex with putidaredoxin is dependent on oxidation state. *J Am Chem Soc* **2013,** *135* (32), 11732-5.
93. Sevrioukova, I. F.; Li, H.; Poulos, T. L., Crystal structure of putidaredoxin reductase from Pseudomonas putida, the final structural component of the cytochrome P450cam monooxygenase. *J Mol Biol* **2004,** *336* (4), 889-902.

94. Kuznetsov, V. Y.; Blair, E.; Farmer, P. J.; Poulos, T. L.; Pifferitti, A.; Sevrioukova, I. F., The putidaredoxin reductase-putidaredoxin electron transfer complex: theoretical and experimental studies. *J Biol Chem* **2005,** *280* (16), 16135-42.

Chapter 2

Substrate Dependent Allosteric Regulation in Cytochrome P450cam (CYP101A1)

Introduction

Cytochrome P450cam (CYP101A1) was first indirectly mentioned by Gunsalas in a communication regarding the microbial degradation of d-camphor in 1959.[1] In this communication, a sewage bacterium, *Pseudomonas putida*, was demonstrated to utilize D-camphor as its sole carbon source via enzymatic hydroxylation of camphor to 5-*exo*-hydroxycamphor. Over the next decade, it would become increasingly clear that this "methylene hydroxylase" was of the same nature as the cytochrome (pigment-450) found in liver extracts that, just 5 years prior, were shown to be responsible for drug metabolism and steroidogenesis. From here, the realization of a highly expressible soluble P450 system that could be "easily" purified in high quantities led to a revolution in our understanding of this important enzyme and by extension, human metabolism. Over the next several decades, many groups worked to elucidate the mechanism of cytochrome P450cam. In particular, Gunsalas' lab was at the forefront of its spectroscopic characterization and efforts were underway to explore all of the capturable states along the reaction pathway in addition to much theoretical work devoted to understanding P450s ability to activate O_2 and C–H bonds.[2-15] These early spectroscopic studies revealed the nature of critical states of the catalytic cycle that guides our thinking of P450s today.

During the early investigation of P450cam, several interesting standards of practice were developed for working with the enzyme system. One of critical importance was the use of excess camphor. Camphor is a small bicyclic monoterpene that has limited solubility in water. Since the

P450cam system is expressed under the control of a camphor-inducible polycistronic operon, the original expression and purification of P450cam components were performed from the native organism in the presence of saturating (excess) camphor.[1, 16-18] To this day, however, it is not agreed upon what the saturating level of camphor is in solution. Even the seemingly most accurate figures disagree with one another; one comes from the Handbook of Aqueous Solubility Data, which cites 1600 mg/L at 25 ˚ C (10.5 mM)[19], another from the International Labor Organization's International Chemical Safety Cards (ILO-ICSC) published values of 0.12 g in 100 mL at 25 ˚ C (7.9 mM)[20] and the Merck index as 1 g in 800 mL at 25 ˚ C (8.2 mM)[21]. This discrepancy has propagated throughout the literature with reported experimental values ranging from 5 mM to 13 mM[17-18, 22] and while this noticeably problematic concentration value is an issue on its own, an increasing level of complexity arises when considering that most of the experiments are performed in buffer and salt at various temperatures potentially broadening an already ambiguous solubility limit.

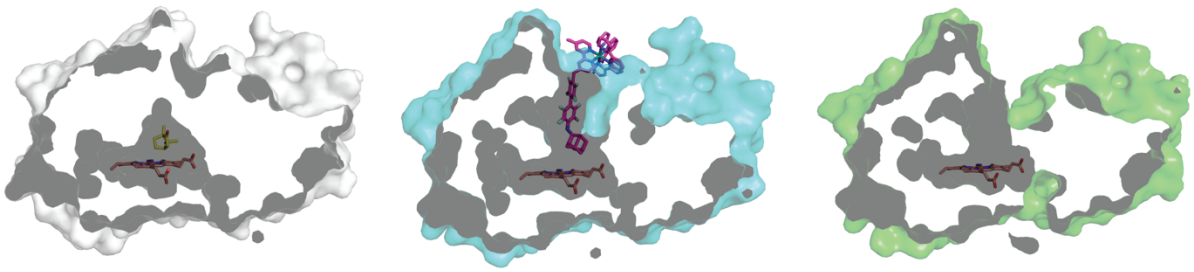

Figure 2-11. Closed camphor bound (left), open with ruthenium linked substrate mimic (magenta) (center), open substrate free (right) structures of P450cam. (PDB: 2CPP, 5IKO, 3L62)

However, this role of substrate concentration, while sitting in the back of my mind, was not the direct reason for the following investigation. It was actually a back of the envelope calculation that really bothered me and gave rise to the following study. Given the *in vitro* rates of NADH consumption and the fact that if *P. putida* survives on camphor, then the use of NADH to produce ATP changes 2-fold, since the ratio 1:1 camphor to acetyl-CoA vs 2:1 glucose to acetyl-CoA (full calculation in Appendix A), it was not possible to reconcile that a cell of *P. putida* could survive on these rates, pointing to flaws in our understanding of the enzymatic system. It also points to an existent hypothesis that P450cam's highly regulated mechanism prevents wasting of valuable reducing equivalents (i.e. uncoupling).[23] If efficiency and effective use of energy is the name of the game, then problems arise when considering the dogma surrounding P450cam's structure-function relationship.

Prior to the determination of the structure in 1985, several solution studies examined substrate binding in P450cam by electronic absorption, magnetic circular dichroism, and EPR spectroscopies.[3, 8, 11-12, 14-15, 24-28] Some of these initial investigations examined the effect of concentration on the spin-state of the enzyme, trying to correlate heme spin state signatures to the binding of camphor. As early as 1975, it was observed that at low-concentrations of camphor, P450cam to substrate stoichiometry remains 1:1, and the high-spin fraction of the enzyme increases with increasing concentration of camphor.[29-30] Yet, at sufficiently high concentrations of camphor, the P450 shifts back to a low-spin state. As pointed out by Lipscomb, the low-spin state (S=1/2) observed in the presence of high-concentrations of camphor (g=1.97) does not yield the same g-values as in its absence (g=1.91), indicating that this low-spin species is distinct from

the resting state. This new feature was not fully characterized, but was attributed to the possibility of a second molecule of camphor binding to P450cam. These results were later corroborated by EPR binding studies by Lange[24, 28-29], as well as Hui bon Hoa[31-33], who demonstrated by high-pressure UV-vis spectroscopy that at high concentrations of camphor there was a shift back to a low-spin species, suggesting a second-binding site.

However, in 1985, the structure of P450cam bound to its substrate revealed a 1:1 stoichiometry between protein and substrate.[34] This crystal structure is debatably, other than the discovery of the enzyme itself, the most important contribution to the P450 field to date as this provided the P450 community with deep insight into the spectroscopic and turnover experiments, revealing atomic details of stereo and regioselective hydroxylation, simultaneously putting an end to the suggestion of a second binding site. However, while camphor was bound to the active site, this structure presented no obvious channel for active site access (Figure 2-1).

For several years that followed this structure determination, computational chemists would be confined to a single set of atomic coordinates to calculate potential pathways of entry and exit. This was somewhat expanded with the determination of P450BM3[35], P450terp[36-37], and P450eryF[38] in the mid to late 90's and led to some ingenious strategies of finding low energy pathways for entry and escape including Random Expulsion Molecular Dynamics (REMD), steered molecular dynamics and metadynamics.[39-42] All these approaches correctly predicted the result of the 2002 crystallographic study where ruthenium tethered substrates revealed the classic entry channel, channel 1.[43] In 2010, a structure of P450cam in the camphor-less "open" state as

well as several other P450 structures supported a common mechanism of substrate binding as they possess a highly conserved fold.[44]

This idea, while elegant, presents an apparent conundrum. Why and how would nature evolve an enzyme that can act as the first step in a mechanism of metabolism to possess a single channel where active site seeking substrate competes against an escaping molecule of hydroxylated product? This idea seemingly violates one of nature's design principles of efficiency and clearly required further investigation.

As an aside, in computational chemistry, we are finally reaching the point where atomistic simulations of incredible complexity can be carried out to time scales that are on par with many

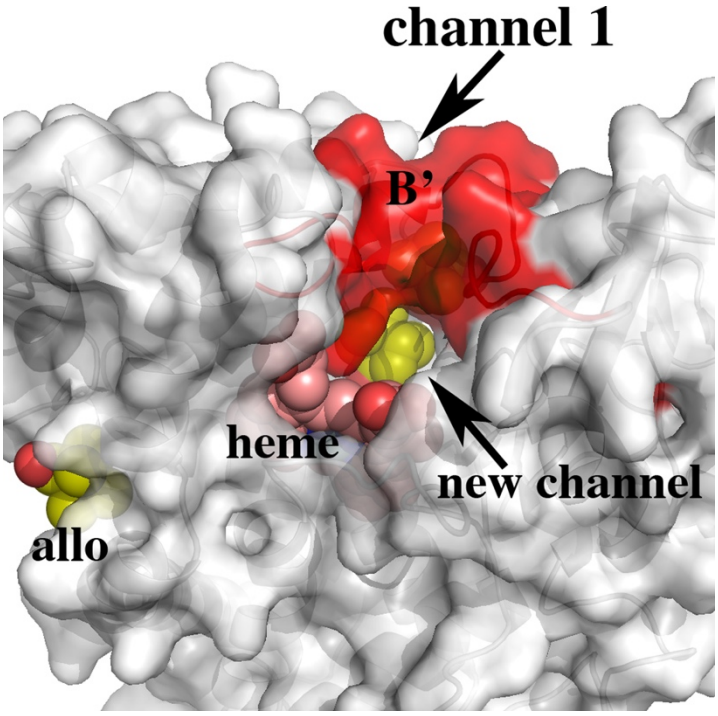

Figure 2-12. Location of the proposed allosteric (labeled **allo**) camphor binding site. Camphor (yellow) is tucked into a hydrophobic pocket between the C and E helices.

of the biological phenomena that we, as biochemists, are interested in. I believe that that this has fundamentally reshaped our thinking of the cellular milieu and biology, as these models are able to bring many critical structures and experimental snapshots "to life". Substrate binding in P450cam, in particular, is reported to occur on the microsecond timescale is now achievable by standard molecular dynamics techniques.

In the following chapter, microsecond timescale unbiassed molecular dynamics simulations are utilized to integrate and begin to answer two outstanding questions in the field of P450cam. 1) Is there second binding site, and if so, where and what is its relevance to catalysis? 2) How does substrate bind to and egress from the active site of P450cam?

Results and Discussion

Identification of an Allosteric Camphor Site

The initial goal of this study was to see if camphor placed in the solvent cushion surrounding the protein would diffuse through channel 1, between the F/G loop and B'-helix, and bind near the heme. To simulate camphor in solution binding to substrate-free P450cam, substrate was placed in the outer solvent cushion. At first, this was done with just one molecule of camphor. Previous studies by our lab utilized principle component analysis (PCA) as a tool to understand the open and closed state conformational dynamics.[45] PCA allows us to reduce a highly dimensional dynamic space with many degrees of freedom down to a finite number of correlated vectors. For molecular dynamics simulations of P450cam, the first two vectors, PC1 and PC2, represent the two dominate correlated motions of the protein and mapped on this new space. The vector that we chose to project on is the average Cα coordinates between the open and closed crystal

structures. This approach is useful for looking at the population of conformational states of P450cam in open and closed during an MD simulation. As can be seen in Figure 2-4, simulations of the open conformation are highly diffuse while the closed conformation is much less diffuse indicating that upon the binding of substrate, the protein tightens down on the camphor molecule. Previously, our lab looked at the effect of the presence of redox partner on the conformational state of P450cam and found that MD simulations of the complex equilibrate between open and closed, or in a "semi-open" state.[45]

Using PCA as a guide, simulations containing one molecule of camphor exhibited a predominately open conformation, starting and ending in the open form. Upon visual inspection, substrate never enters the active site. Increasing to three molecules of substrate, however, a

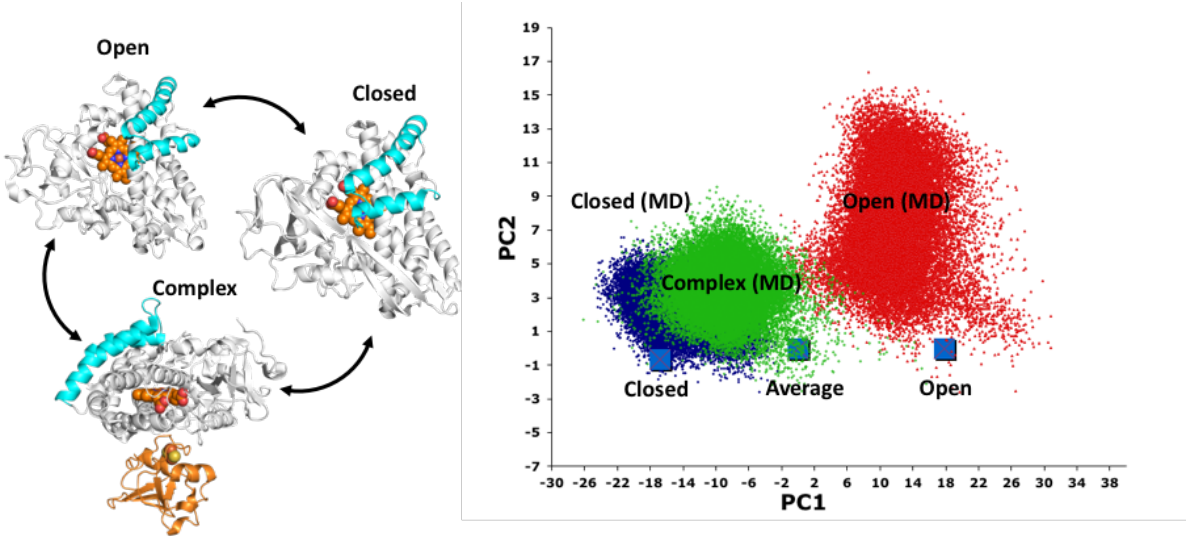

Figure 2-13. Principle component analysis (PCA) of molecular dynamics simulations of the open (red), closed (blue), and Pdx-bound (green) structures for 500 ns each. Crystal structures are plotted as boxes. PCA adapted from Batabyal *et al.*

striking change to the population occurs, where we start in the open, end in the closed, and appear similar to previous simulations of the P450cam-Pdx complex.

In this case, three camphor molecules were placed in the solvent cushion giving an effective three-fold excess, an experimentally relevant condition and within the limit of solubility of camphor in water given the size of the solvent box. In all of these simulations, a molecule of camphor binds to a pocket on the "back side" of the F/G helices in between the C/D/E/F helices (Fig 2-5). This site is defined by V118, V123, K126, L127, L166, and T217 (Figure 2-5) and is the same region that NMR studies found to be perturbed in the presence of high camphor concentrations.[46-47]

These NMR results can be interpreted as either camphor binding to the active site resulting in long-range perturbations at the L166 site or direct binding of camphor to the L166 region. Our MD simulations indicate that perturbation of L166 could be due to direct interactions between camphor and L166.

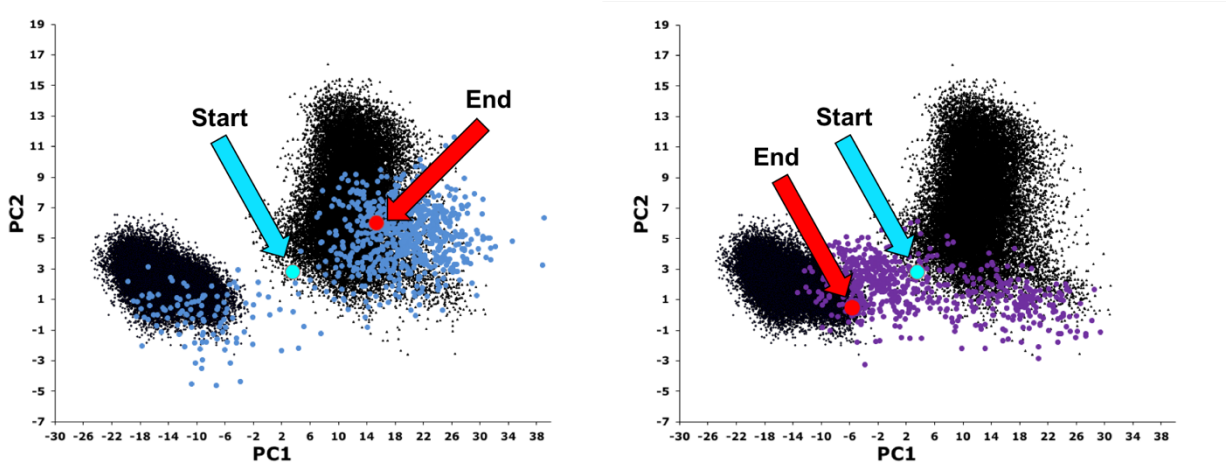

Figure 2-14. PCA of simulations with 1 **(left)** and 3 **(right)** molecules of camphor. Starting coordinates in cyan and final coordinates in red overlaid on open and closed simulations (black).

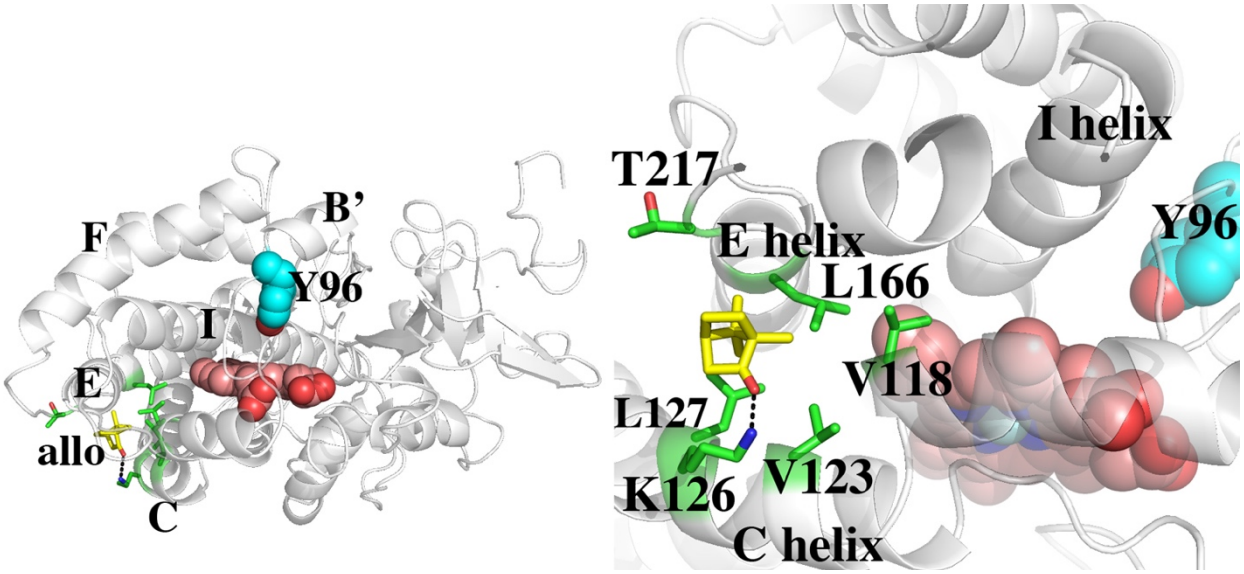

Figure 2-15 The structure of P450cam at 378 ns. Binding of camphor (yellow) to the allosteric site results in the opening of a new active site access channel.

Binding to this allosteric site is accompanied by widening of channel 1 as well as formation of a new active site access channel 2 (Fig 2-1). This second channel was formerly identified as a possible egress channel using modified molecular dynamics techniques such as random expulsion MD (REMD) and metadynamics.[42, 48] Cojocaru *et al.*[42] also suggested the formation of this new channel, but neither the REMD nor metadynamics studies postulated allostery or explored the correlation of channel formation with a second camphor site. We found that a good measure of channel 2 formation is the distance between the Cα atoms of S83 and S102, which is ~5 Å in the closed structures and ~7-13Å when channel 2 is open. Experimentally, S83 was identified by Asciutto *et al.*[49] as a hinge region that undergoes sizable chemical shifts in the absence of camphor. Using the S83-S102 distance as a criterion for channel 2 formation, we determined a strong correlation between occupancy of the allosteric site and formation of this new channel

(Fig. 2-6A). When there is no substrate present in our simulations the S83-S102 distance fluctuates between 5-7 Å (Fig 2-6B). Upon addition of a single camphor in the crystallographic pose, channel 2 remains shut at 5 Å. Binding of camphor to the allosteric site shifts the S83-S102 distance to ~7 Å. In simulations where both binding and egress events occur the second channel opens to nearly 12 Å and the open state is strongly preferred.

If binding to the allosteric site results in formation of a more open active site and binding to that site is much weaker than to the active site, then binding ought to favor low-spin P450cam at high concentrations of camphor. Indeed, multiple studies have found that at concentrations of camphor well beyond that required for saturating the active site, P450cam shifts back toward low-spin.[29, 50-52] This shift was attributed to the binding of a second camphor molecule and is consistent with our results where camphor binding to the L166 allosteric site opens the active site thereby shifting P450cam toward low-spin. At the time of these equilibrium binding studies, the location and relevance of this site was not known. Our simulations also are consistent with the NMR work of Yao *et al.*[53] In this study, a second camphor site with a K_D≈43 µM was located 15-16 Å from the heme iron by paramagnetic T1 relaxation. Uniform labeling with ^{13}C Thr showed that a Thr residue is perturbed at high camphor concentrations but peak overlap prevented determination of its exact location.[53] The allosteric site in our simulations fit these data well as it is ~15 Å from the heme iron and T217 is in the allosteric pocket. Finally, Colthart et al. found that the L166A mutant in the presence of excess camphor favors high-spin P450cam even though enzyme activity was decreased.[46] Camphor binding to the L166 allosteric site should be weakened in the L166A mutant and, as a result, excess camphor will no longer favor low-spin

P450cam. Our MD simulations and allosteric site hypothesis are consistent with NMR[46, 53] and equilibrium binding data[29, 33, 50].

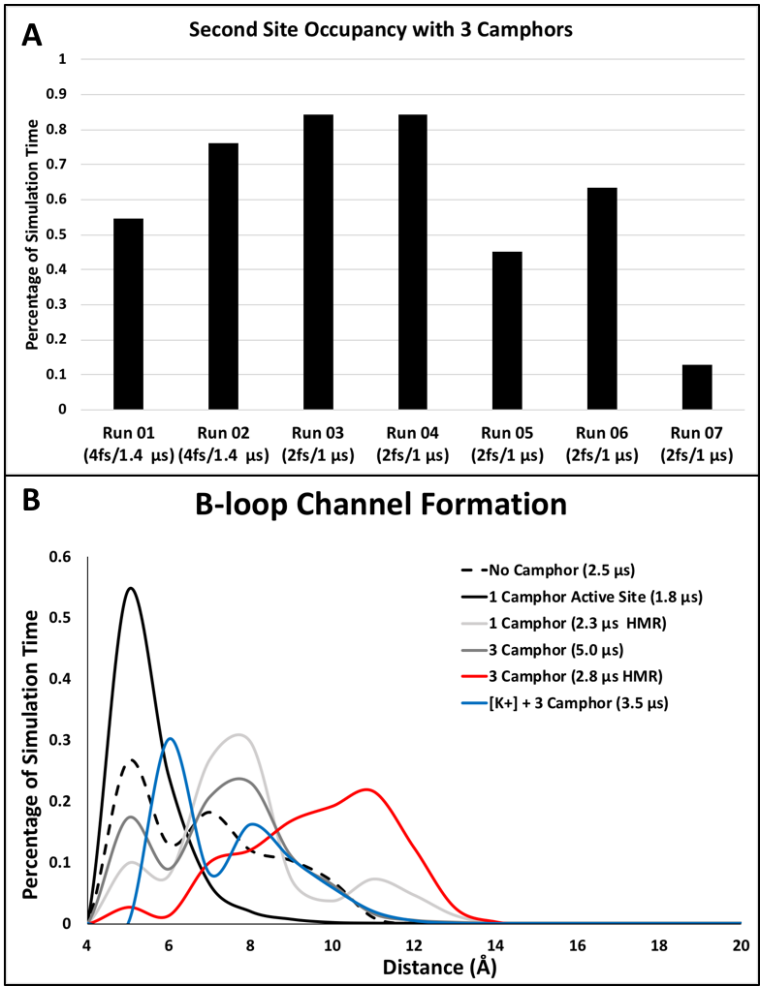

Figure 2-16. (**A**) Camphor population in the allosteric binding pocket as percentage of simulation time. Run 01 and Run 02 were performed with 4 fs time steps and HMR for 1.4 µs each. Run 03-07 were 1 µs each and utilized 2 fs timesteps and no HMR. (**B**) B loop residues S83 to S102 Cα distance as a percentage of total aggregate time in simulations containing no camphor (black dashed), 1 camphor in its crystallographic pose (black solid), 1 molecule using HMR (solid dark grey), 3 camphor molecules with 2 fs steps (solid light grey), 4fs steps and HMR (solid red), and with 3 camphor molecules and potassium counter ions.

Crystallographic Support for the Allosteric Binding Site

Direct observation of camphor binding to our proposed allosteric site would require trapping P450cam in a thermodynamic local minimum of the substrate free open form and then introducing substrate. This is precisely what Lee *et al.*[54] accomplished in solving the crystal structure of substrate-free P450cam in the open state (3L62). In this structure, the B' helix (residues 90-101) is not visible in the electron density due to disorder, which opens channel 2 in a similar way to what we observe in the MD simulations. In a separate study, Liou et al.[55] soaked these same substrate-free P450cam crystals in excess camphor and found that camphor binds in the active site but in multiple conformations (5IK1). If our allosteric model is correct, then we would expect to observe camphor binding to our proposed allosteric site in the 5IK1 structure.

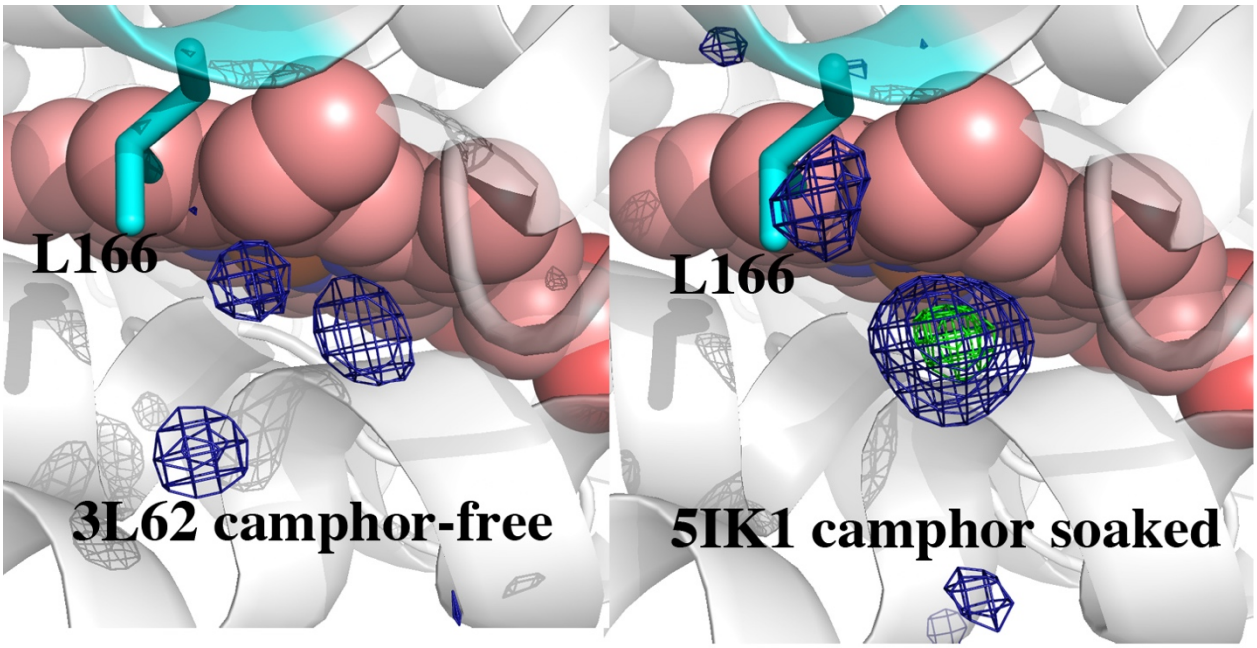

Figure 2-17. F_o-F_c electron density maps contoured at 4.0 σ (blue) and 7.0 σ (green). In the substrate-free 3L62 structure the lobes of electron density are consistent with water molecules as originally modeled. However, in the 5IK1 structure the much larger electron density is not consistent with ordered water but with a much larger molecule(s).

We therefore reexamined the electron density maps for both structures (Fig. 2-7). In the camphor-soaked structure, there is a peak of electron density at 7σ near our proposed allosteric site which is not seen in the camphor-free structure. Since the only difference in the two experiments is soaking with camphor in 5IK1, the larger lobe of electron density near L166 is consistent with an orientationally disordered camphor as predicted by our MD simulations.

Additional crystallographic support for this binding site comes from a P450cam homolog, CYP101D1. CYP101D1, from *Novosphingobium aromaticivorans,* is not the sole P450 for its host organism and possesses 44% sequence identity and a 1.2 Å Cα RMSD to P450cam, however, its camphor-binding and catalytic properties are remarkably close to those of P450cam.[56-57] Of particular interest for this study, is the conservation of the allosteric site, which retains four of

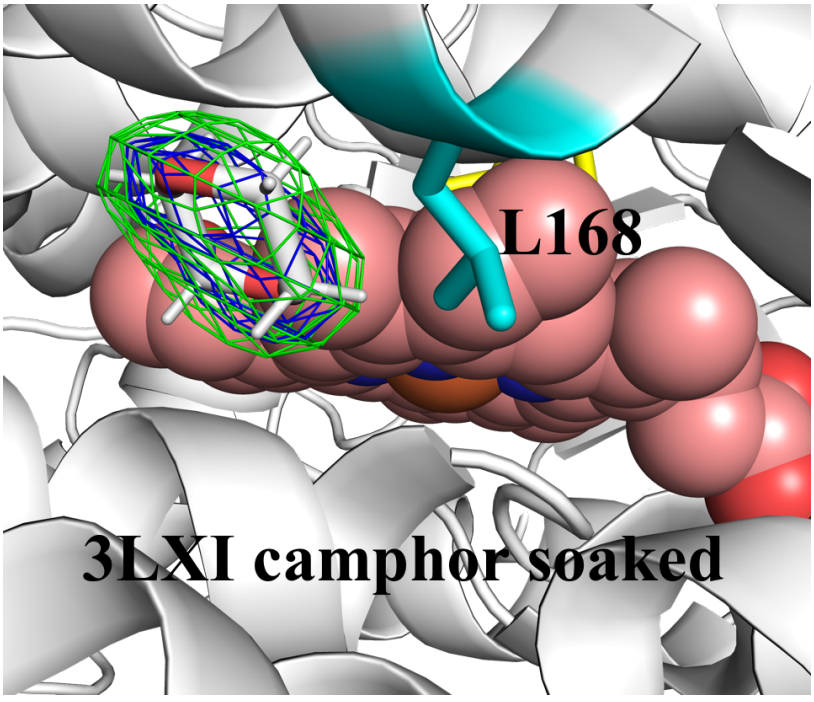

Figure 2-18. CYP101D1 soaked with camphor in the presence of 1,4-dioxane. A polder map (green) contoured at 5 σ and 2Fo-Fc electron density map contoured at 2 σ (blue) with analogous Leucine-168 (cyan).

the six residues identified in our initial MD simulations: K128, L129, L168, T225. The crystallization and structure determination of CYP101D1 was performed both in the absence and presence of camphor.[57] However, within their crystallization solution is 12% 1,4-dioxane, which, in the absence of camphor, binds to the active site. Upon soaking camphor into their crystals, substrate binds to the active site, but additionally, a large peak of density appears around L168, the analogous allosteric region. After further investigation and re-refinement of the deposited structure factors, it is clear that this density should be attributed to a molecule of 1,4-dioxane in both subunits. However, the obvious question becomes, why, when camphor is not present, is dioxane in the active site, but not the allosteric site? And, why, upon camphor soaking does camphor bind to the active site and dioxane bind to the allosteric site given the structures are prepared in the same conditions with the exception of soaking?

An Allosteric Model

The rather dramatic effects of camphor binding to the allosteric site on access channel formation offers a dynamic picture relevant to catalysis and cooperativity. This also provides evidence for the growing realization of how weak transient allosteric interactions can serve to prime and direct enzymatic catalysis.[58-59] A series of snapshots derived from one of the HMR simulations is shown in Fig 2-9. After ~60 ns, one camphor molecule binds to the allosteric site, pulling back on the F/G lid thus widening channel 1 allowing a molecule of camphor to enter the active site. Substrate binding to the allosteric site also pulls on the B' to C-helix loop through mechanical coupling creating a second channel to the active site (Fig. 2-9, channel 2). This is seen in every simulation we performed. This long-range coupling from the allosteric site to the

substrate access channel (about 10 Å) allows for a second molecule of camphor to enter the active site. Once the camphor enters the active site via channel 1 in the 250 ns time range, the F/G helices tighten down on the substrate, which weakens binding to the allosteric site so camphor dissociates from the allosteric site. At 312 ns, the substrate molecule is ejected through channel 2 and Y96 flips out toward solvent. The ability for Y96 to adopt both the "in" and "out"

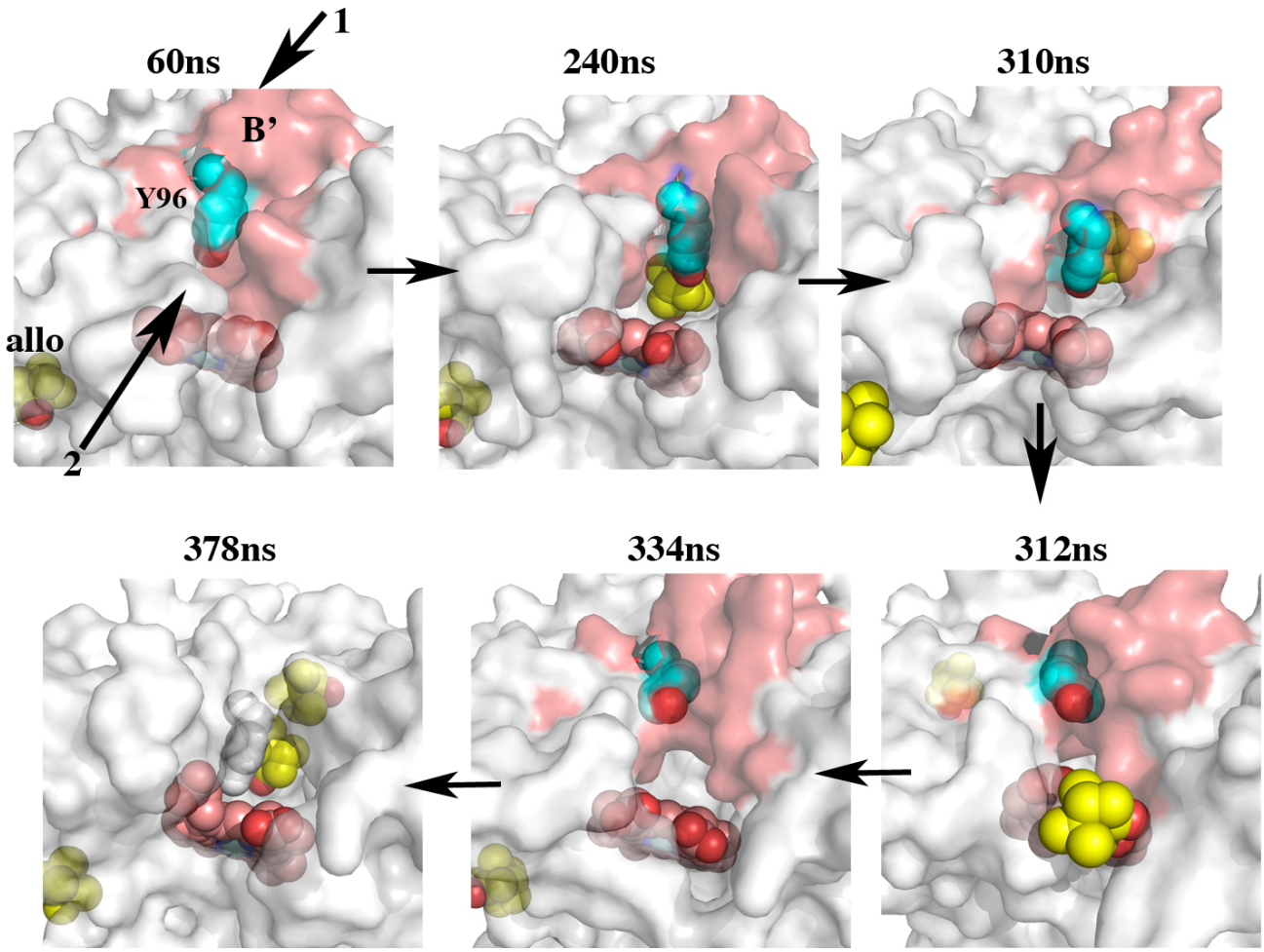

Figure 2-19. The two relevant channels are indicated by 1 and 2. **60 ns-** A camphor molecule (yellow) binds to the allosteric site (allo) priming channel 2 to open. **240 ns-** Binding of a second molecule to the active site widens channel 2. Between 240 and 310 ns, one molecule dissociates from the allosteric site. **310 to 312 ns**- The active site molecule is swept from the active site via Tyr96 (cyan) through the B' region. **334 ns-** A new molecule binds to the allosteric site. **378 ns**- Y96 flips back to the active site upon binding two molecules substrate, restarting the cycle.

orientations is consistent with crystal structures of P450cam in the open state. This also offers an explanation for the potassium specific effects seen in P450cam and why increasing [K^+] slows turnover rates.[60] Potassium is known to increase the high-spin fraction of P450cam.[28-29, 61-62] The K^+ binding site is in the B' loop near Y96 thus stabilizing the B' region in the closed conformation.[62] As a result, binding to the allosteric site is weakened and without the ability to form channel 2 to allow rapid substrate/product binding/egress, activity decreases. We tested this hypothesis by replacing the sodium counter ions that neutralize the charge of our simulations with potassium. As seen in Fig 2-6, the replacement of sodium with potassium shifts the channel to a more closed

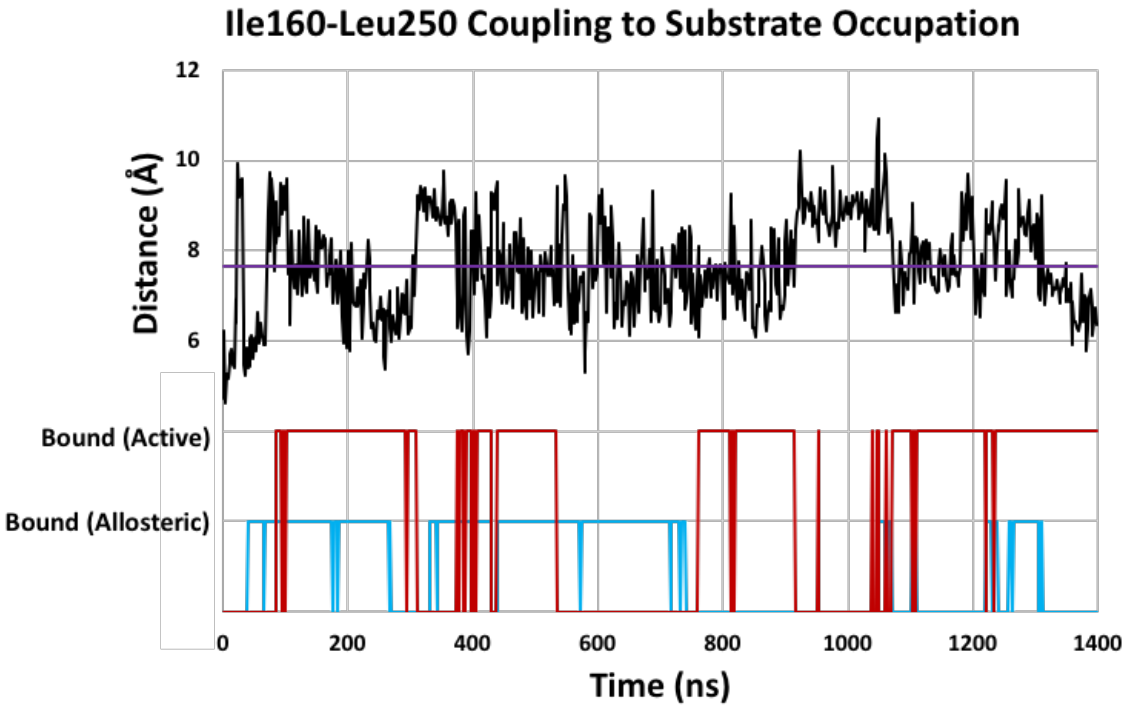

Figure 2-20 Mechanical coupling of the residues I150 and L252 to occupancies of the active and allosteric site. Changes in distances of the sidechains (center of mass) (black) is affected by changes in occupancy of the active site (red) and allosteric site (cyan). There is an average distance of 7.67 Å (purple). Active site occupancy was calculated as ≥10 Å from sidechain O of Thr252. Allosteric site occupancy was calculated as >=8.5 Å from L166 Cγ.

state. However, while the results support experimental conclusions, we have not been able to determine whether the mechanisms of closed state stabilization are the same in our simulations.

Binding to the allosteric site favors the more open form which enables a second camphor molecule to enter the active site and the formation of channel 2 that provides a pathway for rapid substrate binding and product egress. Y96 operates as a swinging arm to "grab" entering substrates when Y96 is in the "up" orientation and then the "in" orientation helps to hold camphor in position for stereo- and regio-selective hydroxylation. Product then can depart via channels 1 or 2, but our data suggests that the channel is unidirectional: entry via channel 1, egress via channel 2. Since active site binding favors the closed form there is a dynamic interplay between the closed/open transition and active site/allosteric site binding.

We observe additional changes that are consistent with NMR studies as detailed by Colthart et al.[46] Using a combination of mutagenesis and chemical shifts, it was demonstrated that I160 in the E helix and L250 in the I helix are mechanically coupled. These two residues directly contact one another in the closed state with a distance between Cα atoms ~5.3 Å. In our HMR simulations where egress is observed, the side chains of Ile160 and L250 have a correlation coefficient of 0.910 over 1.4 μs (1), where C is the average correlation, V is a motion vector per frame and N is the total number of frames.

$$C(a,b) = \frac{\sum Va \cdot Vb}{N}$$

Eq. 2-1. Correlation Coefficient

With an average distance of 7.67 ± 1.05 Å, the fluctuations in distance between the two side chains are driven by events of binding and dissociation at the allosteric and active site (Figure 2-10). However, camphor binding to the allosteric site and opening of channel 2 forces these two residues to break all non-bonded interactions with the distance between Cα atoms now 8.2 Å. In our simulations, just as Colthart et al.[46] described, it is this coupling that allows the I helix to undergo a deformation upon substrate binding and straightening upon camphor ejection/removal from the active site.

Allostery and Redox Partner Binding

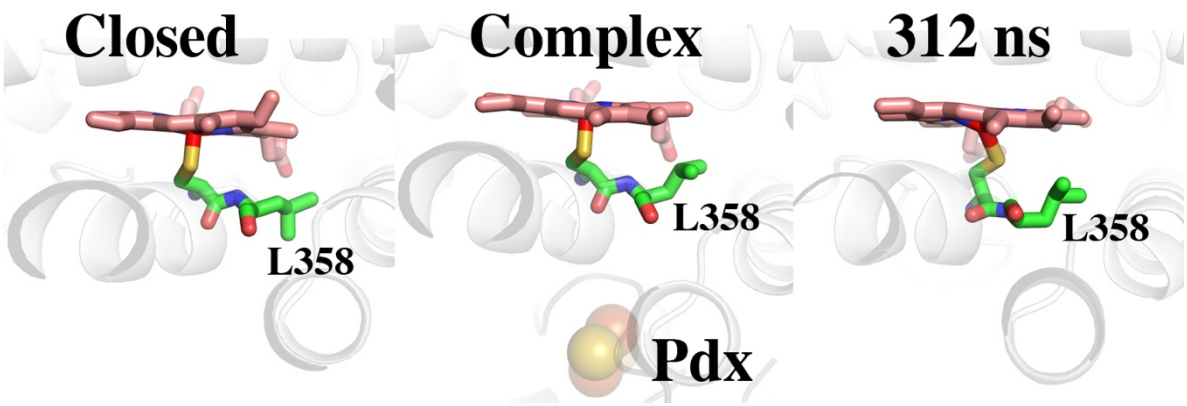

Figure 2-21. L358 adopts a different rotamer in the closed and open states. In the open conformer when Pdx is bound or when the allosteric site is occupied, L358 rotates up to contact the heme.

The cooperative interaction between the allosteric site and active site also has relevance to the binding of Pdx. Since both Pdx binding and allosteric site binding promote the open form, then Pdx and allosteric site binding work synergistically and promote each other's binding. In addition, both Pdx binding and allosteric site binding promote the same structural changes at the Pdx docking site. L358 is positioned at the Pdx binding docking site and must adopt an alternate

rotamer conformation when Pdx binds (Fig. 2-11). As shown in Fig. 2-11, the L358 N-Cα-Cβ-Cγ dihedral is ≈-70˚ in the closed (2CPP) and substrate-free open (3L62) structures.[34, 54] However, in the P450cam-Pdx complexes (4JXI, 4JWU, 3W9C) the L358 dihedral ranges between 55-65˚.[23, 63] This change is necessary to enable Pdx to form a tighter interface with P450cam. Our simulations show that when the allosteric site is occupied with camphor the L358 rotamer becomes more flexible and when substrate is driven through channel 2 the rotamer is the same as in the P450cam-Pdx complex where P450cam is open. Therefore, the allosteric site is not only coupled to the active site, but also the Pdx docking site. When L358 is in the Pdx-bound conformation the Leu side chain is closer to the heme and thus "pushes" on the proximal face of the heme. There is good evidence that this "push" effect is coupled to changes on the opposite side of the heme that favors the open form of P450cam. When O_2 binds to ferrous P450cam the I helix undergoes a significant widening that enables waters essential to catalysis to move into place as part of proton relay network required for O_2 activation. The direction of I helix motion is from closed to partially open. CO, often used as an O_2 mimic, causes none of these changes in wild type P450cam but the CO-L358P mutant more closely mimics those changes induced by O_2 binding.[64-65] This indicates that the L358P mutant can more easily adopt the open conformation.[64-66] The structural basis for these effects is that the more rigid sterically restricted P358 side chain "pushes" on the proximal face of the heme and these changes are transmitted to distal side and I helix. Thus, the L358P mimics the close to open switch accompanying Pdx binding and camphor binding to the allosteric site. These results suggest how two unique interfaces can be presented for electron transfer upon binding of Pdx with and without substrate in the allosteric site. Binding at the

allosteric site which favors open P450cam also favors Pdx binding. As suggested by Tripathi *et al.*[23] the closed state is inactive because the proton relay network involving the essential Asp251 is locked down by tight salt bridges. However, in the open state these salt bridges are broken thus enabling Asp251 to serve its function in proton transfer to the iron linked dioxygen.

We close our discussion with the potential biological implications of these results. While seemingly quite complex, the logic of these transitions in the requirements for balancing rapid turnover with association/dissociation processes and the utilization of camphor as a carbon source is rather simple. The expression of P450cam, PdR, and Pdx is under the control of the CamR repressor although the P450cam proteins are constitutively expressed at low levels in the absence of camphor.[67] Therefore, at low camphor concentrations, the active site, but not the allosteric site, is occupied and the enzyme is in the closed inactive conformation. At higher camphor concentrations, where camphor now can be used as a carbon source, the allosteric site comes into play and together with Pdx binding switches P450cam to the more open active conformation. This view is consistent with what is known about how the CamR repressor that controls the expression of P450cam, Pdx, and Pdr is controlled. CamR is released from the CamR regulatory DNA sequence only at high camphor concentrations.[68] Like many dimeric bacterial repressors, CamR binds two ligand (in this case, camphor) molecules. The first exhibits a $K_D \approx 0.06$ μM, but CamR remains bound to the CamR regulatory DNA sequence. Binding of the second camphor molecule with a $K_D \approx 14$ μM results in the release of CamR and expression of the P450cam gene products. This means P450cam and its redox supporting proteins are highly expressed only at high levels of camphor, >10 μM, which is well above the K_D for camphor binding to the

P450cam active site. Therefore, the entire CamR system including the low amounts of constitutively expressed P450cam are shutdown at low levels of camphor where camphor cannot serve as a useful carbon source thus avoiding the unnecessary consumption of NADH.

Conclusions

The results of our MD simulations provide a detailed structural model on the allosteric interplay between substrate binding, redox partner interactions, and O_2 activation that are consistent with a wealth of experimental data. Most importantly, the novel allosteric binding site identified in this study is consistent with NMR and crystallographic data[46, 55, 69] as well as equilibrium binding data of Lange et al.[29] Changes in specific residues observed in our simulations are consistent with mutagenesis data as well as differences observed in the crystal structures of the open and closed states. From these simulations, it is clear how allosteric regulation in P450cam may affect the formation of a second channel for product egress, the role of Tyr96 and potassium specific effects seen in solution, as well as the distortion of the I helix and long-range mechanical couplings. Such strong correlation with experiments provides a high level of confidence that the allosteric site identified in our simulations and the changes associated with substrate entry and egress provides a realistic structural model of allostery in P450cam. One possible advantage for such a level of allosteric control is to ensure that neither substrate binding/product egress are limiting under steady-state conditions. Therefore, at high levels of camphor, the kinetic processes of substrate binding and allostery are masked and, as observed experimentally, the first electron transfer step becomes limiting.[70]

Experimental Section

Computational Methods

Molecular dynamics (MD) simulations were performed as previously described.[45, 71] In brief, one structure was used for the simulations, the P450cam open structure in 4JX1 where Pdx was removed. The P450cam in this structure is basically the same as the open P450cam crystal structure solved without Pdx (3L62).[54] The rms deviation of Cα atoms between the two structures is 0.37 Å. We chose 4JX1 because in this structure the entire protein is clearly defined in electron density maps while in 3L62 residues 91-94 are not visible. Therefore, using 4JX1 required no modeling to obtain a complete structure for MD simulations. The protein was solvated in a rectangular box of TIP3 waters with a 10 Å cushion and Na^+ ions were added in order to maintain net neutrality. Asp297, which is buried in the active site and forms a H-bond with a heme propionate, was protonated. Camphor was placed manually on the distal side of the protein for simulations including external camphor. One molecule was introduced near the known entry channel and the second and third at a distance ~10 Å from the protein, near the cutoff distance for long-range interactions in our simulations. Structures were minimized for 1000 cycles, allowing only H atoms and solvent molecules to move followed by an additional 1000 cycles where all atoms were allowed to move. Production runs were then carried out using Amber 14 or Amber 16.[72] In order to sample functionally important time scales, we first utilized a technique known as hydrogen mass repartitioning (HMR).[73] In brief, the size of simulation time steps is dictated by the fastest vibrations that occur in the system, which are H atom vibrations. By repartitioning masses of heavy atoms to their adjacent hydrogen atoms, one can effectively slow

down the vibrations of these bonds while preserving the overall mass of the system thereby not increasing viscosity. This allows larger time steps to be taken in order to capture large conformational motions that take place over longer intervals effectively cutting the computational time in half. We later found that motions relevant to allosteric interactions and camphor binding did not require the time scales necessitating HMR. For HMR runs, topology files were modified by the *parmed.py* python script and both protein and water masses were repartitioned using the command *HMassrepartition dowater*.[73] HMR runs were performed using 4 fs timesteps and non-HMR runs were performed using traditional 2 fs steps suggested by the SHAKE algorithm. All simulations were performed using a random initial velocity with each run having a different initial velocity (ig=-1). Two runs were carried out using HMR and 4 fs timesteps for ~1.4 μs each with 3 molecules of camphor. Three runs with HMR and 4 fs timesteps were performed with 1 molecule of camphor for 1.6 μs, 350 nanoseconds and 310 nanoseconds. Five additional runs using 2 fs timesteps and no repartitioning were performed for 1 μs. Five runs were performed for 500 ns with no camphor in the simulation. Five runs were carried out with potassium for a total runtime of 3.5 μs. Data analysis was carried out in cpptraj and VMD.[74-75] Trajectory images were produced in Pymol (Schrodinger).

References

1. Bradshaw, W. H.; Conrad, H. E.; Corey, E. J.; Gunsalus, I. C.; Lednicer, D., Microbiological Degradation of (+)-Camphor. *Journal of the American Chemical Society* **1959,** *81* (20), 5507-5507.
2. Katagiri, M.; Ganguli, B. N.; Gunsalus, I. C., A soluble cytochrome P-450 functional in methylene hydroxylation. *J Biol Chem* **1968,** *243* (12), 3543-6.

3. Gunsalus, I. C.; Ganguli, B. N.; Katagiri, M.; Tsibris, J. C.; Debrunner, P.; Frauenfelder, H., Oxygenation: a specific soluble cytochrome p-450 coupled enzyme complex. *Science* **1968,** *160* (3826), 438-9.
4. Tyson, C. A.; Lipscomb, J. D.; Gunsalus, I. C., The role of putidaredoxin and P450 cam in methylene hydroxylation. *J Biol Chem* **1972,** *247* (18), 5777-84.
5. Gunsalus, I. C.; Lipscomb, J. D.; Marshall, V.; Frauenfelder, H.; Greenbaum, E.; Munck, E., Structure and reactions of oxygenase active centers: cytochrome P-450 and iron sulfur proteins. *Biochem Soc Symp* **1972,** *34*, 135-57.
6. Gunsalus, I. C.; Lipscomb, J. D.; Meeks, J. R., Cytochrome P-450cam Substrate and Effector Interactions. *Annals of the New York Academy of Sciences* **1973,** *212* (1), 107-121.
7. Sligar, S. G.; Debrunner, P. G.; Lipscomb, J. D.; Namtvedt, M. J.; Gunsalus, I. C., A role of the putidaredoxin COOH-terminus in P-450cam (cytochrome m) hydroxylations. *Proc Natl Acad Sci U S A* **1974,** *71* (10), 3906-10.
8. Yu, C.; Gunsalus, I. C., Cytochrome P-450cam. III. Removal and replacement of ferriprotoporphyrin IX. *J Biol Chem* **1974,** *249* (1), 107-10.
9. Yu, C.; Gunsalus, I. C.; Katagiri, M.; Suhara, K.; Takemori, S., Cytochrome P-450cam. I. Crystallization and properties. *J Biol Chem* **1974,** *249* (1), 94-101.
10. Yu, C.; Gunsalus, I. C., Cytochrome P-450cam. II. Interconversion with P-420. *J Biol Chem* **1974,** *249* (1), 102-6.
11. Sharrock, M.; Debrunner, P. G.; Schulz, C.; Lipscomb, J. D.; Marshall, V.; Gunsalus, I. C., Cytochrome P450cam and its complexes, Mössbauer parameters of the heme iron. *Biochimica et Biophysica Acta (BBA) - Protein Structure* **1976,** *420* (1), 8-26.
12. Sligar, S. G.; Gunsalus, I. C., A thermodynamic model of regulation: modulation of redox equilibria in camphor monoxygenase. *Proc Natl Acad Sci U S A* **1976,** *73* (4), 1078-82.
13. Lipscomb, J. D.; Sligar, S. G.; Namtvedt, M. J.; Gunsalus, I. C., Autooxidation and hydroxylation reactions of oxygenated cytochrome P-450cam. *J Biol Chem* **1976,** *251* (4), 1116-24.
14. Gunsalus, I. C.; Sligar, S. G., Equilibrium states and dynamic reactions of iron in the camphor monoxygenase system. *Adv Exp Med Biol* **1976,** *74*, 254-62.
15. Lange, R.; Hui Bon Hoa, G.; Debey, P.; Gunsalus, I. C., A thermodynamic-kinetic analysis of the cytochrome P-450 heme pocket. *Acta Biol Med Ger* **1979,** *38* (2-3), 143-52.
16. Conrad, H. E.; Dubus, R.; Gunsalus, I. C., An enzyme system for cyclic ketone lactonization. *Biochem Biophys Res Commun* **1961,** *6*, 293-7.
17. Hedegaard, J.; Gunsalus, I. C., Mixed function oxidation. IV. An induced methylene hydroxylase in camphor oxidation. *J Biol Chem* **1965,** *240* (10), 4038-43.
18. Conrad, H. E.; Dubus, R.; Namtvedt, M. J.; Gunsalus, I. C., Mixed Function Oxidation. Ii. Separation and Properties of the Enzymes Catalyzing Camphor Lactonization. *J Biol Chem* **1965,** *240*, 495-503.
19. Yalkowsky, S. H. H. Y. J. P., *Handbook of Aqueous Solubility Data Second Edition*. 2 ed.; CRC Press: Boca Raton, Fl, 2010; p 721-721.
20. Camphor. http://www.ilo.org/dyn/icsc/showcard.display?p_version=2&p_card_id=1021.

21. O'Neil, M. J., *The Merck index: an encyclopedia of chemicals, drugs, and biologicals*. RSC Publishing: 2013.
22. Keller, R. M.; Wuthrich, K.; Debrunner, P. G., Proton magnetic resonance reveals high-spin iron (II) in ferrous cytochrome P450 cam from Pseudomonas putida. *Proc Natl Acad Sci U S A* **1972,** *69* (8), 2073-5.
23. Tripathi, S.; Li, H.; Poulos, T. L., Structural basis for effector control and redox partner recognition in cytochrome P450. *Science* **2013,** *340* (6137), 1227.
24. Lange, R.; Hui Bon Hoa, G.; Debey, P.; Gunsalus, I. C., Ionization dependence of camphor binding and spin conversion of the complex between cytochrome P-450 and camphor. Kinetic and static studies at sub-zero temperatures. *Eur J Biochem* **1977,** *77* (3), 479-85.
25. Champion, P. M.; Gunsalus, I. C., Resonance Raman spectra of cytochrome P450cam. *J Am Chem Soc* **1977,** *99* (6), 2000-2.
26. Philson, S. B.; Debrunner, P. G.; Schmidt, P. G.; Gunsalus, I. C., The effect of cytochrome P-450cam on the NMR relaxation rate of water protons. *J Biol Chem* **1979,** *254* (20), 10173-9.
27. Sligar, S. G.; Gunsalus, I. C., Proton coupling in the cytochrome P-450 spin and redox equilibria. *Biochemistry* **1979,** *18* (11), 2290-5.
28. Lange, R.; Hui Bon Hoa, G.; Debey, P.; Gunsalus, I. C., Spin transition of camphor-bound cytochrome P-450. 2. Kinetics following rapid changes of the local paH at sub-zero temperatures. *Eur J Biochem* **1979,** *94* (2), 491-6.
29. Lange, R.; Bonfils, C.; Debey, P., The low-spin/high-spin transition equilibrium of camphor-bound cytochrome P-450. Effects of medium and temperature on equilibrium data. *Eur J Biochem* **1977,** *79* (2), 623-8.
30. Lipscomb, J. D. Energy Transfer and Segregation: Mixed Function Oxidation by Cytochrome P450(cam) and Putidaredoxin. University of Illinois at Urbana-Champaign, 1975.
31. Marden, M. C.; Hui Bon Hoa, G., Dynamics of the spin transition in camphor-bound ferric cytochrome P-450 versus temperature, pressure and viscosity. *Eur J Biochem* **1982,** *129* (1), 111-7.
32. Hui Bon Hoa, G.; Marden, M. C., The pressure dependence of the spin equilibrium in camphor-bound ferric cytochrome P-450. *Eur J Biochem* **1982,** *124* (2), 311-5.
33. Hui Bon Hoa, G.; Di Primo, C.; Dondaine, I.; Sligar, S. G.; Gunsalus, I. C.; Douzou, P., Conformational changes of cytochromes P-450cam and P-450lin induced by high pressure. *Biochemistry* **1989,** *28* (2), 651-6.
34. Poulos, T. L.; Finzel, B. C.; Gunsalus, I. C.; Wagner, G. C.; Kraut, J., The 2.6-A crystal structure of Pseudomonas putida cytochrome P-450. *J Biol Chem* **1985,** *260* (30), 16122-30.
35. Ravichandran, K. G.; Boddupalli, S. S.; Hasermann, C. A.; Peterson, J. A.; Deisenhofer, J., Crystal structure of hemoprotein domain of P450BM-3, a prototype for microsomal P450's. *Science* **1993,** *261* (5122), 731-6.
36. Boddupalli, S. S.; Hasemann, C. A.; Ravichandran, K. G.; Lu, J. Y.; Goldsmith, E. J.; Deisenhofer, J.; Peterson, J. A., Crystallization and preliminary x-ray diffraction analysis of P450terp and the hemoprotein domain of P450BM-3, enzymes belonging to two distinct classes of the cytochrome P450 superfamily. *Proc Natl Acad Sci U S A* **1992,** *89* (12), 5567-71.

37. Hasemann, C. A.; Ravichandran, K. G.; Peterson, J. A.; Deisenhofer, J., Crystal structure and refinement of cytochrome P450terp at 2.3 A resolution. *J Mol Biol* **1994,** *236* (4), 1169-85.
38. Cupp-Vickery, J. R.; Poulos, T. L., Structure of cytochrome P450eryF involved in erythromycin biosynthesis. *Nat Struct Biol* **1995,** *2* (2), 144-53.
39. Helms, V.; Deprez, E.; Gill, E.; Barret, C.; Hui Bon Hoa, G.; Wade, R. C., Improved binding of cytochrome P450cam substrate analogues designed to fill extra space in the substrate binding pocket. *Biochemistry* **1996,** *35* (5), 1485-99.
40. Ludemann, S. K.; Lounnas, V.; Wade, R. C., How do substrates enter and products exit the buried active site of cytochrome P450cam? 2. Steered molecular dynamics and adiabatic mapping of substrate pathways. *J Mol Biol* **2000,** *303* (5), 813-30.
41. Wade, R. C.; Winn, P. J.; Schlichting, I.; Sudarko, A survey of active site access channels in cytochromes P450. *J Inorg Biochem* **2004,** *98* (7), 1175-82.
42. Cojocaru, V.; Winn, P. J.; Wade, R. C., The ins and outs of cytochrome P450s. *Biochim. Biophys. Acta, Gen. Subj.* **2007,** *1770*, 390.
43. Dmochowski, I. J.; Dunn, A. R.; Wilker, J. J.; Crane, B. R.; Green, M. T.; Dawson, J. H.; Sligar, S. G.; Winkler, J. R.; Gray, H. B., Sensitizer-linked substrates and ligands: ruthenium probes of cytochrome P450 structure and mechanism. *Methods Enzymol* **2002,** *357*, 120-33.
44. Lee, Y. T.; Wilson, R. F.; Rupniewski, I.; Goodin, D. B., P450cam visits an open conformation in the absence of substrate. *Biochemistry* **2010,** *49* (16), 3412-9.
45. Batabyal, D.; Richards, L. S.; Poulos, T. L., Effect of Redox Partner Binding on Cytochrome P450 Conformational Dynamics. *J. Am. Chem. Soc.* **2017,** *139*, 13193.
46. Colthart, A. M.; Tietz, D. R.; Ni, Y.; Friedman, J. L.; Dang, M.; Pochapsky, T. C., Detection of substrate-dependent conformational changes in the P450 fold by nuclear magnetic resonance. *Sci. Rep.* **2016,** *6*, 22035.
47. Asciutto, E. K.; Pochapsky, T. C., Some Surprising Implications of NMR-directed Simulations of Substrate Recognition and Binding by Cytochrome P450cam (CYP101A1). *J. Mol. Biol.* **2018,** *430*, 1295.
48. Rydzewski, J.; Nowak, W., Thermodynamics of camphor migration in cytochrome P450cam by atomistic simulations. *Sci. Rep.* **2017,** *7*, 7736.
49. Asciutto, E. K.; Young, M. J.; Madura, J.; Pochapsky, S. S.; Pochapsky, T. C., Solution structural ensembles of substrate-free cytochrome P450(cam). *Biochemistry* **2012,** *51*, 3383.
50. Marden, M. C.; Hui Bon Hoa, G., P-450 binding to substrates camphor and linalool versus pressure. *Arch. Biochem. Biophys.* **1987,** *253*, 100.
51. Lipscomb, J. D., Electron paramagnetic resonance detectable states of cytochrome P-450cam. *Biochemistry* **1980,** *19*, 3590.
52. Narasimhulu, S.; Havran, L. M.; Axelsen, P. H.; Winkler, J. D., Interactions of substrate and product with cytochrome P450: P4502B4 versus P450cam. *Arch. Biochem. Biophys.* **1998,** *353*, 228.
53. Yao, H.; McCullough, C. R.; Costache, A. D.; Pullela, P. K.; Sem, D. S., Structural evidence for a functionally relevant second camphor binding site in P450cam: model for substrate entry into a P450 active site. *Proteins* **2007,** *69* (1), 125-38.

54. Lee, Y. T.; Wilson, R. F.; Rupniewski, I.; Goodin, D. B., P450cam visits an open conformation in the absence of substrate. *Biochemistry* **2010,** *49*, 3412.
55. Liou, S. H.; Mahomed, M.; Lee, Y. T.; Goodin, D. B., Effector Roles of Putidaredoxin on Cytochrome P450cam Conformational States. *J. Am. Chem. Soc.* **2016,** *138* (32), 10163.
56. Bell, S. G.; Wong, L. L., P450 enzymes from the bacterium Novosphingobium aromaticivorans. *Biochem Biophys Res Commun* **2007,** *360* (3), 666-72.
57. Yang, W.; Bell, S. G.; Wang, H.; Zhou, W.; Hoskins, N.; Dale, A.; Bartlam, M.; Wong, L. L.; Rao, Z., Molecular characterization of a class I P450 electron transfer system from Novosphingobium aromaticivorans DSM12444. *J Biol Chem* **2010,** *285* (35), 27372-84.
58. Wand, A. J., Dynamic activation of protein function: a view emerging from NMR spectroscopy. *Nat. Struct. Biol.* **2001,** *8*, 926.
59. Wand, A. J., On the dynamic origins of allosteric activation. *Science* **2001,** *293*, 1395.
60. Batabyal, D.; Li, H.; Poulos, T. L., Synergistic effects of mutations in cytochrome P450cam designed to mimic CYP101D1. *Biochemistry* **2013,** *52* (32), 5396-402.
61. Deprez, E.; Gill, E.; Helms, V.; Wade, R. C.; Hui Bon Hoa, G., Specific and non-specific effects of potassium cations on substrate-protein interactions in cytochromes P450cam and P450lin. *J Inorg Biochem* **2002,** *91* (4), 597-606.
62. OuYang, B.; Pochapsky, S. S.; Pagani, G. M.; Pochapsky, T. C., Specific effects of potassium ion binding on wild-type and L358P cytochrome P450cam. *Biochemistry* **2006,** *45* (48), 14379.
63. Hiruma, Y.; Hass, M. A.; Kikui, Y.; Liu, W. M.; Olmez, B.; Skinner, S. P.; Blok, A.; Kloosterman, A.; Koteishi, H.; Lohr, F.; Schwalbe, H.; Nojiri, M.; Ubbink, M., The structure of the cytochrome p450cam-putidaredoxin complex determined by paramagnetic NMR spectroscopy and crystallography. *J. Mol. Biol.* **2013,** *425*, 4353.
64. Tosha, T.; Yoshioka, S.; Ishimori, K.; Morishima, I., L358P mutation on cytochrome P450cam simulates structural changes upon putidaredoxin binding: the structural changes trigger electron transfer to oxy-P450cam from electron donors. *J. Biol. Chem.* **2004,** *279*, 42836.
65. Nagano, S.; Tosha, T.; Ishimori, K.; Morishima, I.; Poulos, T. L., Crystal structure of the cytochrome p450cam mutant that exhibits the same spectral perturbations induced by putidaredoxin binding. *J. Biol. Chem.* **2004,** *279*, 42844.
66. Yoshioka, S.; Tosha, T.; Takahashi, S.; Ishimori, K.; Hori, H.; Morishima, I., Roles of the proximal hydrogen bonding network in cytochrome P450cam-catalyzed oxygenation. *J. Am. Chem. Soc.* **2002,** *124*, 14571.
67. Koga, H.; Aramaki, H.; Yamaguchi, E.; Takeuchi, K.; Horiuchi, T.; Gunsalus, I. C., camR, a negative regulator locus of the cytochrome P-450cam hydroxylase operon. *J Bacteriol* **1986,** *166* (3), 1089-95.
68. Aramaki, H.; Kabata, H.; Takeda, S.; Itou, H.; Nakayama, H.; Shimamoto, N., Formation of repressor-inducer-operator ternary complex: negative cooperativity of d-camphor binding to CamR. *Genes Cells* **2011,** *16*, 1200.
69. Yao, H.; McCullough, C. R.; Costache, A. D.; Pullela, P. K.; Sem, D. S., Structural evidence for a functionally relevant second camphor binding site in P450cam: model for substrate entry into a P450 active site. *Proteins: Struct., Funct., Genet.* **2007,** *69*, 125.

70. Kuznetsov, V. Y.; Poulos, T. L.; Sevrioukova, I. F., Putidaredoxin-to-cytochrome P450cam electron transfer: differences between the two reductive steps required for catalysis. *Biochemistry* **2006,** *45*, 11934.
71. Hollingsworth, S. A.; Batabyal, D.; Nguyen, B. D.; Poulos, T. L., Conformational selectivity in cytochrome P450 redox partner interactions. *Proc. Natl. Acad. Sci. U. S. A.* **2016,** *113*, 8723.
72. Salomon-Ferrer, R.; Gotz, A. W.; Poole, D.; Le Grand, S.; Walker, R. C., Routine Microsecond Molecular Dynamics Simulations with AMBER on GPUs. 2. Explicit Solvent Particle Mesh Ewald. *J. Chem. Theory Comput.* **2013,** *9*, 3878.
73. Hopkins, C. W.; Le Grand, S.; Walker, R. C.; Roitberg, A. E., Long-Time-Step Molecular Dynamics through Hydrogen Mass Repartitioning. *J. Chem. Theory Comput.* **2015,** *11*, 1864.
74. Roe, D. R.; Cheatham, T. E., PTRAJ and CPPTRAJ: Software for Processing and Analysis of Molecular Dynamics Trajectory Data. *J. Chem. Theory Comput.* **2013,** *9*, 3084.
75. Humphrey, W.; Dalke, A.; Schulten, K., VMD: visual molecular dynamics. *J. Mol. Graphics* **1996,** *14*, 33.

Chapter 3

Ligand and Redox Partner Binding Generates a New Conformational State in Cytochrome P450cam (CYP101A1)

Introduction

As discussed in chapters 1 and 2, after binding substrate and displacement of the active site water, P450cam undergoes a low to high spin transition. High-spin P450cam's redox potential is sufficiently high enough to abstract an electron from its native redox partner, putidaredoxin (Pdx). This is followed by the binding of O_2 to the open axial coordination site on P450cam's heme active site.[1] The first ET is the rate limiting step of the P450 catalytic cycle.[2] Therefore, to prepare any of the critical intermediates, an electron must first be transferred to P450cam. This first electron transfer only requires a reductant of the appropriate potential such as dithionite or cytochrome b5 and thus many of the P450cam intermediates have been studied in the absence of Pdx. Although, in its native context, putidaredoxin is present during both electron transfers and its influence on P450cam's conformation those intermediate complexes are unknown.

In particular, a hallmark of the P450cam system is that the second electron transfer step can be supported by only Pdx so it has long been thought that Pdx plays an effector/allosteric role.[3] This effector role has been demonstrated by numerous spectroscopic methods,[4-10] but the underlying conformational dynamics that give rise to its specificity have only recently begun to emerge. Crystal structures of P450-redox partner complexes are challenging and rare with only three structures to date.[11-13] The most recent are the covalent and non-covalent structures of P450cam-Pdx determined by both X-ray crystallography and NMR.[13-14] These structures provided

the first direct structural evidence of how allosteric effects of Pdx may be achieved. The binding of Pdx to substrate bound P450 pushes P450cam towards the open conformation consistent with earlier spectroscopic evidence that demonstrated Pdx binding shifted substrate-bound P450cam back towards the low-spin state.[10] This shift to an open conformation was hypothesized to allow for the formation of a water mediated proton relay network to enter the active-site channel and

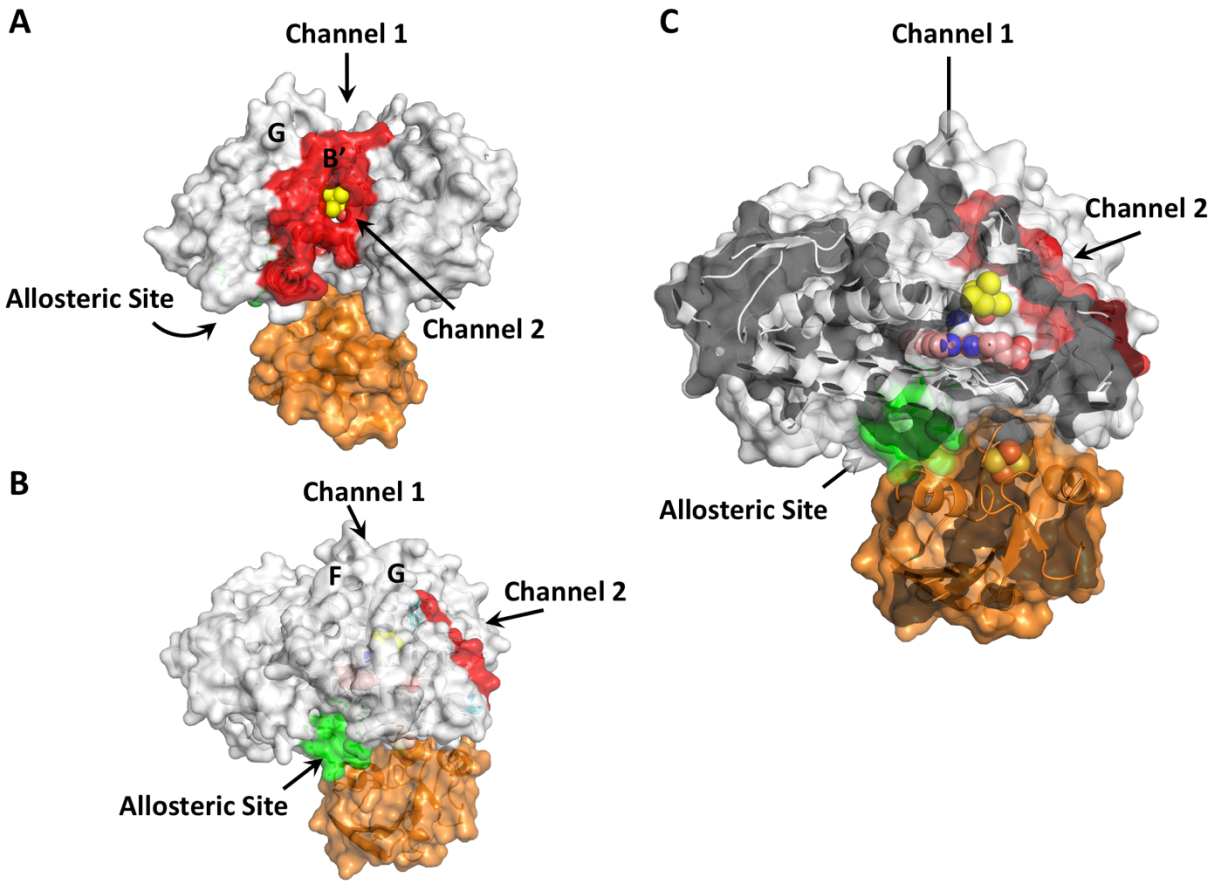

Figure 3-1. (A) P450cam (white) with the B-C loop (red) forming channel 2 in complex with Pdx (orange). **(B)** Rotated by 90˚ counter clockwise to show the allosteric site (green). **(C)** A cross section of the complex.

free active site residue Asp251 from a strong ion pair with F helix residue Arg186, which participates in a proton delivery relay to the distal heme-bound oxygen for O-O bond scission.[13, 15]

Related to both substrate and Pdx binding is perhaps the most important step of the P450 catalytic cycle, the binding and activation of molecular dioxygen. The synergistic timing of O_2 binding, activation, and turnover is critical to ensure efficient coupling and prevent unproductive turnover and release of O_2 as reactive oxygen species (ROS) such as superoxide or peroxide. While these interactions have been extensively investigated within the context of P450cam-camphor interactions,[3, 16] Pdx's involvement with substrate and O_2 dynamics are not well understood. While the structure of substrate-bound P450cam and dioxygen has been solved crystallographically, determination of the analogous structure of the oxy-complex bound to Pdx is not as straight forward. It has been previously demonstrated that in the presence of substrate and Pdx, X-ray radiation alone can reduce either P450cam and/or Pdx to initiate substrate turnover and form product within the crystal.[13] Beyond the challenges related to the instability of the oxy complex, formation of the oxygenated intermediate within the crystallized complex would surely bring a similar result upon X-ray exposure.

In order to study the effects of oxygenated intermediates of P450, both cyanide and carbon monoxide have been utilized as stable mimics of O_2.[17-18] However, binding of CO to P450 does not confer many of the conformational changes that are known to occur upon dioxygen binding.[5, 18] This may be due to electronic changes that occur upon CO binding and a lack of charge on the distal oxygen. Oxy complexes of heme proteins are best described as ferric-superoxide rather

than ferrous-oxy so the distal O_2 oxygen atom carries a negative charge.[19-20] The ferric-superoxide complex is electronically similar to the ferric-cyanide complex as CN^- has a negative charge on

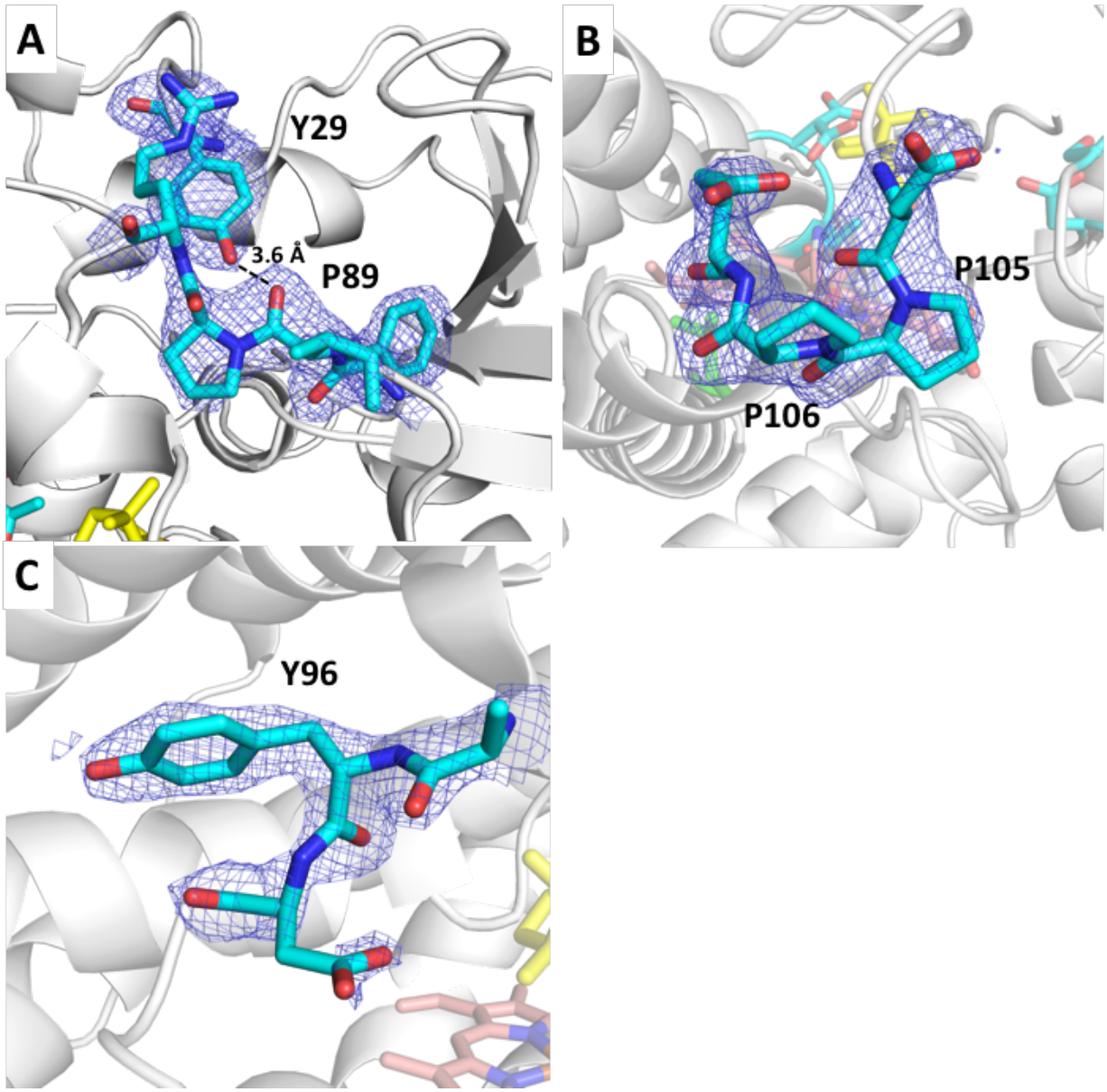

Figure 3-2. Several changes occur in the B-C loop of P450cam. Two prolines in the structure undergo *cis-trans* isomerization including **(A)** Pro89 that also moves to a distance of 3.6 Å from Tyr29 as well as **(B)** Pro105. **(C)** Tyr96 also rotates out of the active site where it H-bonds with the camphor carbonyl oxygen. Camphor (yellow) Heme (red). $2F_o$-F_c maps at 1 σ (blue).

the distal nitrogen. Indeed, the P450cam-CN^- complex results in the same changes in local protein and solvent structure as the O_2-bound intermediate, while CO and NO complexes do not.[17, 21-23]

In this chapter, the structure of substrate bound P450cam-Pdx complexed with cyanide as an axial ligand at a resolution of 2.15 Å is presented. Quite unexpectedly, we found that cyanide induces large structural changes that results in the formation of a new opening to the active site we have termed channel 2. Our recent molecular dynamics (MD) simulations showed that binding of the substrate, camphor, to a site on the protein well removed from the active site results in the formation of this same channel 2.[24] Thus, the present work provides experimental verification of structural change predicted by MD simulations as well as defining a novel conformational state of P450cam that may have relevance to enzyme function.

Results and Discussion

In Chapter 2, MD simulations demonstrated how allosteric control of P450cam by a second molecule of camphor may provide a mechanism of activation by opening a primary and secondary channel. To date, the formation of the second channel has never been verified experimentally. Owing to the limits of classical MD, the role of O_2 binding, product formation, and Pdx interaction were not demonstrated in our proposed model, but these processes are intricately governed by protein-substrate interactions.

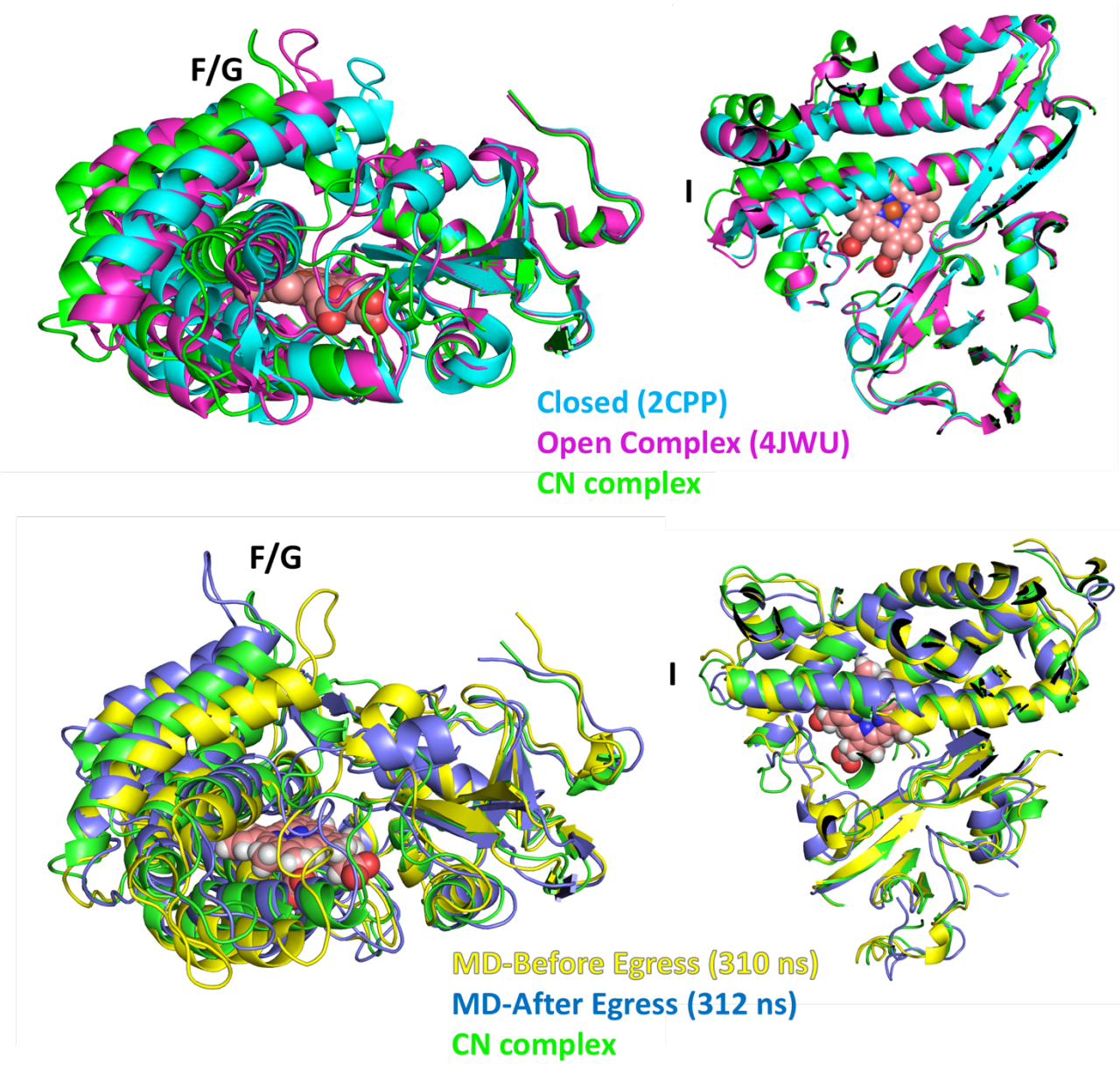

Figure 3-3. Alignment of P450cam crystal structures and molecular dynamics snapshots. Top: Crystal structure of the closed complex (cyan), Pdx bound complex (magenta) and Pdx-CN complex (green) showing the degree of movement of both the F/G helices (left) and I helix right. Bottom: Molecular dynamics snapshots revealing the degree of similarity between the Pdx-CN structure (green) and simulation before (yellow) and after (blue) egress of camphor from the active site through channel 2.

P450cam and Pdx were covalently crosslinked using a bismaleimide crosslinker between two non-native cysteines far from the protein-protein interface. The protein complex was crystallized and soaked with excess cyanide. To confirm the binding of CN^-, a UV-vis spectrum of the crystal was taken using the microfocus beamline and the Soret peak is significantly red shifted indicating the presence of bound CN^- (Fig 3-6). The most significant stuctural changes between the complexes with and without CN^- bound are the widening of the F/G loop and opening of the B' channel (channel 2, Fig 3-1). This indicates that the binding of CN^- to the heme induces large, ordered conformational rearrangements within the crystal.

In Chapter 2, it was suggested how substrate binding to a second site may prime the opening of a second channel and how Pdx may preferentially bind to this open structure to contribute to product egress *via* mechanical coupling. Overlaying the CN^- bound complex structure with our prior simulation egress event reveals significant similarities (Fig 3-3). Unlike the other P450cam-Pdx complexes, the F/G helices have moved to a completely open conformation. This allows for breakage of the Arg186-Asp-251 ion pair, which, in our structure, is present in two rotameric conformations revealing how binding of dioxygen and Pdx may break this pair allowing for Asp251 to participate in proton delivery as suggested by Tripathi *et al*.[13] Polder maps demonstrate the bifurcation of the Asp251 residue (Fig 3-3). The rotamer where Asp251 is oriented in toward the active site is in an ideal position to mediate proton transfer to dioxygen.

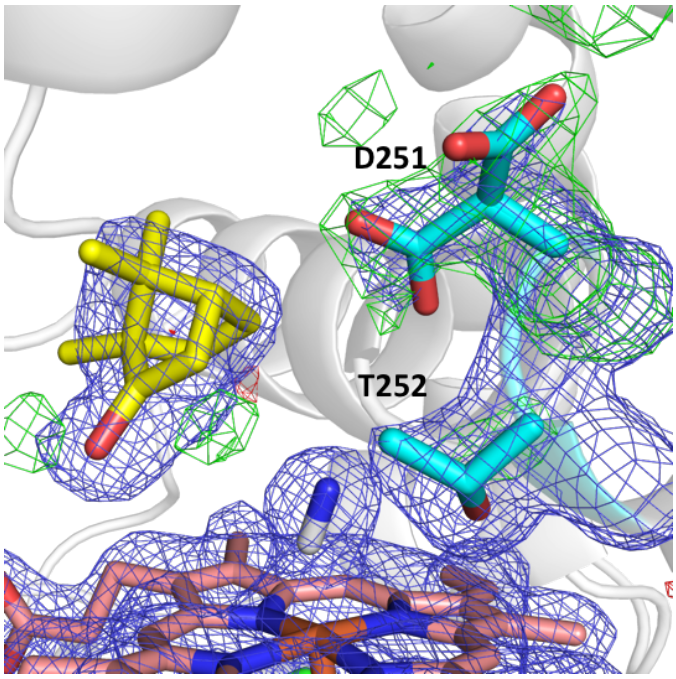

Figure 3-4. Polder Map of Asp-251 in two rotameric conformations. $2F_o$-F_c at 1 σ (blue) and Polder map at 4 σ (green).

However, the substrate access channel (channel 1) is not completely exposed in either of the molecules as the B' helix has lost nearly all secondary structure but remains hydrogen bonded to the F/G loop. The movement of the F/G loop and the unfolding of the B' helix leads to channel 2 formation while channel 1 remains closed. This new channel provides an egress path for product and is associated with dynamic movement of Tyr96. This is important since in the closed state Tyr96 provides an H-bond to the camphor carbonyl oxygen. However, when CN^- binds to the P450cam-Pdx complex Tyr96 flips out of the active site (Fig 3-2C). To demonstrate the dynamics of this channel, we previously utilized the Ser83 to Ser102 Cα distance as a measure of channel 2 formation, which in all crystal structures where the B loop is ordered, is ~5 Å.[24] In the

CN^- complex structure, however, the S83 to S102 distance is ~9.5 Å, which is in good agreement with our simulations that in order for substrate egress to occur channel 2 opens to beyond 7 Å.

NMR studies hypothesized that conformational switching in P450cam is dictated by an X-proline (X-Pro) *cis-trans* isomerization, but this has never been observed in a crystal structure. Specifically, OuYang *et al*. identified Pro89 as the most likely candidate for controlling this process.[25] They observed two distinct camphor orientations when substrate bound P450cam was reduced and bound to carbon monoxide (CYP-S-CO) and was then titrated with reduced Pdx (Pdx^r). The time scales of the observed chemical shifts were in good agreement with reported time scales of catalyzed proline *cis-trans* isomerization. Catalyzed X-Pro *cis-trans* isomerizations are accelerated ~10^6 times faster than uncatalyzed transitions (~0.01 s^{-1}).[25] The binding of CN^- to P450cam-Pdx results in the *cis* to *trans* isomerization of the Ile88-Pro89 bond which breaks a bifurcated hydrogen bond from the carbonyl of Pro89 to the NH groups of Ala92 and Gly93 that allows the B'helix to lose secondary structure but remain hydrogen bonded to the F/G loop. NMR-directed molecular dynamics suggested that the barrier of this isomerization is lowered by a distortion of the ideally planar Ile88-Pro89 O-C-N-C_∂ (ω) dihedral from 180˚ to ~166˚ in the *trans* form. The conclusions of those simulations are supported by the Ile88-Pro89 ω dihedral angles in our structure, which are distorted to 167˚ and 169˚. Tyr29 was also hypothesized to be important in the controlling the isomerization process, and, when compared to the closed structure, has moved from a distance of ~2.7 Å to 3.6 Å, nearly out of hydrogen bonding range (Fig 4A). Pro106 also undergoes *cis* to *trans* isomerization assisting in the opening of channel 2 and forces greater alignment of the backbone carbonyls effectively increasing the stability of the

C-helix (Fig 4B). The Pro-Pro motif at the end of the B-C loop is conserved in a number of bacterial P450s and suggests that this mechanism may not be unique to P450cam.[26]

One surprising observation from the structure is the orientation of the 7-propionate group. In every crystallographic structure of P450cam deposited in the Protein Data Bank, the

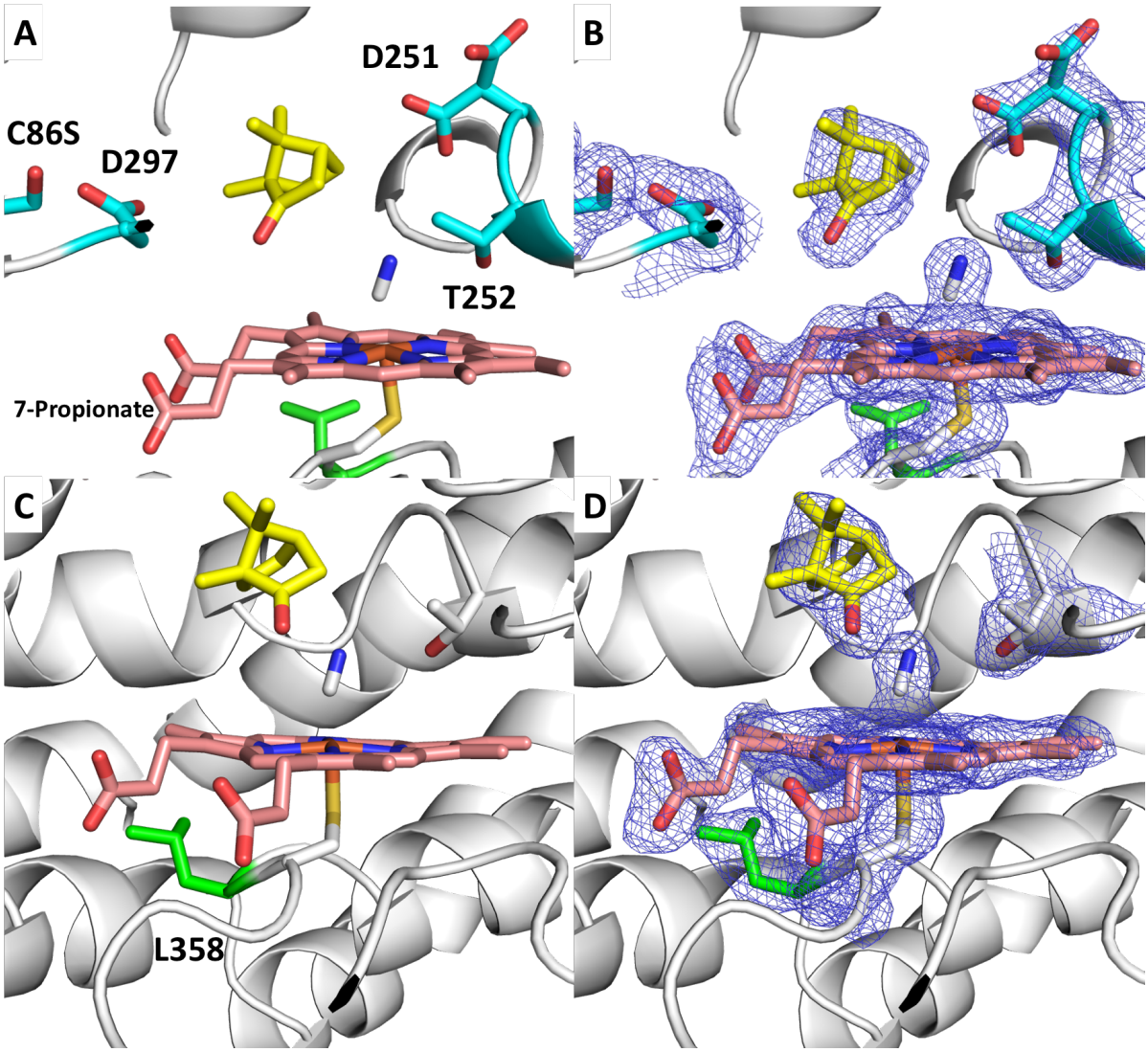

Figure 3-5. Two different views of the active site of P450cam with camphor (yellow) and CN (grey) bound to heme (red). Leu358 (green) has rotated to accommodate Pdx and pushes on the heme, where the 7-propionate has rotated and broken its interactions with Asp297. 2Fo-Fc contoured at 1 σ (blue, right).

propionates take on identical conformations, with 7-propionate C1A-C2A-CAA-CBA dihedral between -100˚ and -110˚. In the cyanide structure presented here, the 7-propionate dihedral has rotated by ~180˚ to 89.9˚ and 85.3˚ respectively (Fig 3-5). Hayashi *et al*. reconstituted P450cam with a "one-legged" heme to demonstrate how the 7-propionate along with Asp297, Arg299, and Gln322 act to protect the active site from solvent entry.[27] Asp297 is believed to be protonated (H++ server: http://biophysics.cs.vt.edu/) and involved in hydrogen bonding with heme 7-propionate. In the CN^- complex, Asp297 breaks this hydrogen bond with the propionate revealing how Asp297 may participate in hydrogen bonding to camphor after binding O_2 allowing for retained regio-stereoselectivity. In our unrestrained MD simulations, this same H-bond breakage of 7-propionate is associated with substrate egress. (One NMR structure exhibits a similar geometry; however the heme structure was determined by molecular dynamics.)

We previously postulated that the dihedral rotation of the Leu358 side chain had relevance in Pdx binding and product formation.[24] Once again, Leu358 N-Cα-Cβ-Cγ rotates ~130˚ from the open-closed structure (2CPP) ~-70˚ to a dihedral angle of 59.3˚ and 56.9˚ in each monomer, respectively. This rotation allows for Pdx to create a tighter interface with P450cam and has been associated with the "push" effect coupled to changes on the distal side of the heme that favors the open form of P450cam.[5-6, 28] Here, we can see how Leu358 rotates upon CN^- and Pdx binding and induces changes on the distal side of the heme as well as the heme itself that favor an open state.

Why CN^- binding induces such large changes illustrates the intricate coupling of distant regions of P450cam with one another which have been well documented by NMR studies.[25, 28-33]

To make room for CN^- the I helix must move and since the F and G helices contact the I helix and the F/G loop region contacts the B' helix, all these regions move in concert. These large changes are possible because Pdx is holding P450cam in the partially open state. In the closed state, O_2 and CN^- binding, P450cam is locked down in the closed state and these large changes cannot take place. Even so, O_2 and CN^- binding to closed P450cam results in local change in the I helix which are in the direction toward the open state.[17, 22] Pdx binding releases these restraints thereby enabling the protein to undergo these large conformational rearrangements.

Conclusions

The P450cam-Pdx-CN^- structure illustrates the magnitude of conformational changes that P450s can undergo and defines a new conformational state of P450cam. We were quite surprised that these large changes including *cis-trans* proline isomerization can occur within the confines of a crystal lattice. Although CN^- is a good mimic of O_2, the current structure cannot represent an active complex owing to the location of the camphor in channel 1. In our original structure of the P450cam-Pdx complex the product, 5-*exo*-hydroxycamphor, is positioned in the substrate binding site but a second camphor molecule is bound just above the product in channel 1 (PDB 4JX1). In the CN^--complex, camphor is positioned about 2 Å up the channel away from the productive binding site and thus cannot represent the structure just prior to O–O bond cleavage and substrate hydroxylation. We postulate that opening of channel 2 has allowed productively bound substrate to escape while rearrangements of the F/G and B' regions trap the second camphor molecule in channel 1. It is unlikely that O_2 alone can result in the same changes we observe with CN^- primarily because the oxy-P450cam complex is very unstable when bound to

oxidized Pdx while clearly the CN^- complex is quite stable. This is probably because Pdx shifting P450cam to the open state in the absence of electron transfer promotes rapid autoxidation of the oxy-complex. It thus seems more likely that the stability of the CN^- complex has enabled trapping of P450cam in this new open conformational state. What provides an additional level of confidence that the CN^--induced structural changes are functionally relevant is the consistency with our previous MD simulations that show an allosterically regulated change in structure resulting in the formation of channel 2 very similar to what happens when CN^- binds. This is reasonable since the regions in the immediate vicinity of CN^- binding in the I helix and those of the proposed allosteric substrate binding site ~16 Å away are mechanically coupled. Perturbing one perturbs the other. Therefore, the CN^- complex provides a snapshot along the reaction coordinate after substrate hydroxylation and product egress through channel 2 while the substrate molecule in channel 1 is poised for movement to the productive binding site once Pdx dissociates.

Table 3-1. X-ray crystallography data collection and refinement statistics for P450cam-Pdx-CN complex. Values in parentheses are for the highest resolution shell.

	P450cam-Pdx-CN
Data collection	
Space group	P 1 21 1
Cell dimensions	
a, b, c	57.36 110.30 88.62
α, β, γ	90, 107.67, 90
Resolution (Å)	40.6 - 2.15 (2.227 - 2.15)
R_{merge}	5.0 (34.76)
Total reflections	108983 (10818)
Unique reflections	54970 (5453)
$CC_{1/2}$	0.997 (0.632)
I/σ	10.42 (2.46)
Completeness	96.26 (96.33)
Redundancy	2.0 (2.0)
Refinement	
R_{work}/R_{free}	0.1979 (0.2714)/ 0.2558 (0.3457)
Number of atoms	8572
Protein	8015
Water	395
Ligands	162
RMSD Bond lengths (Å)	0.005
RMSD Bond angles	0.63
Average B factor	40.26
Ramachandran Favored/Outliers (%)	97.03/ 0.00

Materials and Methods

Crystallization

P450cam-Pdx crystals were prepared by hanging drop method as previously described.[13] To prepare the CN^--bound complex, crystals were soaked in mother liquor containing 50mM KCN for 15 min. Mother liquor supplemented with 15% glycerol was used as a cryo-protectant and crystals were flash frozen in liquid nitrogen before data collection.

Data collection and Refinement

Data were collected from single crystals at the Stanford Synchrotron Radiation Lightsource (SSRL). Diffraction images were indexed, integrated, and scaled using Mosflm and Scala in the CCP4 package.[34] P450cam-Pdx complex crystals structure (4JWS)[13] without cofactor was used as a search model in molecular replacement using Phaser. The final structure contains two molecules of the P450cam-Pdx complex per asymmetric unit. The Phenix suite[35] was used for structure refinement. All reflections were used for refinement except for 5% excluded for R_{free} calculations.[35] The structural model was revised in real space with the program COOT[36-37] based on sigma-A weighted 2Fo-Fc and Fo-Fc electron density maps. The final refinement statistics are given in Table 3-1. The final structure was refined to 2.15 Å resolution with an R_{free} of 25.6 % and R_{work} of 19.8%.

Structural Analysis

The final refined model consists of two molecules of complex (P450cam A-chain + Pdx C-chain, P450cam B-chain + Pdx D-chain) in the asymmetric unit. All four chains are highly ordered and more than 97.0% of the residues were located in the core region of Ramachandran plots as determined by MolProbity.[38] We did not observe any significant change in Pdx although during data collection the Fe_2S_2 center in Pdx very likely gets reduced. When Pdx is reduced the 45-46 peptide flips allowing the peptide NH group to donate a hydrogen bond to the Fe_2S_2 center in the reduced state. In our structure, this peptide is in the reduced conformation.

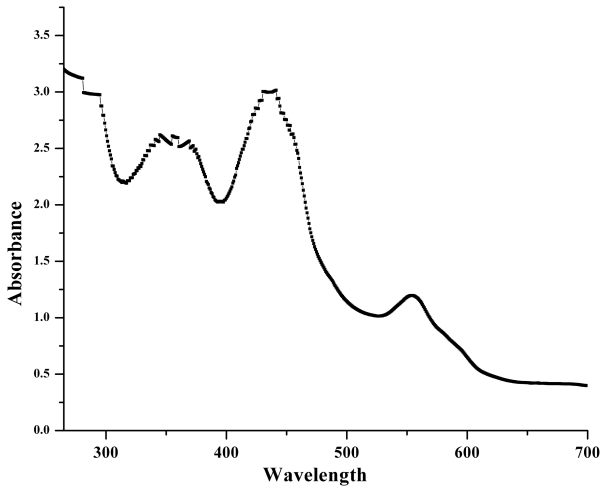

Figure 3-6. Single Crystal UV-vis of P450cam-Pdx-CN complex.

References:

1. Poulos, T. L., Heme enzyme structure and function. *Chem. Rev.* **2014,** *114*, 3919.
2. Brewer, C. B.; Peterson, J. A., Single turnover kinetics of the reaction between oxycytochrome P-450cam and reduced putidaredoxin. *J Biol Chem* **1988,** *263* (2), 791-8.
3. Lipscomb, J. D.; Sligar, S. G.; Namtvedt, M. J.; Gunsalus, I. C., Autooxidation and hydroxylation reactions of oxygenated cytochrome P-450cam. *J. Biol. Chem.* **1976,** *251* (4), 1116.

4. Gunsalus, I. C.; Sligar, S. G., Redox regulation of cytochrome P450cam mixed function oxidation by putidaredoxin and camphor ligation. *Biochimie* **1976,** *58*, 143.
5. Nagano, S.; Tosha, T.; Ishimori, K.; Morishima, I.; Poulos, T. L., Crystal structure of the cytochrome p450cam mutant that exhibits the same spectral perturbations induced by putidaredoxin binding. *J. Biol. Chem.* **2004,** *279*, 42844.
6. Tosha, T.; Yoshioka, S.; Ishimori, K.; Morishima, I., L358P mutation on cytochrome P450cam simulates structural changes upon putidaredoxin binding: the structural changes trigger electron transfer to oxy-P450cam from electron donors. *J. Biol. Chem.* **2004,** *279*, 42836.
7. Myers, W. K.; Lee, Y. T.; Britt, R. D.; Goodin, D. B., The conformation of P450cam in complex with putidaredoxin is dependent on oxidation state. *J. Am. Chem. Soc.* **2013,** *135*, 11732.
8. Liou, S. H.; Mahomed, M.; Lee, Y. T.; Goodin, D. B., Effector Roles of Putidaredoxin on Cytochrome P450cam Conformational States. *J Am Chem Soc* **2016,** *138* (32), 10163-72.
9. Liou, S. H.; Myers, W. K.; Oswald, J. D.; Britt, R. D.; Goodin, D. B., Putidaredoxin Binds to the Same Site on Cytochrome P450cam in the Open and Closed Conformation. *Biochemistry* **2017,** *56* (33), 4371.
10. Unno, M.; Christian, J. F.; Benson, D. E.; Gerber, N. C.; Sligar, S. G.; Champion, P. M., Resonance Raman Investigations of Cytochrome P450cam Complexed with Putidaredoxin. *J. Am. Chem. Soc.* **1997,** *119* (28), 6614.
11. Sevrioukova, I. F.; Li, H.; Zhang, H.; Peterson, J. A.; Poulos, T. L., Structure of a cytochrome P450-redox partner electron-transfer complex. *Proc. Natl. Acad. Sci. U. S. A.* **1999,** *96* (5), 1863.
12. Strushkevich, N.; MacKenzie, F.; Cherkesova, T.; Grabovec, I.; Usanov, S.; Park, H. W., Structural basis for pregnenolone biosynthesis by the mitochondrial monooxygenase system. *Proc. Natl. Acad. Sci. U. S. A.* **2011,** *108* (25), 10139.
13. Tripathi, S.; Li, H.; Poulos, T. L., Structural basis for effector control and redox partner recognition in cytochrome P450. *Science* **2013,** *340* (6137), 1227.
14. Hiruma, Y.; Hass, M. A.; Kikui, Y.; Liu, W. M.; Olmez, B.; Skinner, S. P.; Blok, A.; Kloosterman, A.; Koteishi, H.; Lohr, F.; Schwalbe, H.; Nojiri, M.; Ubbink, M., The structure of the cytochrome p450cam-putidaredoxin complex determined by paramagnetic NMR spectroscopy and crystallography. *J. Mol. Biol.* **2013,** *425*, 4353.
15. Gerber, N. C.; Sligar, S. G., A role for Asp-251 in cytochrome P-450cam oxygen activation. *J. Biol. Chem.* **1994,** *269* (6), 4260.
16. Sjodin, T.; Christian, J. F.; Macdonald, I. D.; Davydov, R.; Unno, M.; Sligar, S. G.; Hoffman, B. M.; Champion, P. M., Resonance Raman and EPR investigations of the D251N oxycytochrome P450cam/putidaredoxin complex. *Biochemistry* **2001,** *40* (23), 6852.
17. Fedorov, R.; Ghosh, D. K.; Schlichting, I., Crystal structures of cyanide complexes of P450cam and the oxygenase domain of inducible nitric oxide synthase-structural models of the short-lived oxygen complexes. *Arch. Biochem. Biophys.* **2003,** *409* (1), 25.
18. Raag, R.; Poulos, T. L., Crystal structure of the carbon monoxide-substrate-cytochrome P-450CAM ternary complex. *Biochemistry* **1989,** *28* (19), 7586.

19. Luthra, A.; Denisov, I. G.; Sligar, S. G., Spectroscopic features of cytochrome P450 reaction intermediates. *Arch. Biochem. Biophys.* **2011,** *507* (1), 26.
20. Huang, X.; Groves, J. T., Oxygen Activation and Radical Transformations in Heme Proteins and Metalloporphyrins. *Chem. Rev.* **2018,** *118* (5), 2491.
21. Conner, K. P.; Woods, C. M.; Atkins, W. M., Interactions of cytochrome P450s with their ligands. *Arch. Biochem. Biophys.* **2011,** *507* (1), 56.
22. Schlichting, I.; Berendzen, J.; Chu, K.; Stock, A. M.; Maves, S. A.; Benson, D. E.; Sweet, R. M.; Ringe, D.; Petsko, G. A.; Sligar, S. G., The catalytic pathway of cytochrome p450cam at atomic resolution. *Science* **2000,** *287* (5458), 1615.
23. Kuhnel, K.; Blankenfeldt, W.; Terner, J.; Schlichting, I., Crystal structures of chloroperoxidase with its bound substrates and complexed with formate, acetate, and nitrate. *J. Biol. Chem.* **2006,** *281* (33), 23990.
24. Follmer, A. H.; Mahomed, M.; Goodin, D. B.; Poulos, T. L., Substrate-Dependent Allosteric Regulation in Cytochrome P450cam (CYP101A1). *J Am Chem Soc* **2018,** *140* (47), 16222-16228.
25. OuYang, B.; Pochapsky, S. S.; Dang, M.; Pochapsky, T. C., A functional proline switch in cytochrome P450cam. *Structure* **2008,** *16* (6), 916.
26. Nelson, D. R., The cytochrome p450 homepage. *Hum Genomics* **2009,** *4* (1), 59.
27. Hayashi, T.; Harada, K.; Sakurai, K.; Shimada, H.; Hirota, S., A role of the heme-7-propionate side chain in cytochrome P450cam as a gate for regulating the access of water molecules to the substrate-binding site. *J. Am. Chem. Soc.* **2009,** *131* (4), 1398.
28. OuYang, B.; Pochapsky, S. S.; Pagani, G. M.; Pochapsky, T. C., Specific effects of potassium ion binding on wild-type and L358P cytochrome P450cam. *Biochemistry* **2006,** *45* (48), 14379.
29. Asciutto, E. K.; Madura, J. D.; Pochapsky, S. S.; OuYang, B.; Pochapsky, T. C., Structural and dynamic implications of an effector-induced backbone amide cis-trans isomerization in cytochrome P450cam. *J. Mol. Biol.* **2009,** *388* (4), 801.
30. Dang, M.; Pochapsky, S. S.; Pochapsky, T. C., Spring-loading the active site of cytochrome P450cam. *Metallomics* **2011,** *3* (4), 339.
31. Asciutto, E. K.; Young, M. J.; Madura, J.; Pochapsky, S. S.; Pochapsky, T. C., Solution structural ensembles of substrate-free cytochrome P450(cam). *Biochemistry* **2012,** *51*, 3383.
32. Colthart, A. M.; Tietz, D. R.; Ni, Y.; Friedman, J. L.; Dang, M.; Pochapsky, T. C., Detection of substrate-dependent conformational changes in the P450 fold by nuclear magnetic resonance. *Sci. Rep.* **2016,** *6*, 22035.
33. Asciutto, E. K.; Pochapsky, T. C., Some Surprising Implications of NMR-directed Simulations of Substrate Recognition and Binding by Cytochrome P450cam (CYP101A1). *J. Mol. Biol.* **2018,** *430*, 1295.
34. Battye, T. G.; Kontogiannis, L.; Johnson, O.; Powell, H. R.; Leslie, A. G., iMOSFLM: a new graphical interface for diffraction-image processing with MOSFLM. *Acta Crystallogr., Sect. D: Biol. Crystallogr.* **2011,** *67* (4), 271.
35. Adams, P. D.; Afonine, P. V.; Bunkoczi, G.; Chen, V. B.; Davis, I. W.; Echols, N.; Headd, J. J.; Hung, L. W.; Kapral, G. J.; Grosse-Kunstleve, R. W.; McCoy, A. J.; Moriarty, N. W.; Oeffner, R.;

Read, R. J.; Richardson, D. C.; Richardson, J. S.; Terwilliger, T. C.; Zwart, P. H., PHENIX: a comprehensive Python-based system for macromolecular structure solution. *Acta Crystallogr., Sect. D: Biol. Crystallogr.* **2010,** *66* (2), 213.
36. Emsley, P.; Cowtan, K., Coot: model-building tools for molecular graphics. *Acta Crystallogr., Sect. D: Biol. Crystallogr.* **2004,** *60* (12), 2126.
37. Emsley, P.; Lohkamp, B.; Scott, W. G.; Cowtan, K., Features and development of Coot. *Acta Crystallogr., Sect. D: Biol. Crystallogr.* **2010,** *66* (4), 486.
38. Williams, C. J.; Headd, J. J.; Moriarty, N. W.; Prisant, M. G.; Videau, L. L.; Deis, L. N.; Verma, V.; Keedy, D. A.; Hintze, B. J.; Chen, V. B.; Jain, S.; Lewis, S. M.; Arendall, W. B.; Snoeyink, J.; Adams, P. D.; Lovell, S. C.; Richardson, J. S.; Richardson, D. C., MolProbity: More and better reference data for improved all-atom structure validation. *Protein Sci.* **2018,** *27* (1), 293.

Chapter 4

Redox Partner Interactions with P450terp (CYP108A1)

Introduction

The importance of cytochromes P450 in biological processes cannot be overstated. However, as discussed in chapter 1, a significant portion of these enzymes exist as membrane tethered, multi-component systems (Fig 1-7) presenting a significant challenge for both high-yield expression and purification, as well as experimentation (e.g. crystallization). Hence, the utility of the highly expressible and soluble P450cam system is immeasurable and while its global

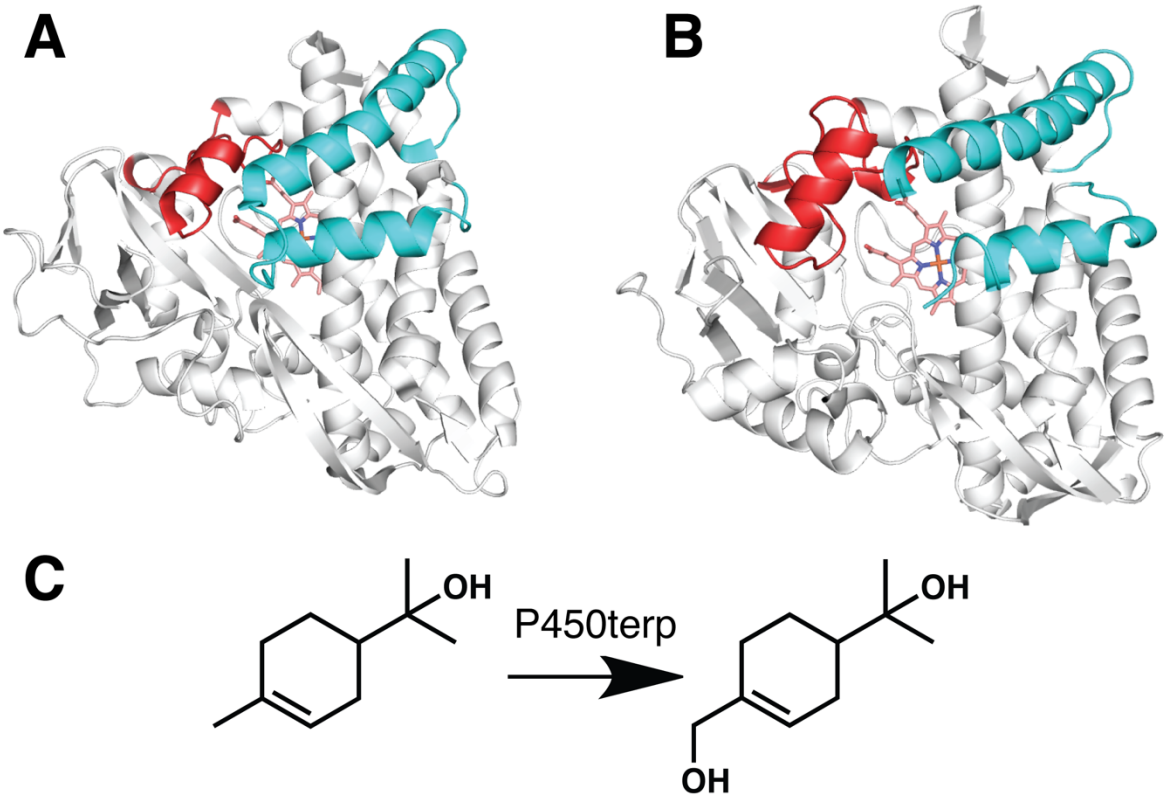

Figure 4-1. Comparison of P450cam (PDB: 2CPP) **(A)** and P450terp (PDB: 1CPT) **(B)**. F/G helices (cyan) and B/C loop (red). **(C)** Hydroxylation of α-terpineol to 7-hydroxy-α-terpineol catalyzed by P450terp.

properties such as architecture and general mechanistic intermediates are conserved, it remains unclear to what extent the exact mechanistic transitions (i.e. effector role of the redox partner) of P450cam can be generalized to the superfamily.

As discussed in the previous chapters, the working hypothesis is that the redox partners act in an effector role to push P450s to an open conformation allowing the iron-linked O_2 access to solvent protons for proton coupled ET (PCET). However, only three structures of P450 redox complexes have been solved crystallographically, P450BM3-BM3FMN reductase[1], P450scc-Adx[2], and P450cam-Pdx[3], so limited structural information is available to guide our understanding of these processes. The complex of P450BM3 to its FMN-containing reductase domain, while from a prokaryote like P450cam, was solved in the substrate-free form. Therefore, questions remain whether redox-partner induced structural rearrangements occur in the presence of substrate. The P450scc-Adx complex is mammalian and does not exhibit these same structural changes and leads us to our second hypothesis, that this effector role is perhaps specific to bacterial P450s. In bacterial systems, where a single, plasmid encoded P450 is responsible for the metabolism of some carbon source, it is necessary for tightly coupled regulation of substrate binding, redox partner binding, and conformational changes to ensure efficient metabolism and prevent wasting of potentially valuable reducing equivalents. Recent work by the Plettner group has provided critical insight into the toxicity of camphor to *Pseudomonas putida*[4], as well as the ability for *P. putida* to undergo P450cam-dependent camphor-induced taxis[5], thus supporting the notion that increased regulation is required for energetic efficiency and survival of the organism. In order to

investigate the extension of the mechanism discussed and developed in chapters 2 and 3, it is necessary to examine homologous systems to P450cam.

P450terp or CYP108A1 is a close homologue of P450cam that serves as the sole P450 for its host *Pseudomonad*, and, in addition, is a plasmid-borne inducible system that allows its host to utilize a small terpenoid, α-terpineol, as its sole carbon source.[6] P450terp catalyzes the transformation of α-terpineol to 7-hydroxy-α-terpineol (Fig 4-1). Similar to P450cam, P450terp requires an electron transfer (ET) from a small Fe_2S_2 ferredoxin, terpredoxin (Tdx), which is first reduced by an FAD-containing reductase, terpredoxin reductase (TdR), which oxidizes NADH. While highly homologous in its biological role, atomically, P450terp possesses only 22% sequence identity to P450cam. Additionally, its redox partner, terpredoxin, shares a 36% identity with Pdx and does not possess an analogous C-terminal tryptophan (W106), which plays an important role in the P450cam-Pdx interactions.[3, 7]

Other than P450cam, P450terp is one of the first P450s to be crystallographically characterized.[8-9] The Peterson lab, similar to the lab of Gunsalus, was intrigued by the use of microbial metabolism for the controlled functionalization of organic substrates and isolated P450terp by cultural enrichment of growth media containing α-terpineol from a swamp in North Dallas.[6] The genetic structure and sequence were determined in 1992 and was followed shortly by a substrate free structure of P450terp in 1994 at 2.3 Å resolution.[6, 8] A few additional works by Peterson, as well as the lab of Hui Bon Hoa, characterized some thermodynamic and kinetic properties of the enzyme[10-11], but none were performed with respect to the interactions with its redox partner, terpredoxin (Tdx). Although, an NMR structure of Tdx was published by

Pochapsky, the active site was necessarily homology modeled due to paramagnetic broadening by the two high-spin Fe sites.[12]

This chapter focuses on the recombinant expression and purification of the P450terp system and investigates its selectivity with regard to its redox partner.

Results and Discussion

While the structure of P450terp was solved in the by Hasemann *et al.*[8], it was solved in the absence of substrate. As a result, a large portion of the F/G loop is unresolved and the binding mode of the substrate remains unknown. To this end, crystallization of all components of the P450terp system was attempted. However, the only successful conditions were the repetition of the structure in the substrate free form which showed no deviation from the previous solution, and terpredoxin.

Structure of Tdx

Like many ferredoxins, terpredoxin is a relatively small Fe_2S_2 protein with high acidic amino acid content (pI = 3.8). Its iron-sulfur cluster is ligated by four of five total cysteines present in the protein: C39, C45, C48, C86 and C43 is non-ligating. While initially expressed and purified as the wild-type (WT) protein, crystallization of WT (even in the presence of excess dithiothreitol) led to small needle-like crystals that could not be easily separated and thus did not lend themselves to diffraction. This is similar to the situation encountered with the crystallization of putidaredoxin (Pdx), the native redox partner of P450cam.[13] In Pdx, there are six cysteine residues, and in order to achieve long-term stability and successful crystallization conditions, the two non-ligating cysteines were mutated to serines (C75S and C85S). It was believed that these

free cysteines may be reactive and contribute to the formation of intermolecular disulfide bridges. As Tdx also possesses one non-ligating cysteine (C43), mutation of this residue was hypothesized to improve the overall stability and aid in crystallization of the protein.

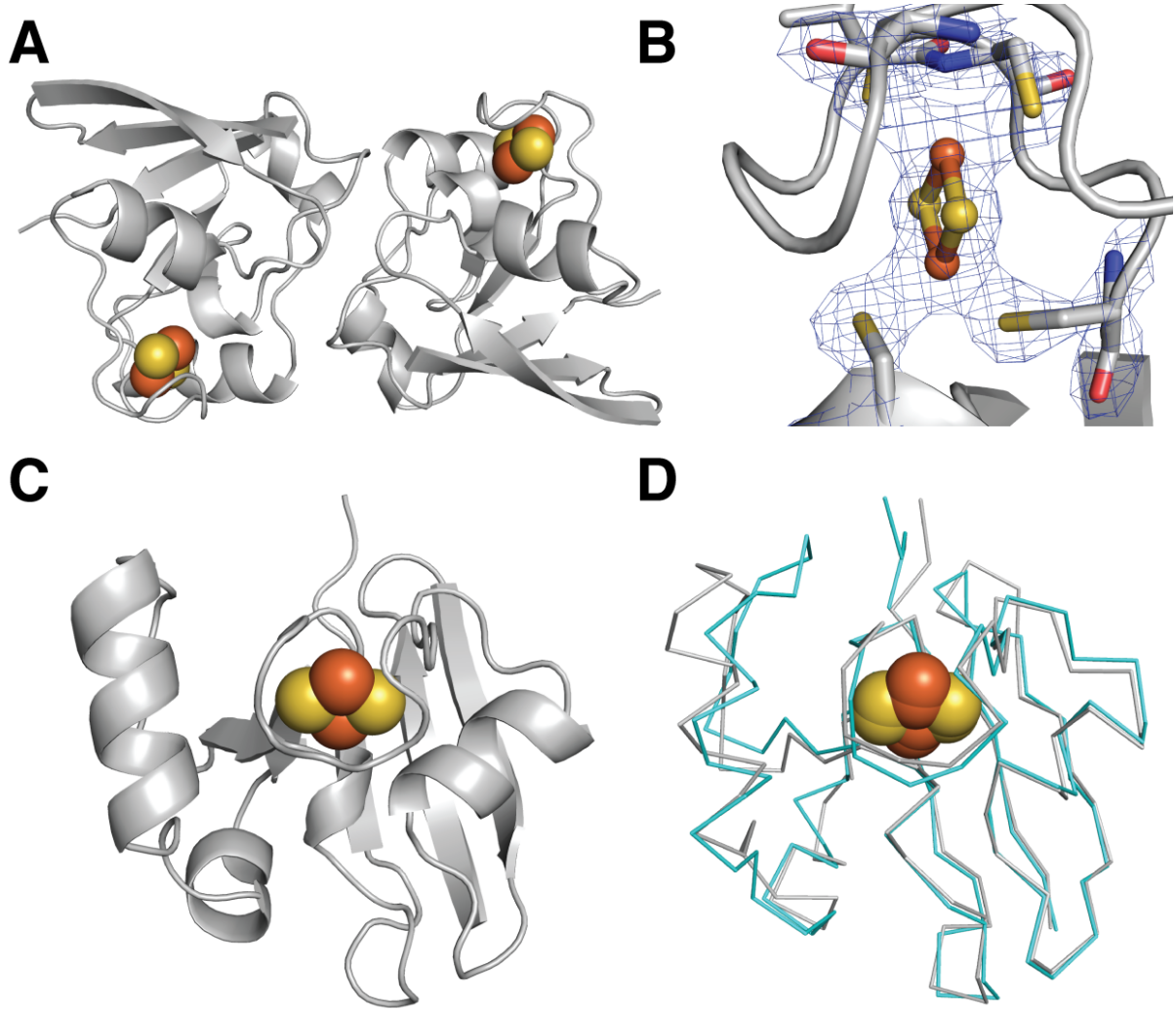

Figure 4-2. (A) Asymmetric unit of the C43S Tdx forms a dimer similar to Pdx. **(B)** The $2F_o$-F_c electron density map at the [2Fe–2S] cluster in the Tdx structure contoured at 1 σ. **(C)** Alternative view of a cartoon representation of a monomer of Tdx. **(D)** An overlay of the ribbon structure C73S/C85S Pdx crystal structure (PDB: 1XLO) (cyan) and C43S Tdx (gray).

The Tdx C43S mutant yielded small plate-like crystals that diffracted to 2.15 Å. Pdx and Tdx share 36% sequence identity. However, attempts to utilize either the NMR solution structure or Pdx as molecular replacement search models were unsuccessful. However, bioinformatic analyses revealed a ferredoxin from *Rhodobacter capsultus* possessing a 41% sequence identity with a crystal structure available. FdxE or Ferredoxin-6 (PDB: 1E9M) was used a successful molecular replacement search model.[14]

Modeling of the Complex

Utilizing the crystal structure of P450terp (PDB: 1CPT) and the crystal structure of Tdx-C43S, we can construct a model of the potential complex based on the structure of P450cam-Pdx.[3] We find that, while the RMSD is 0.65 Å between Pdx and Tdx and critical electron transfer residues are conserved in each P450, these two ferredoxins have significantly different interfaces presented to their respective P450s (Fig 4-3). In particular, at the C-terminus of Pdx is a tryptophan residue (Trp-106) which is necessary for the effector role that regulates ET.[3, 7] This residue is not present in Tdx. Not only is it not present, the C-terminus of Tdx ends in an alanine (A105 which was disordered within our structure) and does not extend to reach to potential interface between the two proteins. Additionally, arginine-66 of Pdx forms an ion pair with glutamate-76 of P450cam while Tdx-P450terp has a potential charge reversal of this ion pair with aspartate-66 of Tdx and lysine-65 of P450terp. While the analogous residue to Asp38 of Pdx is a glutamate (E38) in Tdx, this residue has been shown to be critical for activity and highly sensitive to mutation.[16]

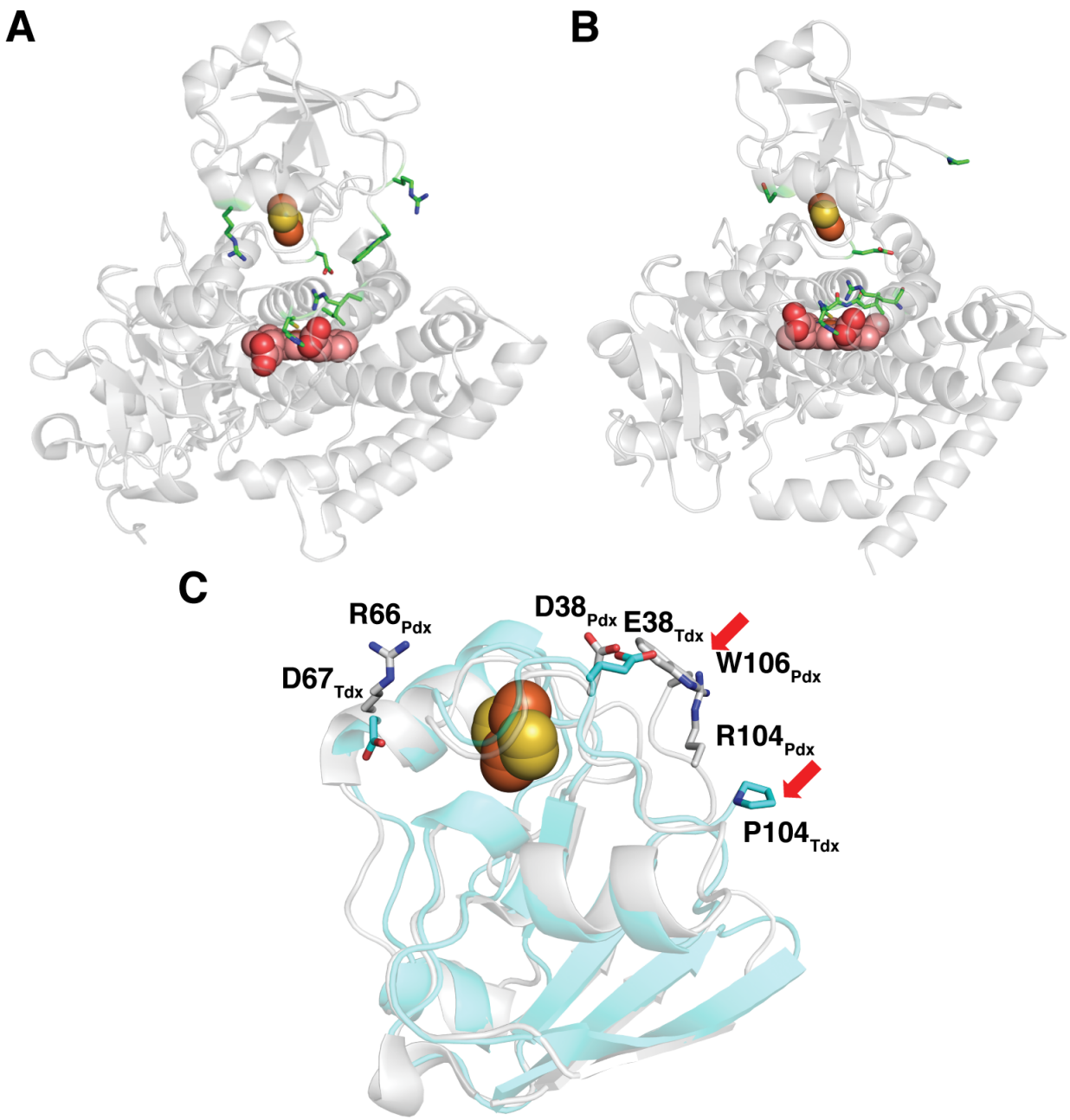

Figure 4-3. (A) P450cam-Pdx complex with interface residues highlighted in green with heme in pink spheres (PDB: 4JWS). **(B)** Modelled complex of P450terp-Tdx based on P450cam complex with analogous residues highlighted in green sticks. **(C)** Superposition of Tdx on Pdx from complex (4JWS) (gray) and Tdx (cyan). Key residues in Pdx that interact with P450cam are shown in sticks and their analogous residues in Tdx. C-termini are shown with red arrows.

Additionally, it is known that crystals of oxidized ferredoxins, such as Pdx, undergo significant photoreduction upon exposure to synchrotron radiation.[15] As such, Tdx is assumed to be in the reduced conformation as no precautions were taken to minimize this process. This is partially justified by the geometry of the C45-A46 peptide. Upon reduction, ferredoxins, including Pdx, a peptide bond flips to readjust the hydrogen bonding to the sulfurs of both the cluster and ligating cysteine residues. This was originally documented in *Anabena* PCC7119 where, upon reduction, the Cys46-Ser47 peptide bond flips to provide a hydrogen bond to sulfur S1 and stabilize the increased negative charge on the cofactor.[15] The same conformational change of Cys45-Ala46 has been documented in Pdx.[16] In the Tdx-C43S structure, the Cys45-Ala46 peptide is in the CO-out conformation and A46's nitrogen is 3.3 Å from sulfur 1 of the cluster supporting a reduced state.

Stability of the Oxygen Complex of P450terp

One of the first ways the effector role of Pdx was demonstrated was by the destabilization of the oxygenated complex of P450cam in the presence of camphor.[17] Presumably, oxidized Pdx should not react with the oxycomplex of P450cam. However, oxidized Pdx accelerates the decay of the oxycomplex P450 by 150-fold. We hypothesize that this rate acceleration is due to the conformational change induced by Pdx, which from both crystallographic and spectroscopic studies is a closed to open transition.[3, 17-18] Thus, Pdx opens the active site and accelerates the oxidation of the oxycomplex back to the ferric high spin resting state. A similar effect was observed in the P450cam homologue, CYP101D1, and its native redox partner Arx. In the case of 101D1, the decay rate of the oxycomplex was accelerated ~33-fold in the presence of Arx.[19]

However, by UV-vis and resonance Raman spectroscopic experiments, the effector role of Arx pushes CYP101D1 towards a high-spin state; opposite of Pdx's influence on P450cam which increases of the population of the low-spin species.[19]

In an effort to understand if a similar effector role is exhibited by terpredoxin on P450terp

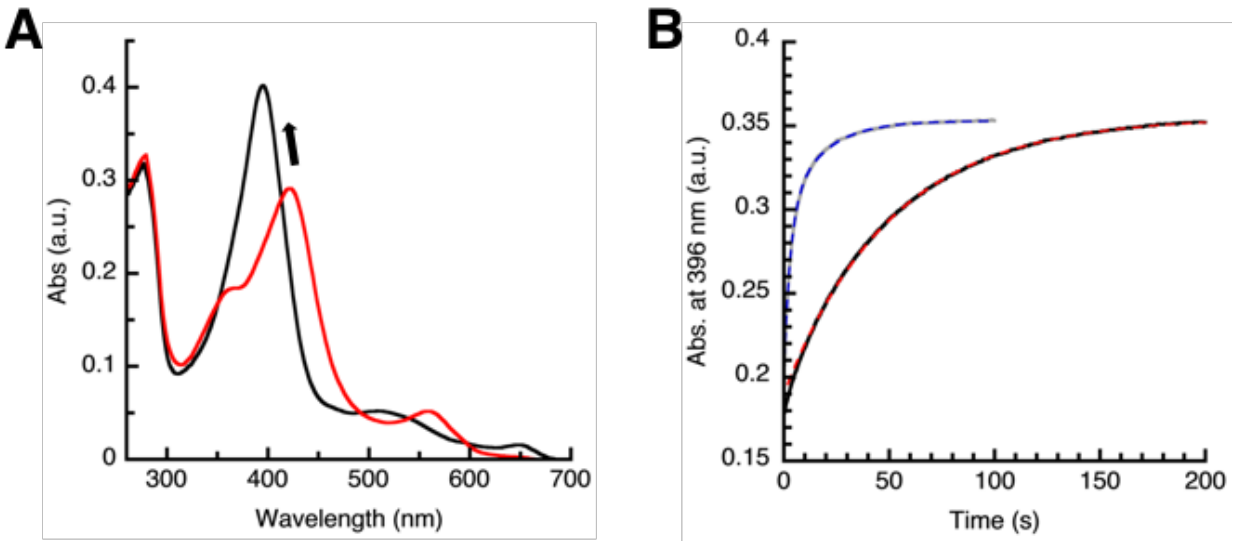

Figure 4-4. (A) Oxy-P450terp (red) decays to high-spin ferric P450terp (black). **(B)** Decay of the oxycomplex in the absence (data-black solid, fit-red dashed) and presence of two-fold Tdx (data- solid gray, fit- dashed blue) at room temperature (23 ˚C).

in the absence of a complex crystal structure, the decay of the oxygenated complex of P450terp was monitored by stopped-flow UV-vis spectroscopy. Terpredoxin exhibits a similar effect as Pdx and Arx, but its effect is not as pronounced. Addition of a 2-fold excess of oxidized Tdx to P450terp decreases the stability of the oxy complex by ~16-fold with rate of 0.3200 ± 0.04 s^{-1} compared to an autooxidation rate of 0.0212 ± 0.002 s^{-1} in the absence of Tdx (Fig 4-4). While the destabilization is not as prominent as P450cam or 101D1, it is significantly faster than the rate of

auto-oxidation and suggests that Tdx may exhibit a similar conformational change in P450terp as is observed in P450cam.

NADH Oxidation

Associated with the conformational change induced by Pdx, a hallmark feature of the P450cam system is the lack of cross-reactivity with any ferredoxin other than its native Pdx.[20-22] To examine whether this selectivity is generalizable to other P450s, P450terp was tested for cross-reactivity with a selection of redox partners from homologous systems. The standard method for examining selectivity is monitoring the substrate dependent consumption of NAD(P)H by its characteristic absorbance at 340 nm. In these experiments, NADH is incubated in the presence of all of the protein components required for turnover of substrate and a background rate of NADH oxidation is determined. After mixing and incubation, substrate is added to the reaction. If the redox partner can successfully provide electrons for turnover to the P450, there is a substantial increase in the rate of NAD(P)H oxidation. These rates are reported

Reductase	**Redoxin**	**P450**	**NADH (min^{-1})**
TdR	Tdx	P450terp	691.72 ± 24.716
PdR	Pdx	P450terp	N.R.
FldR*	Cdx	P450terp	N.R.
ArR	Arx	P450terp	272.5 ± 12.75
TdR	Tdx	P450cam	N.R.
TdR	Tdx	P450cin	N.R.
TdR	Tdx	P450lin	N.R.
PdR	Pdx	P450cam	973.08 ± 146.15

Table 4-1. Substrate dependent NADH oxidation rates. *-NADPH. N.R- No Reactivity.

in Table 4-1. Of the systems tested, only the native system, Tdx, and Arx, from the 101D1 system, allowed for successful NADH consumption. However, the observation that P450terp exhibits cross-reactivity with Arx contradicts the current hypothesis of redox partner selectivity to preserve energetic equivalents. Moreover, Arx was also shown to exhibit cross reactivity with another *Pseudomonad* P450, P450lin that oxidizes a monoterpene, linalool, which it can utilize as its sole carbon source (data not shown). Additionally, Tdx was not able to provide electrons to the homologous P450s.

Conclusion

Our initial hypothesis was that *Pseudomonad* P450s that are plasmid borne and function as the first step of oxidative assimilation of a non-glucose carbon source are necessarily tightly coupled and selective for their redox partners in order to prevent the wasting of valuable energetic equivalents (i.e. NAD(P)H). Additionally, we hypothesized that this selectivity is conformationally regulated. However, the extreme selectivity for redox partner may not extend beyond P450cam as Arx is able to pass electrons to P450terp and P450lin. While the degree of coupling of non-native redox partners remains to be determined, it appears that there still is a degree of selectivity and that some form conformational regulation may be involved. Preliminary resonance Raman data suggest that the behavior of P450terp may be similar to CYP101D1 upon redox partner binding, where the high spin fraction is increased upon introduction of redox partner exactly the opposite of P450cam.

Materials and Methods

Terpredoxin Reductase (TdR)

A pET-28A expression vector containing TdR gene with a thrombin cleavable N-terminal His-tag was ordered from GenScript. The plasmid was transformed into *E. coli* C41 cells. A 100 mL starter culture was inoculated and shaken at 180 rpm overnight at 37° C. The starter culture was used to inoculate 7 L of TB media and the cells were grown at 37° C at 225 rpm to an optical density (OD) of ≥1.0 before induction via 1mM IPTG. At this time, growth conditions were slowed to 80 rpm and cooled to 18° C. Cells were harvested after 48 hours. The cells were broken by microfluidization, high-speed centrifuged, and the supernatant was loaded onto a Nickel-NTA column. TdR was washed with buffer containing increasing concentrations of imidazole in a step-wise fashion until elution with 150 mM imidazole. To remove the His-tag, a thrombin digest (50:1) was performed for 2 hours at room temperature. Completion of digestion was assessed by MALDI-TOF mass spectrometry. TdR was loaded back on to the Ni-NTA column and the flow through was collected. The protein was concentrated and purified further by size-exclusion chromatography. Purified protein was assessed by SDS-PAGE and UV-vis spectroscopy (Fig 4-5). In addition, the extinction coefficient was determined by denaturation assay[23] to be 12.2 $mM^{-1}cm^{-1}$ at 455nm.

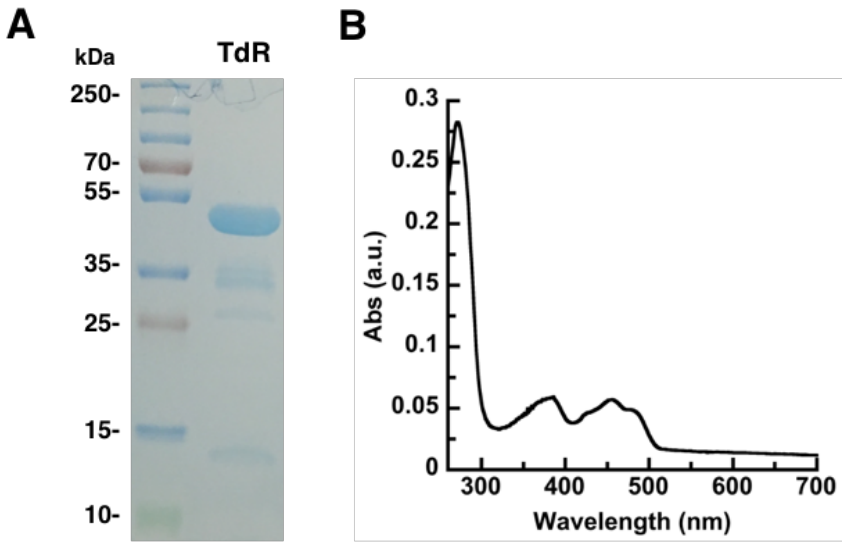

Figure 4-5. (A) SDS-PAGE gel of Terpredoxin Reductase. **(B)** UV-vis spectrum of TdR.

Terpredoxin (Tdx)

A pET-28A expression vector containing Tdx gene with a thrombin cleavable N-terminal His-tag was ordered from GenScript. This expression vector did not work and the Tdx gene was cloned (*vide infra*) into a pET-17b vector with no His-tag. The plasmid was transformed into *E. coli* C41 cells. A 100 mL starter culture was inoculated and shaken at 180 rpm overnight at 37° C. The starter culture was used to inoculate 14 L of 2xYT media and the cells were grown at 23° C (RT) at 80 rpm for 48 hours. The flasks were then removed and allowed to stand for 2 days. Cells were then harvested, washed with 20 mM potassium phosphate buffer (KPi) pH 7.4 containing 5 mM DTT, and lysed by microfluidization. Cell lysate was centrifuged and the supernatant was loaded on to DE-52 anionic exchange column. The column was washed with an excess of buffer (20 mM KPi pH 7.4, 5 mM DTT) and the brown band (Tdx) was excised and loaded onto a clean

DE-52 column. The protein was eluted with a gradient of 0-600 mM KCl. Fractions exhibiting $A_{280/415}$>0.3 were combined and concentrated then loaded onto a Q-sepharose column. The column was washed with 20 mM Kpi pH 7.4, 50 mM KCl, 5 mM DTT and eluted over a gradient of 0-600mM KCl. Fractions with $A_{280/415}$>0.6 were combined, concentrated, and purified further by size-exclusion chromatography. Purified protein was assessed by SDS-PAGE and UV-vis spectroscopy (Fig 4-6). In addition, the extinction coefficient was determined by BCA assay to be 6.5 $mM^{-1}cm^{-1}$ at 415 nm.

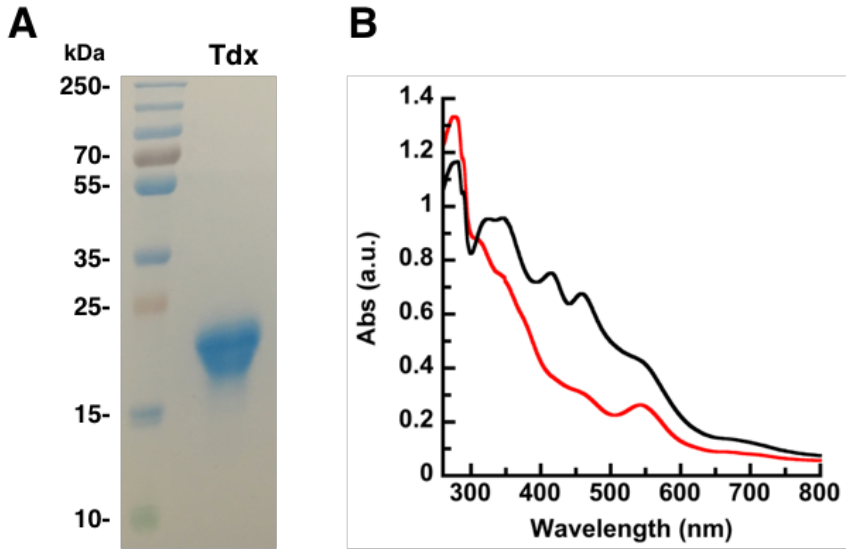

Figure 4-6. (A) SDS-PAGE gel of Terpredoxin. **(B)** UV-vis spectrum of oxidized (black) and reduced (red) Tdx.

Cloning of Tdx from pET-28A to pET-17b

The pET-28a plasmid was digested with restriction enzymes NDE1 and XHO1 for 2 hours at 37 ˚C. The digestion products were run on a 0.8 % agarose gel, extracted and purified with a

Nucleospin gel extraction kit. Purification was assessed by an additional 0.8% agarose gel. Ligation into the pET-17b plasmid was performed overnight at 15 ˚C. The ligated mixture was transformed into competent Gold cells. Successful transformations were confirmed by blue-white X-gal assay.

Site-directed mutagenesis of Tdx-WT to C43S

Tdx plasmid (100 ng/µL) was incubated with PFU Turbo DNA polymerase and 20 µM of forward and reverse primers: F: 5'-GTGCGGCGGCTCAAGTGTCTGCGCTAC-3', R: 5'-GTAGCGCAGACACTTGAGCCGCCGCAC-3'. The reaction mixture was PCR cycled for 18 rounds with a Tm of 68 ˚C. The mixture was DPN1 digested for two hours at 37 ˚C. The reaction mixture was plated on antibiotic resistant LB plates. Successful transformants were confirmed by gene-sequencing.

P450terp

A pET-28A expression vector containing P450terp gene with a thrombin cleavable N-terminal His-tag was ordered from GenScript. The plasmid was transformed into *E. coli* C41 cells. A 100 mL starter culture was inoculated and shaken at 180 rpm overnight at 37° C. The starter culture was used to inoculate 7 L of TB media and the cells were grown at 37° C at 225 rpm to an optical density (OD) of ≥1.0 before induction via 1 mM IPTG and supplemented with 1 mM D-aminolevulinic acid (D-ALA). At this time, growth conditions were slowed to 80 rpm and cooled to 18° C. Cells were harvested after 48 hours. The cells were broken by microfluidization and high-speed centrifuged. The supernatant was brought to 30% ammonium sulfate and clarified by centrifugation. The soluble cut was brought to 40% ammonium sulfate and centrifuged. The

supernatant of the 40% cut was loaded onto a Nickel-NTA column. The column was washed with lysis buffer (50 mM KPi pH 7.4, 100 mM KCl, 5 mM βME) and protein was eluted from Ni-NTA column using a 0-30 mM histidine-free base. Fractions with $A_{418/280}$>1.2 were collected, concentrated, and loaded onto DEAE column and washed with buffer. Protein was eluted from the column with a gradient of 0-500 mM KCl. Total protein content was calculated and a thrombin digest (50:1) was performed for 12 hours at 4° C and digestion was confirmed by MALDI-TOF mass spectrometry. After digestion, the protein was loaded back onto a Ni-NTA column and washed and eluted with a gradient of 0-5 mM His-free base. Fractions with $A_{418/280}$>1.4 were combined and concentrated and purified further by size-exclusion chromatography. Protein concentration was determined using previously determined extinction coefficients ε_{418}=120 mM^{-1} cm^{-1} (substrate free) and ε_{396}= 96 mM^{-1} cm^{-1} (substrate bound).[6]

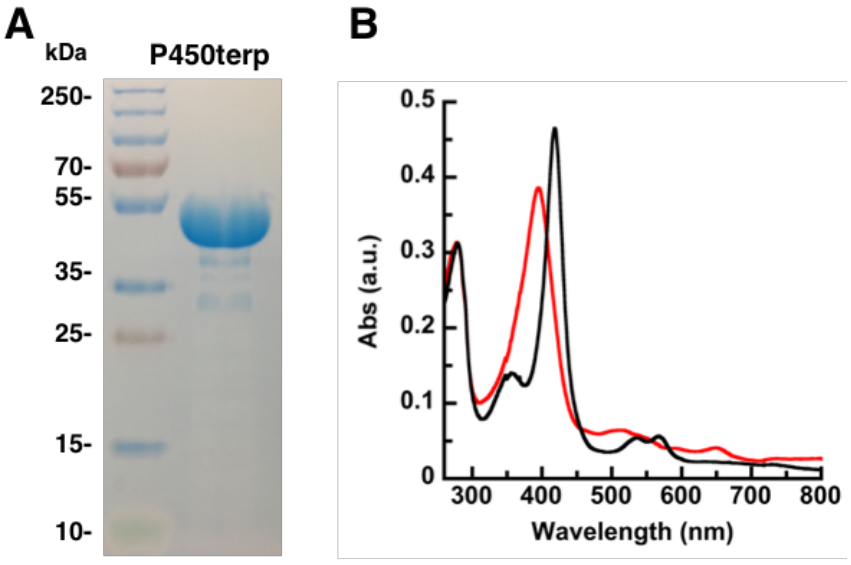

Figure 4-7. (A) SDS-PAGE gel of P450terp. **(B)** UV-vis spectrum of substrate free (black) and α-terpineol bound (red) P450terp.

Crystallization of Tdx C43S:

Tdx C43S was crystallized at a concentration of 13 mg/mL in 1.6 M Na_3Citrate pH 6.5 in a hanging drop tray by vapor diffusion with a protein:precipitant ratio of 1:1. Crystals of Tdx C43S were cryoprotected into paratone oil before flash freezing in liquid nitrogen.

Table 4-2. X-ray crystallography data collection and refinement statistics for Tdx-C43S structure. Values in parentheses are for the highest resolution shell.

	Tdx C43S
Data collection	
Space group	P 21 21 21
Cell dimensions	
a, b, c	30.97 80.45 86.14
α, β, γ	90, 90, 90
Resolution (Å)	37.97 - 2.15 (2.227 - 2.15)
R_{merge}	10.6 (81.57)
Total reflections	23412 (2110)
Unique reflections	11865 (1084)
$CC_{1/2}$	0.989 (0.619)
I/σ	4.78 (0.84)
Completeness	96.00 (89.64)
Redundancy	2.0 (1.9)
Refinement	
R_{work}/R_{free}	0.2147 (0.3184) / 0.2680 (0.3185)
Number of atoms	1595
Protein	1532
Water	55
Ligands	8
RMSD Bond lengths (Å)	0.010
RMSD Bond angles	1.30
Average B factor	33.12
Ramachandran Favored/Outliers (%)	95.59/ 0.00

Data Collection and Refinement

Data were collected from single crystals at the Advanced Lightsource (ALS) beamline 8.2.1. Diffraction images were indexed, integrated, and scaled using Mosflm.[24] The 1E9M crystal structure without cofactor was used as a search model in molecular replacement using Phaser.[25] The final structure contains two molecules of the Tdx per asymmetric unit. The Phenix suite[25] was used for structure refinement. All reflections were used for refinement except for 5% excluded for R_{free} calculations. The structural model was revised in real space with the program COOT[26] based on $2F_o$-F_c and F_o-F_c electron density maps. The final refinement statistics are given in Table 4-2. The final structure was refined to 2.15 Å resolution with an R_{free} of 21.5% and R_{work} of 26.8%.

Stopped Flow Kinetics

Oxygen complex formation and decay were measured using an SX.18MV stopped flow apparatus from Applied Photophysics at 23 °C. Briefly, ferric P450terp in buffer [50 mM potassium phosphate (pH 7.4) and 1 mM α-terpineol] was first degassed and purged with argon and then reduced inside an anaerobic cuvette and monitored on an Agilent Cary 300 UV-vis spectrophotometer by careful titration with a 5 mM sodium dithionite stock (in the same buffer). Stopped flow syringes were washed first with a 5 mM sodium dithionite solution to remove oxygen followed by washing with degassed and nitrogen-purged buffer 50 mM potassium phosphate (pH 7.4) and 1 mM α-terpineol to wash away the dithionite. First, reduced ferrous P450terp in 50 mM potassium phosphate (pH 7.4) and 1 mM α-terpineol was mixed with the

same air-saturated buffer to form the oxy complex. In the second experiment, the reduced ferrous P450terp was mixed with air-saturated buffer that contained a 2-fold excess of oxidized Tdx to compare the stability of the oxygen complex in the presence Tdx. The final concentrations of P450terp and Tdx after mixing in the stopped flow were around 4 and 8 μM, respectively. Data were fitted using Sigma Plot.

NADH Consumption Assays

NADH oxidation rates for P450terp enzymes were determined in steady state kinetic experiments using a Reductase/Ferredoxin (Flavodoxin)/P450 system in a 1:10:1 ratio, respectively. Experiments were performed as previously described.[27] In brief, all enzymatic components were added at a ratio of 0.5 μM: 5 μM: 0.5 μM and mixed. 200 μM NAD(P)H was then added to the cuvette, mixed, and the 340 nm absorbance was monitored. This provides a background NAD(P)H oxidation rate. After a minute or more, substrate for the P450 was introduced, mixed, and the rate of NAD(P)H oxidation was measured as a function of decrease in 340 nm absorbance.

References

1. Sevrioukova, I. F.; Li, H.; Zhang, H.; Peterson, J. A.; Poulos, T. L., Structure of a cytochrome P450-redox partner electron-transfer complex. *Proc. Natl. Acad. Sci. U. S. A.* **1999,** *96* (5), 1863.
2. Strushkevich, N.; MacKenzie, F.; Cherkesova, T.; Grabovec, I.; Usanov, S.; Park, H. W., Structural basis for pregnenolone biosynthesis by the mitochondrial monooxygenase system. *Proc. Natl. Acad. Sci. U. S. A.* **2011,** *108* (25), 10139.
3. Tripathi, S.; Li, H.; Poulos, T. L., Structural basis for effector control and redox partner recognition in cytochrome P450. *Science* **2013,** *340* (6137), 1227.
4. Prasad, B.; Rojubally, A.; Plettner, E., Identification of camphor oxidation and reduction products in Pseudomonas putida: new activity of the cytochrome P450cam system. *J Chem Ecol* **2011,** *37* (6), 657-67.

5. Balaraman, P.; Plettner, E., Chemotaxis by Pseudomonas putida (ATCC 17453) towards camphor involves cytochrome P450cam (CYP101A1). *Biochim Biophys Acta Gen Subj* **2019,** *1863* (2), 304-312.
6. Peterson, J. A.; Lu, J. Y.; Geisselsoder, J.; Graham-Lorence, S.; Carmona, C.; Witney, F.; Lorence, M. C., Cytochrome P-450terp. Isolation and purification of the protein and cloning and sequencing of its operon. *Journal of Biological Chemistry* **1992,** *267* (20), 14193-14203.
7. Stayton, P. S.; Sligar, S. G., Structural microheterogeneity of a tryptophan residue required for efficient biological electron transfer between putidaredoxin and cytochrome P-450CAM. *Biochemistry* **1991,** *30* (7), 1845-1851.
8. Hasemann, C. A.; Ravichandran, K. G.; Peterson, J. A.; Deisenhofer, J., Crystal structure and refinement of cytochrome P450terp at 2.3 A resolution. *J Mol Biol* **1994,** *236* (4), 1169-85.
9. Boddupalli, S. S.; Hasemann, C. A.; Ravichandran, K. G.; Lu, J. Y.; Goldsmith, E. J.; Deisenhofer, J.; Peterson, J. A., Crystallization and preliminary x-ray diffraction analysis of P450terp and the hemoprotein domain of P450BM-3, enzymes belonging to two distinct classes of the cytochrome P450 superfamily. *Proc Natl Acad Sci U S A* **1992,** *89* (12), 5567-71.
10. Sevrioukova, I. F.; Peterson, J. A., Reaction of carbon monoxide and molecular oxygen with P450terp (CYP108) and P450BM-3 (CYP102). *Arch Biochem Biophys* **1995,** *317* (2), 397-404.
11. Fruetel, J. A.; Mackman, R. L.; Peterson, J. A.; Ortiz de Montellano, P. R., Relationship of active site topology to substrate specificity for cytochrome P450terp (CYP108). *J Biol Chem* **1994,** *269* (46), 28815-21.
12. Mo, H.; Pochapsky, S. S.; Pochapsky, T. C., A Model for the Solution Structure of Oxidized Terpredoxin, a Fe2S2 Ferredoxin from Pseudomonas. *Biochemistry* **1999,** *38* (17), 5666-5675.
13. Sevrioukova, I. F.; Garcia, C.; Li, H.; Bhaskar, B.; Poulos, T. L., Crystal structure of putidaredoxin, the [2Fe-2S] component of the P450cam monooxygenase system from Pseudomonas putida. *J Mol Biol* **2003,** *333* (2), 377-92.
14. Armengaud, J.; Sainz, G.; Jouanneau, Y.; Sieker, L. C., Crystallization and preliminary X-ray diffraction analysis of a [2Fe-2S] ferredoxin (FdVI) from Rhodobacter capsulatus. *Acta Crystallogr D Biol Crystallogr* **2001,** *57* (Pt 2), 301-3.
15. Morales, R.; Charon, M.-H.; Hudry-Clergeon, G.; Pétillot, Y.; Norager, S.; Medina, M.; Frey, M., Refined X-ray Structures of the Oxidized, at 1.3 Å, and Reduced, at 1.17 Å, [2Fe−2S] Ferredoxin from the Cyanobacterium Anabaena PCC7119 Show Redox-Linked Conformational Changes. *Biochemistry* **1999,** *38* (48), 15764-15773.
16. Sevrioukova, I. F., Redox-dependent Structural Reorganization in Putidaredoxin, a Vertebrate-type [2Fe-2S] Ferredoxin from Pseudomonas putida. *Journal of Molecular Biology* **2005,** *347* (3), 607-621.
17. Lipscomb, J. D.; Sligar, S. G.; Namtvedt, M. J.; Gunsalus, I. C., Autooxidation and hydroxylation reactions of oxygenated cytochrome P-450cam. *J. Biol. Chem.* **1976,** *251* (4), 1116.
18. Unno, M.; Christian, J. F.; Benson, D. E.; Gerber, N. C.; Sligar, S. G.; Champion, P. M., Resonance Raman Investigations of Cytochrome P450cam Complexed with Putidaredoxin. *J. Am. Chem. Soc.* **1997,** *119* (28), 6614.

19. Batabyal, D.; Lewis-Ballester, A.; Yeh, S.-R.; Poulos, T. L., A Comparative Analysis of the Effector Role of Redox Partner Binding in Bacterial P450s. *Biochemistry* **2016,** *55* (47), 6517-6523.
20. Tyson, C. A.; Lipscomb, J. D.; Gunsalus, I. C., The Roles of Putidaredoxin and P450cam in Methylene Hydroxylation. *Journal of Biological Chemistry* **1972,** *247* (18), 5777-5784.
21. Geren, L.; Tuls, J.; O'Brien, P.; Millett, F.; Peterson, J. A., The involvement of carboxylate groups of putidaredoxin in the reaction with putidaredoxin reductase. *Journal of Biological Chemistry* **1986,** *261* (33), 15491-5.
22. Tsai, R. L.; Gunsalus, I. C.; Dus, K., Composition and structure of camphor hydroxylase components and homology between putidaredoxin and adrenodoxin. *Biochemical and Biophysical Research Communications* **1971,** *45* (5), 1300-1306.
23. Prongay, A. J.; Engelke, D. R.; Williams, C. H., Jr., Characterization of two active site mutations of thioredoxin reductase from Escherichia coli. *J Biol Chem* **1989,** *264* (5), 2656-64.
24. Battye, T. G.; Kontogiannis, L.; Johnson, O.; Powell, H. R.; Leslie, A. G., iMOSFLM: a new graphical interface for diffraction-image processing with MOSFLM. *Acta Crystallogr., Sect. D: Biol. Crystallogr.* **2011,** *67* (4), 271.
25. Adams, P. D.; Afonine, P. V.; Bunkoczi, G.; Chen, V. B.; Davis, I. W.; Echols, N.; Headd, J. J.; Hung, L. W.; Kapral, G. J.; Grosse-Kunstleve, R. W.; McCoy, A. J.; Moriarty, N. W.; Oeffner, R.; Read, R. J.; Richardson, D. C.; Richardson, J. S.; Terwilliger, T. C.; Zwart, P. H., PHENIX: a comprehensive Python-based system for macromolecular structure solution. *Acta Crystallogr., Sect. D: Biol. Crystallogr.* **2010,** *66* (2), 213.
26. Emsley, P.; Cowtan, K., Coot: model-building tools for molecular graphics. *Acta Crystallogr., Sect. D: Biol. Crystallogr.* **2004,** *60* (12), 2126.
27. Bell, S. G.; Dale, A.; Rees, N. H.; Wong, L. L., A cytochrome P450 class I electron transfer system from Novosphingobium aromaticivorans. *Appl Microbiol Biotechnol* **2010,** *86* (1), 163-75.

Chapter 5

CYP102L1 and the occurrence of P450s in viruses

Introduction

Cytochromes P450 are ubiquitous throughout the biosphere and recently their prevalence has been extended to life's gray area of viruses.[1-2] However, their role in viral biology remains unclear. Recently, Lamb *et al.* reported unique P450s in megaviral genomes that inhabit amoeba.[2] Since this report, a growing number of genes encoding for unique potential P450s in both giant and non-giant viruses have been annotated. In particular, one bacteriophage, *Mycobacterium phage Adler*, which infects *Mycobacteroides* (previously *Mycobacterium*) *abscessus subsp. bolletii* F1660, has a gene predicted to encode a cytochrome P450 (Genbank protein accession number AHB79207; genome sequence locus tag: CH35_gp012). The predicted 471 amino acid protein defines a new CYP102 subfamily and gene, CYP102L1, within the broader CYP102 family. A P450 subsequently found in the mycobacterial host is 98% identical to the phage P450 and, therefore, it is also classified as CYP102L1 (Fig 5-2A). Additional members of the new CYP102L subfamily (CYP102L1-8) have now been found in other *Mycobacterioides* species (Fig 5-5). The phage CYP102L1 shows lower sequence identity with genes in other CYP102 subfamilies (CYP102AZ). It shares only 34% identity yet retains remarkable structural similarity with the P450 domain of CYP102A1 (P450BM3), an extensively characterized P450 (Fig 5-2B).

This chapter reports the structure and analysis of CYP102L1 along with the binding of several fatty acids and discuss the potential consequences of cytochromes P450 in viruses.

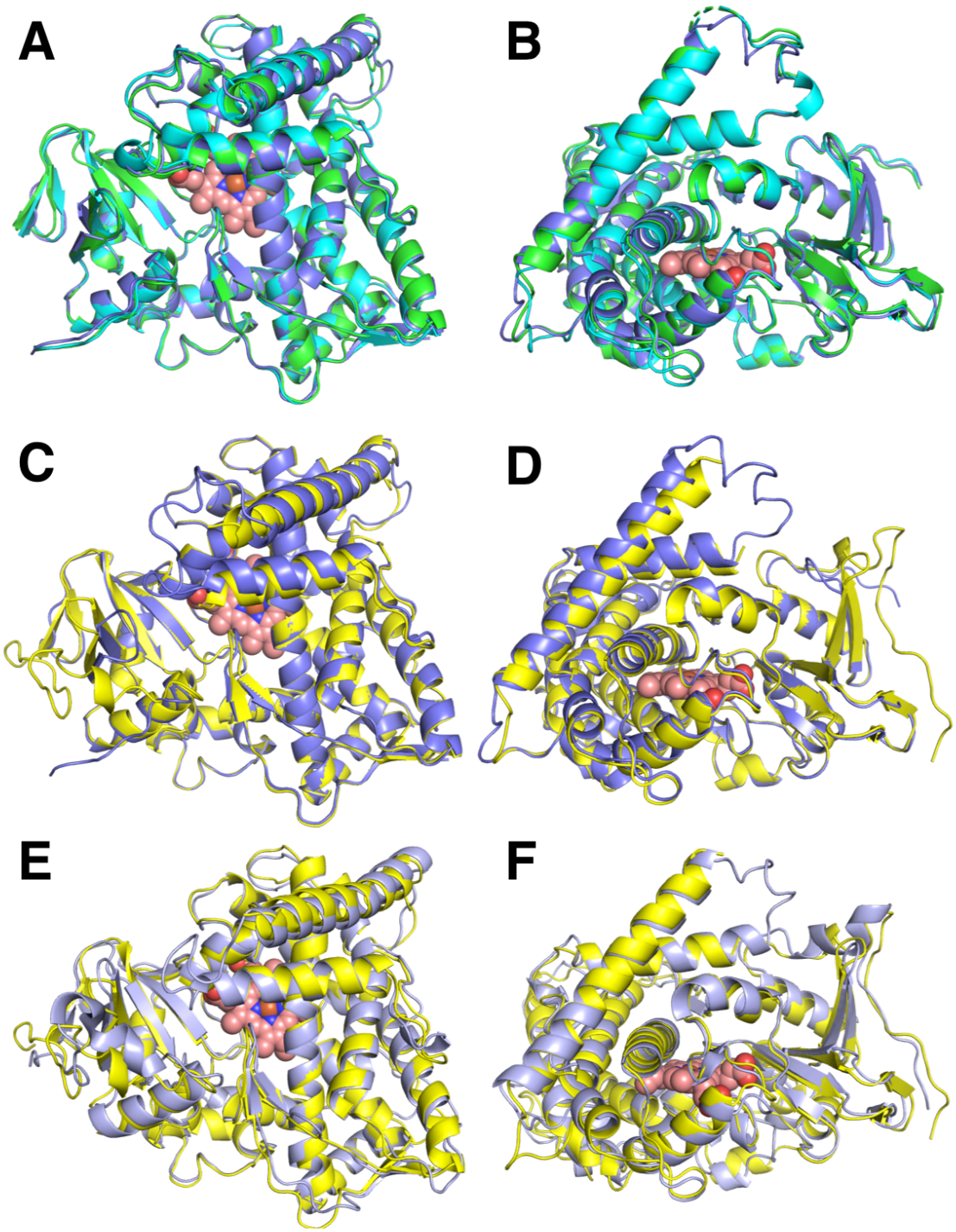

Figure 5-1. Top-down **(A)** and side-on **(B)** overlay of CYP102L1 chains A (blue), C (cyan), and D (green). Top-down **(C)** and side-on **(D)** overlay of CYP102L1 chains A (blue), and B (yellow). Top-down **(E)** and side-on **(F)** overlay of CYP102L1 chain B (yellow) and CYP102A1 (pale blue).

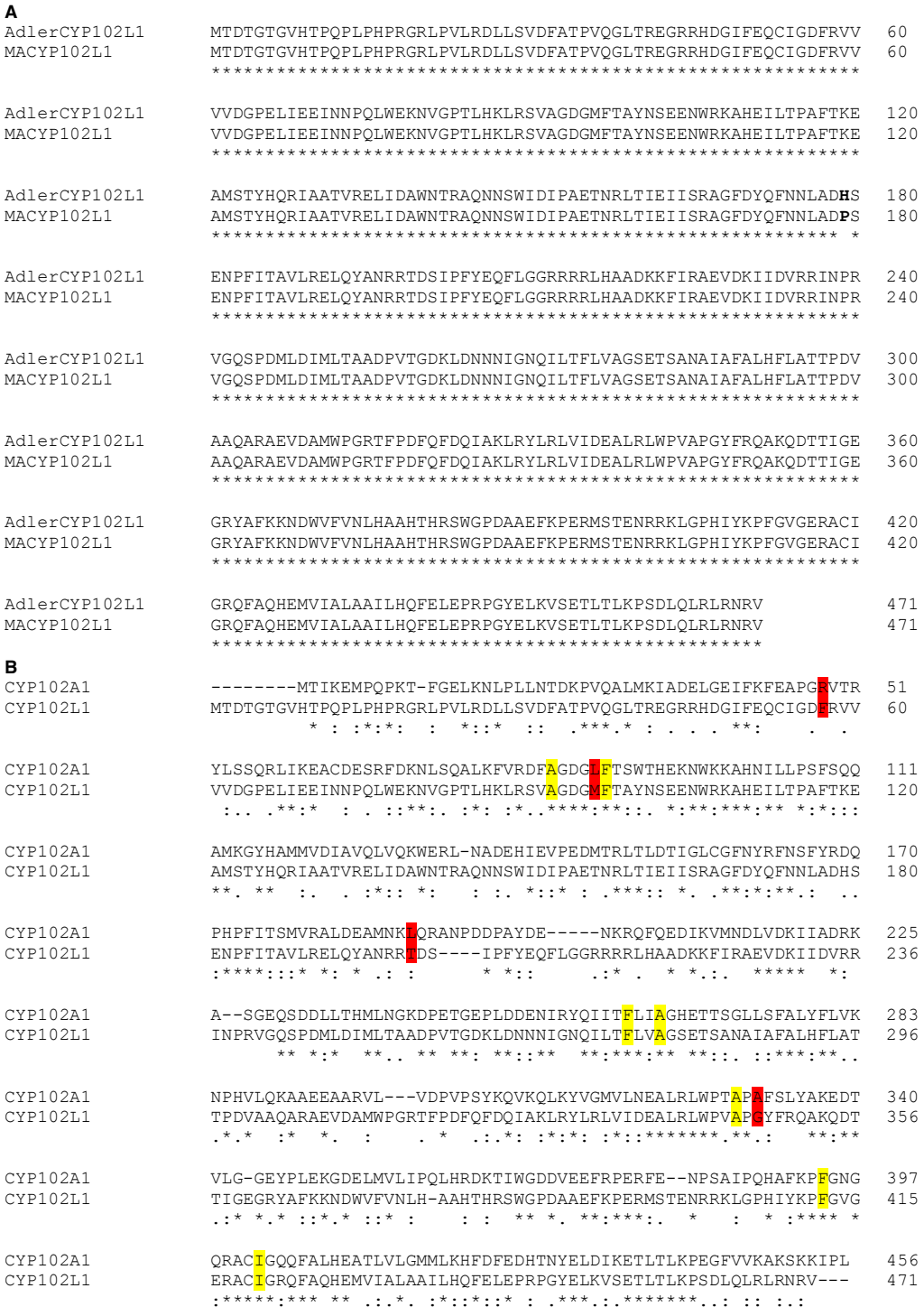

Figure 5-2 (A) Alignment of amino acid sequences of *Mycobacteria phage Adler* CYP102L1 and the wild-type *Mycobacteroides abscessus subsp. bolletii* CYP102L1 showing the substitution of the proline to histidine (red) in the viral P450. **(B)** Amino acid sequence alignment of *Mycobacteria phage Adler* CYP102L1 against the B. megaterium CYP102A1 heme domain. Critical residues of 102A1 are highlighted with conserved residues in yellow and mutations in red.

Structure and function of mycophage CYP102L1

The protein in the open state was crystallized and the structure was determined by single-wavelength anomalous diffraction (SAD) and was refined with a maximum resolution of 2.5 Å. The overall structure of the CYP102L1 exhibits the typical P450 fold consisting of α-helical and β sheet domains as seen in all other known archaeal, bacterial, and eukaryotic P450 structures (Fig 5-1).[1] The heme cofactor is located between the α-helical domain and the β-sheet domain to create a substrate-binding pocket. The CYP102L1 has a conserved cysteine (Cys419) that serves as the fifth axial thiolate ligand to the heme iron, as in all P450s. The structure solved is strikingly similar to that for the P450 domain of the *Bacillus megaterium* CYP102A1 (Fig 5-1E,F).

Comparison of CYP102L1 and CYP102A1

Despite the low sequence identity to 102A1, the structure of the two proteins is remarkably conserved. As backbone or Cα RMSD values only provide averaged information of the pairwise distances of atoms in space and are not sensitive to similarities of local geometries, the TMscore developed by Zhang *et al.* provides a more useful metric for understanding similarities of the global fold in a length independent manner.[3-4] The TM-scoring scale is from 0 to 1, where a score of < 0.3 is random structural similarity and are essentially unrelated, >0.5 possess generally the same fold, and a score of 1 is a perfect match. In Table 5-1, each monomer of CYP102L1 was aligned using TM-align and compared one another and then to the substrate free structure of P450BM3 (1FAH).[5] As a negative control, all structures are compared to a substrate free crystal structure of P450cam (3L62)[6] demonstrating that a general P450 architecture still possesses significantly different TM scores than those of well-aligned structures. The alignment

Chain B in both CYP102L1 and 102A1 (1FAH), have the highest TM-score and lowest RMSD, 0.94361 and 1.53 Å respectively.

Table 5-1. TM-scores of Cyp102L1 monomers aligned to each monomer within the asymmetric unit. 1FAH - Substrate free Cyp102A1 monomers. 3L62 - Substrate free open structure of P450cam. The number of residues used for the alignment and RMSD (Å) are shown in parenthesis.

	CYP102L1-A	**CYP102L1-B**	**CYP102L1-C**	**CYP102L1-D**	**102A1-A (1FAH)**	**102A1-B (1FAH)**	**P450cam (3L62)**
CYP102L1-A	1.00000 (446:0.00)	0.94536 (432:1.36)	0.99195 (446:0.72)	0.99226 (434:0.73)	0.91571 (435:2.42)	0.91973 (435:2.31)	0.80318 (375:3.38)
CYP102L1-B		1.00000 (448:0.00)	0.94936 (432:1.38)	0.95363 (423:1.41)	0.93979 (437:1.62)	0.94361 (437:1.53)	0.81736 (379:3.25)
CYP102L1-C			1.00000 (446:0.00)	0.99315 (434:0.64)	0.91488 (434:2.39)	0.91963 (434:2.23)	0.80397 (375:3.35)
CYP102L1-D				1.00000 (434:0.00)	0.92407 (426:2.35)	0.92841 (426:2.22)	0.79078 (370:3.41)
102A1-A (1FAH)					1.00000 (455:0.00)	0.99079 (455:0.76)	0.82567 (383:3.29)
102A1-B (1FAH)						1.00000 (455:0.00)	0.82930 (382:3.18)
P450cam (3L62)							1.00000 (400:0.00)

Some noteworthy aspects of this structure are the differences of monomer chains A, C, D that possess TM-scores around 0.99 and RMSDs of less than 1 Å, while chain B is the most dissimilar from these with a TM-score around .95 and RMSDs around 1.4 Å against the other monomers. However, chain B is the most structurally similar to CYP102A1. Specifically, a portion of the first 24 residues that are not resolvable at the N-termini of chains A, C, D is visible in chain B, which is missing only 9 residues from the N-terminus. The 15 visible residues begin to accommodate some of the beta sheet domain seen at the N-term of CYP102A1. Additionally, the B chain monomer has a more closed G helix than chains A, C, D by ~3 Å. This is most likely attributable to crystal packing, as monomer contacts occur at the F/G loops in these three chains.

It is these crystal-packing interactions that may provide stability to the F/G loops in chains A, C, D, hence why their loops are more resolvable than that in chain B.

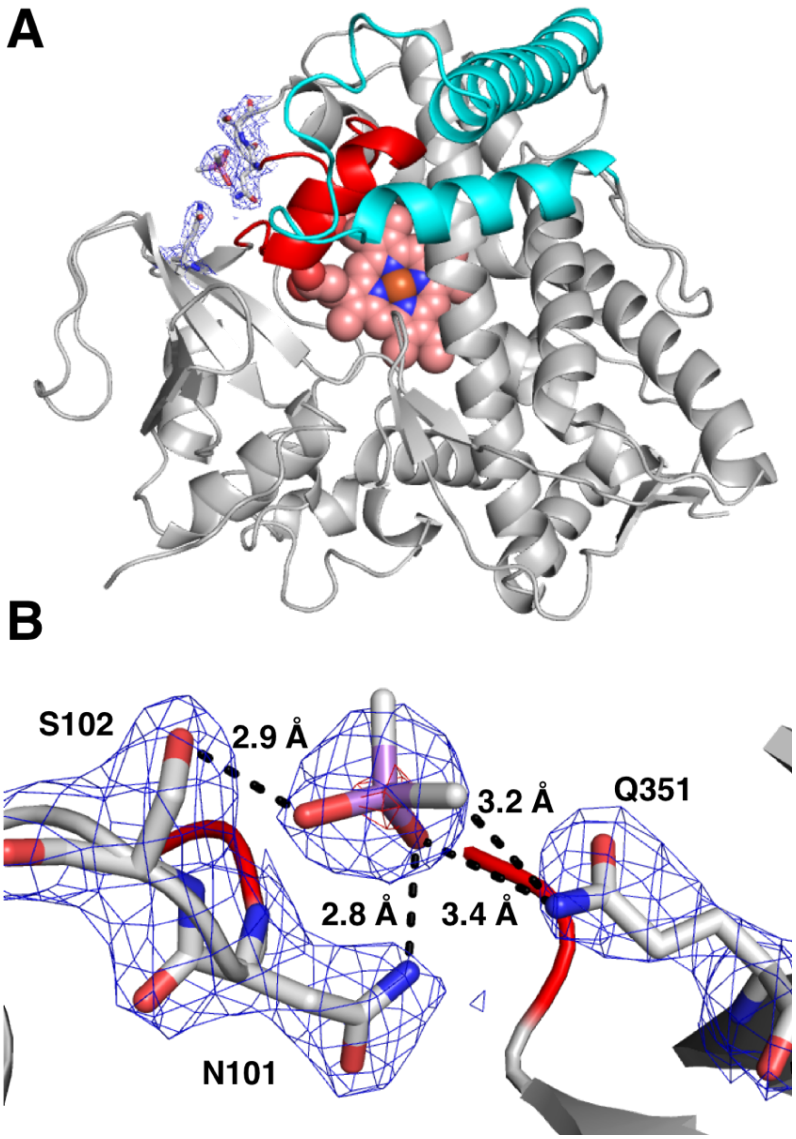

Figure 5-3. (A) Overview of CYP102L1 with F/G helices in cyan and B/C loop in red. **(B)** Cacodylate (purple) binding site with residues within hydrogen bonding distance. $2F_o$-F_c displayed in mesh at 1.5 σ (blue) and 7 σ (red).

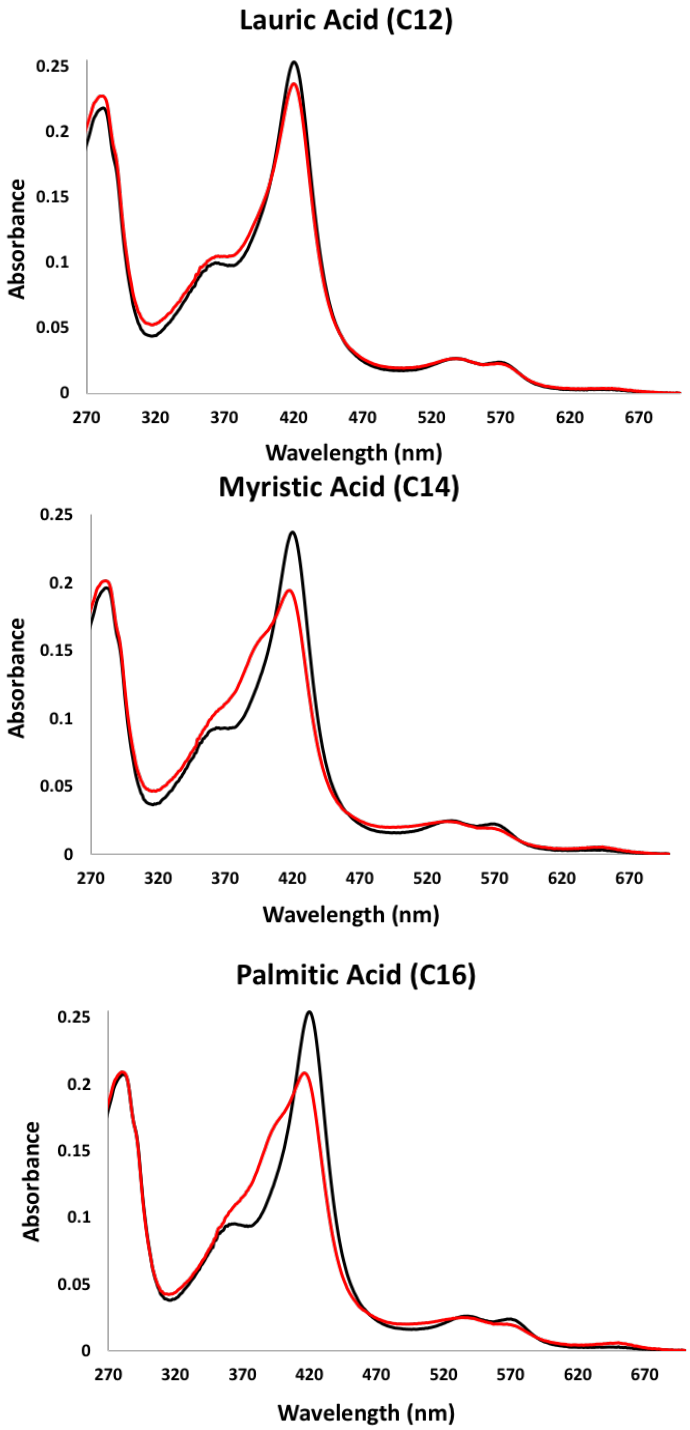

Figure 5-4. Spectral shift analysis of Mycobacteria phage Adler CYP102L1 (2 µM) with the fatty acids lauric acid (200 µM), myristic acid (50 µM), palmitic acid (50 µM). Absolute spectra are shown, with differential absorbance in the inset.

While sequence identity to 102A1 is quite low, retention of a number of resides that have been implicated in substrate binding affinity, turnover, and electron transfer are conserved. With 102L1 residues in parenthesis, mutation of residues A82(92)[7], I401(420)[8-9] in CYP102A1 affect substrate binding and turnover, while F87 (97)[10], T268 (282)[5, 11], A328 (245)[12], A330 (347)[13] affect substrate selectivity. F261 (275)[8], A264 (278)[14-15], T268 (282)[5, 11], and F393(412)[11, 16] affect electron transfer through either tuning the redox potential and/or changing the ET rate. CYP102A1 residues that are not conserved are R47 (F57)[17], L86 (M96)[8], and L188 (T199)[10] and, upon mutation of CYP102A1, affect substrate binding, redox potential and electron transfer, and substrate selectivity, respectively.

Another site of interest is a cacodylate binding site in the B/C loop. Orientation of the cacodylate molecule is not possible at this resolution, but residues in the region provide a number of possible hydrogen bonding contacts such as N101, S102, and Q351. Attribution of this density to cacodylate comes from the strong anomalous signal of arsenic that extends to ~7 σ (Fig 5-3).

Fatty Acid Binding

Type I spectral shift changes were observed following the addition of the fatty acids lauric acid (C12), myristic acid (C14), or palmitic acid (C16) to recombinant CYP102L1, suggesting these fatty acids are substrates (Fig 5-4). Metabolism experiments using the exogenous CYP102A1 reductase domain, eukaryotic POR and bacterial redox systems as electron donor proteins for CYP102L1 have yielded inconsistent results with palmitic acid as a potential substrate. An as yet undiscovered, CYP102L1 redox system may actually be necessary for phage CYP102L1 function.

Conversely, phage CYP102L1 may be the first CYP102 described to-date that does not function in fatty acid metabolism. Additional experiments are required to unravel this conundrum.

Conclusion

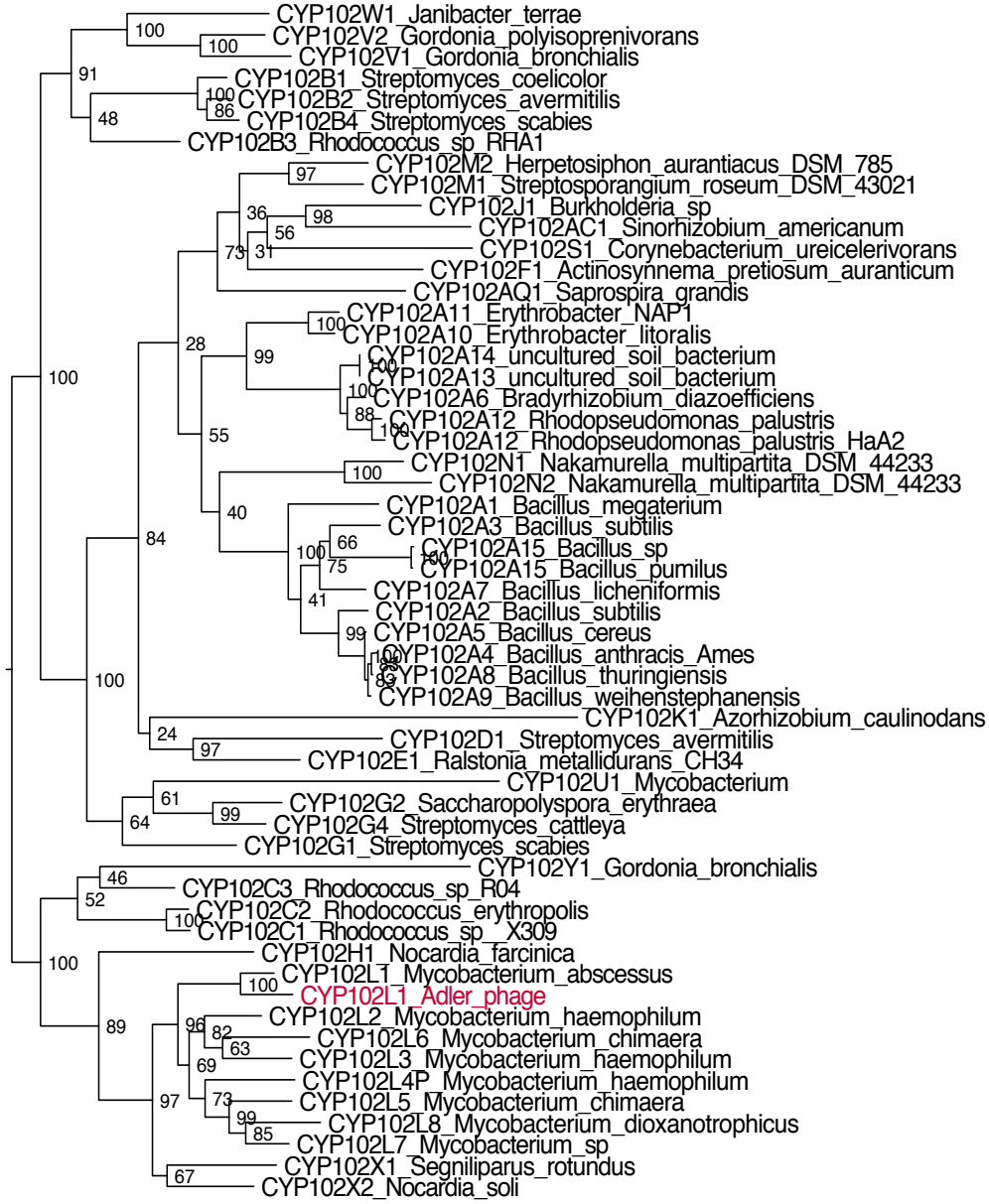

Figure 5-5. Known CYP102 sequences in most cases are predicted from the nucleotide sequences. Mycobacterium phage Adler shown in red.

Searching all available viral genomes, we discovered a surprising number, diversity and distribution of P450 genes, significantly in numerous giant viruses, including genes encoding unique P450 proteins. We also uncovered P450 genes in a phage and a herpes virus. In animals, other eukaryotes, and bacteria P450 enzymes have extremely broad metabolic roles in altering endogenous and exogenous chemicals in synthetic and degradation pathways not thought to be relevant in viruses.

The similarity of the P450 in mycobacteriophage Adler and a P450 in the *Mycobacteroides* host indicates that the phage almost certainly acquired this gene from the host. However, the situation is quite different in the giant viruses. P450s in giant viruses of amoebae are remarkably unlike any of the P450s in a common *Acanthamoeba* host. The P450 gene found in this mycobacteriophage defined a new subfamily and gene, CYP102L1. To date, only one CYP102 protein has been examined structurally: CYP102A1 (aka P450 BM3). The crystal structure of phage CYP102L1 adds a second new CYP102 structure to this gene family. The CYP102L1 structure closely resembles that of CYP102A1 (P450 BM3), suggesting that other CYP102s might have retained similar structural architecture. The high degree of protein sequence identity suggests the phage CYP102L1 was directly derived from the host. This apparent shuttling of a P450 gene on a small dsDNA virus resembles the occurrence of many P450 genes found encoded in natural plasmids, for example the occurrence of CYP101A1 (P450cam) on a plasmid that affords the bacterium Pseudomonas putida the ability to utilize camphor as a sole carbon source.

The presence of P450s in viruses leaves us with an important question. Where do the electrons come from? CYP102A1 possesses covalent redox partners with its FMN and FAD

cofactor-containing proteins attached, but CYP102l1 only seems to possess a heme domain and bioinformatic searches have been unsuccessful in identifying potential endogenous redox partners in viral genomes.

Materials and Methods

Mycobacteria phage Adler CYP102L1 protein expression and purification

Protein was expressed from *pET28a* plasmid (Genscript) with a thrombin cleavable N-terminal 6x-His-tag. The plasmid was transformed into C41 cells and expressed in 7 L of TB media shaken at 37 ˚C at 225 rpm overnight. The cells were inoculated with 1 mM IPTG and supplemented with 1 mM δ-ALA. The temperature was decreased to 27 ˚C and the shaking speed to 130 rpm. The cells were harvested 24 hours later and re-suspended in 50 mM potassium

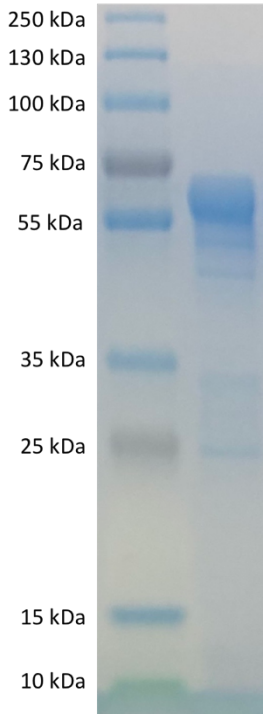

Figure 5-6. SDS-PAGE gel showing the isolation of Adler phage CYP102L1. Lane 1, molecular-mass markers; lane 2, CYP eluate obtained.

phosphate pH 7.5, 500 mM NaCl, 10% (v/v) glycerol, 2 mM β-mercaptoethanol. Cells were lysed by sonication and cellular debris removed by centrifugation at 15,000 rpm at 4 ˚C for 60 min.

The supernatant was loaded onto a 25 mL Ni^{2+}-NTA agarose column and washed with 500 mL lysis buffer containing 7 mM L-Histidine overnight. Cyp102L1 was eluted from the column over a gradient of 7- 100 mM L-His. The protein was buffer exchanged into 50 mM potassium phosphate pH 6, 20 mM NaCl, 10% (v/v) glycerol, 2 mM β-mercaptoethanol and loaded onto a 100 mL CM-Sepharose column. The column was washed with a gradient of 500 mL 50 mM potassium phosphate pH 6, 20-250 mM NaCl, 10% (v/v) glycerol, 2 mM β-mercaptoethanol and eluted with CM buffer containing 250 to 350 mM NaCl. The protein was concentrated and buffer exchanged by a 25 mL Sephacryl-S200 size exclusion column into 50 mM potassium phosphate pH 8, 2 mM DTT. Purity of the protein was assessed by SDS-PAGE (Fig. 5-6) and UV-vis spectroscopy. R/Z >1.6 was used for crystallization.

By SDS-PAGE and MALDI-TOF mass spectrometry, it was observed that thrombin cleavage exhibited two major products. We attributed this to a thrombin like cleavage site near the N-term of CYP102L1's sequence. We performed site directed mutagenesis to make the R17K mutant. Primers for this mutation were: **F:**5'-TGCCGCACCCGAATCGTCTGCCGGTT-3' and the **R:** 5'-AACCGGCAGACGATTCGGGTGCGGCA-3'. This substantially decreased the amount of the secondary product.

Table 5-2. X-ray crystallography data collection and refinement statistics for CYP102L1 structure. Values in parentheses are for the highest resolution shell.

CYP102L1	PDB: 6N6Q
Wavelength	1.734
Resolution range	66.56 - 2.5 (2.589 - 2.5)
Space group	I 2 2 2
Unit cell	119.899 174.09 203.469 90 90 90
Total reflections	142946 (14259)
Unique reflections	73160 (7248)
Multiplicity	2.0 (2.0)
Completeness (%)	99.16 (99.49)
Mean I/sigma(I)	7.55 (0.83)
Wilson B-factor	62.03
CC1/2	0.994 (0.396)
CC*	0.998 (0.753)
Reflections used in refinement	73117 (7241)
Reflections used for R-free	3764 (365)
R-work	0.2302 (0.3551)
R-free	0.2887 (0.3921)
CC(work)	0.938 (0.629)
CC(free)	0.923 (0.579)
Number of non-hydrogen atoms	14644
macromolecules	14326
ligands	197
solvent	121
Protein residues	1777
RMS(bonds)	0.002
RMS(angles)	0.51
Ramachandran favored (%)	95.80
Ramachandran allowed (%)	3.91
Ramachandran outliers (%)	0.28
Rotamer outliers (%)	1.13
Clashscore	5.95
Average B-factor	69.10
macromolecules	69.41
ligands	55.40
solvent	54.40

CYP102L1 crystallization

Crystallization was performed using hanging drop diffusion. After initial screening and optimization, crystal hits were found in a condition containing 0.1 M Sodium cacodylate pH 6.5 and 1.26 M $(NH_4)_2SO_4$. Diffraction quality crystals were obtained using an additive screen that yielded the final condition of 0.1 M Sodium Cacodylate pH 6.5, 1.26 M $(NH_4)_2SO_4$ and 4.2 % (w/v) Dextran Sulfate. Hanging drops were set up at with a 1:1 ratio of protein to precipitant with a protein concentration of 12 mg/mL.

Data Collection and Structure Determination

The structure of CYP102L1 was solved to a resolution of 2.5 Å by single wavelength anomalous diffraction at the iron K-edge (7150 eV). Images were processed, integrated, and scaled with the iMosflm package.[18] Crystals belonged to the space group I 2 2 2, with 4 molecules of CYP102L1 in the asymmetric unit, where the dimensions of the unit cell were determined to be a=119.899 Å b= 174.09 Å c= 203.469 Å α=β=γ= 90˚. A hybrid substructure search (HySS) within the phenix suite of programs found 2 potential iron sites (of the 4 expected in the asymmetric unit). Phenix.autosol was utilized to find the remaining sites and phenix.autobuild built a partial model.[19] The rest of the structural model was built manually in Coot and refined iteratively with phenix.refine.[19-21] The final structure was refined to possess an Rfree = 28.8% and Rwork of 23.0%. Crystallographic data is reported below (Table 5-2).

CYP102L1 fatty acid spectral shifts

Preparation and titrations of fatty acids were carried out as previously described.[22] Stocks were 100 mM lauric acid in 50 mM K_2CO_3, and 10 mM myristic and palmitic acids in DMSO.

Experiments were performed in 1000 µL total volume at 30˚C and measurements made on an Agilent Cary 300 UV-vis spectrophotometer.

References

1. Poulos, T. L., Heme enzyme structure and function. *Chem Rev* **2014,** *114* (7), 3919-62.
2. Lamb, D. C.; Lei, L.; Warrilow, A. G.; Lepesheva, G. I.; Mullins, J. G.; Waterman, M. R.; Kelly, S. L., The first virally encoded cytochrome p450. *J Virol* **2009,** *83* (16), 8266-9.
3. Zhang, Y.; Skolnick, J., Scoring function for automated assessment of protein structure template quality. *Proteins* **2004,** *57* (4), 702-10.
4. Zhang, Y.; Skolnick, J., TM-align: a protein structure alignment algorithm based on the TM-score. *Nucleic Acids Res* **2005,** *33* (7), 2302-9.
5. Yeom, H.; Sligar, S. G.; Li, H.; Poulos, T. L.; Fulco, A. J., The role of Thr268 in oxygen activation of cytochrome P450BM-3. *Biochemistry* **1995,** *34* (45), 14733-40.
6. Lee, Y. T.; Wilson, R. F.; Rupniewski, I.; Goodin, D. B., P450cam visits an open conformation in the absence of substrate. *Biochemistry* **2010,** *49*, 3412.
7. Huang, W. C.; Westlake, A. C.; Marechal, J. D.; Joyce, M. G.; Moody, P. C.; Roberts, G. C., Filling a hole in cytochrome P450 BM3 improves substrate binding and catalytic efficiency. *J Mol Biol* **2007,** *373* (3), 633-51.
8. Girvan, H. M.; Levy, C. W.; Williams, P.; Fisher, K.; Cheesman, M. R.; Rigby, S. E.; Leys, D.; Munro, A. W., Glutamate-haem ester bond formation is disfavoured in flavocytochrome P450 BM3: characterization of glutamate substitution mutants at the haem site of P450 BM3. *Biochem J* **2010,** *427* (3), 455-66.
9. Whitehouse, C. J.; Bell, S. G.; Yang, W.; Yorke, J. A.; Blanford, C. F.; Strong, A. J.; Morse, E. J.; Bartlam, M.; Rao, Z.; Wong, L. L., A highly active single-mutation variant of P450BM3 (CYP102A1). *Chembiochem* **2009,** *10* (10), 1654-6.
10. Budde, M.; Morr, M.; Schmid, R. D.; Urlacher, V. B., Selective hydroxylation of highly branched fatty acids and their derivatives by CYP102A1 from Bacillus megaterium. *Chembiochem* **2006,** *7* (5), 789-94.
11. Clark, J. P.; Miles, C. S.; Mowat, C. G.; Walkinshaw, M. D.; Reid, G. A.; Daff, S. N.; Chapman, S. K., The role of Thr268 and Phe393 in cytochrome P450 BM3. *J Inorg Biochem* **2006,** *100* (5-6), 1075-90.
12. Haines, D. C.; Hegde, A.; Chen, B.; Zhao, W.; Bondlela, M.; Humphreys, J. M.; Mullin, D. A.; Tomchick, D. R.; Machius, M.; Peterson, J. A., A single active-site mutation of P450BM-3 dramatically enhances substrate binding and rate of product formation. *Biochemistry* **2011,** *50* (39), 8333-41.
13. Whitehouse, C. J.; Yang, W.; Yorke, J. A.; Rowlatt, B. C.; Strong, A. J.; Blanford, C. F.; Bell, S. G.; Bartlam, M.; Wong, L. L.; Rao, Z., Structural basis for the properties of two single-site proline mutants of CYP102A1 (P450BM3). *Chembiochem* **2010,** *11* (18), 2549-56.

14. Girvan, H. M.; Toogood, H. S.; Littleford, R. E.; Seward, H. E.; Smith, W. E.; Ekanem, I. S.; Leys, D.; Cheesman, M. R.; Munro, A. W., Novel haem co-ordination variants of flavocytochrome P450BM3. *Biochem J* **2009,** *417* (1), 65-76.
15. Girvan, H. M.; Seward, H. E.; Toogood, H. S.; Cheesman, M. R.; Leys, D.; Munro, A. W., Structural and spectroscopic characterization of P450 BM3 mutants with unprecedented P450 heme iron ligand sets. New heme ligation states influence conformational equilibria in P450 BM3. *J Biol Chem* **2007,** *282* (1), 564-72.
16. Ost, T. W.; Munro, A. W.; Mowat, C. G.; Taylor, P. R.; Pesseguiero, A.; Fulco, A. J.; Cho, A. K.; Cheesman, M. A.; Walkinshaw, M. D.; Chapman, S. K., Structural and spectroscopic analysis of the F393H mutant of flavocytochrome P450 BM3. *Biochemistry* **2001,** *40* (45), 13430-8.
17. Hegde, A.; Haines, D. C.; Bondlela, M.; Chen, B.; Schaffer, N.; Tomchick, D. R.; Machius, M.; Nguyen, H.; Chowdhary, P. K.; Stewart, L.; Lopez, C.; Peterson, J. A., Interactions of substrates at the surface of P450s can greatly enhance substrate potency. *Biochemistry* **2007,** *46* (49), 14010-7.
18. Battye, T. G.; Kontogiannis, L.; Johnson, O.; Powell, H. R.; Leslie, A. G., iMOSFLM: a new graphical interface for diffraction-image processing with MOSFLM. *Acta Crystallogr., Sect. D: Biol. Crystallogr.* **2011,** *67* (4), 271.
19. Adams, P. D.; Afonine, P. V.; Bunkoczi, G.; Chen, V. B.; Davis, I. W.; Echols, N.; Headd, J. J.; Hung, L. W.; Kapral, G. J.; Grosse-Kunstleve, R. W.; McCoy, A. J.; Moriarty, N. W.; Oeffner, R.; Read, R. J.; Richardson, D. C.; Richardson, J. S.; Terwilliger, T. C.; Zwart, P. H., PHENIX: a comprehensive Python-based system for macromolecular structure solution. *Acta Crystallogr., Sect. D: Biol. Crystallogr.* **2010,** *66* (2), 213.
20. Emsley, P.; Cowtan, K., Coot: model-building tools for molecular graphics. *Acta Crystallogr., Sect. D: Biol. Crystallogr.* **2004,** *60* (12), 2126.
21. Emsley, P.; Lohkamp, B.; Scott, W. G.; Cowtan, K., Features and development of Coot. *Acta Crystallogr., Sect. D: Biol. Crystallogr.* **2010,** *66* (4), 486.
22. Rowlatt, B.; Yorke, J. A.; Strong, A. J.; Whitehouse, C. J.; Bell, S. G.; Wong, L. L., Chain length-dependent cooperativity in fatty acid binding and oxidation by cytochrome P450BM3 (CYP102A1). *Protein Cell* **2011,** *2* (8), 656-71.

Chapter 6

Conclusion

Together these works highlight the complexity and importance of dynamics in the cytochrome P450 mechanism. As discussed in chapter one, the changes that occur in Nature's aircraft carrier are to regulate and control a powerful reaction, and here we have taken a further step in progressing our understanding of the structure-function relationship that governs P450 chemistry.

In chapter 2, we utilized molecular dynamics simulations to understand the mechanism of substrate binding in cytochrome P450cam. The results of these unbiased simulations revealed a number of surprising transitions that resulted in the prediction of a second molecule of camphor acting as an allosteric activator and the formation of a second active site access channel. The activation of P450cam by a second molecule of substrate through a distant binding pocket is consistent with a number of crystallographic and spectroscopic studies that extend back to the enzyme's discovery. Additionally, it was the activation by the allosteric site that led to the formation of a new channel between the B/C loop. This channel has been suggested by biased molecular dynamics approaches but never observed experimentally or captured in a bias-free simulation and/or associated with allosteric interactions. The opening of this new channel presented the active site camphor with a channel for egress and is associated with a number of coupled mechanistic transitions that allow for the product to escape. While the allosteric site activation and egress channel were new findings, the limits of classical molecular dynamics left a number of lingering questions since after substrate binds to the active site, several critical

interactions take place before product egresses. These dynamic interactions include putidaredoxin (Pdx) binding, electron transfer, O_2 binding, and hydroxylation and are the focus of future simulation work.

The predictions of chapter 2 were tackled experimentally in chapter 3. The simulations predicted a number of changes that would presumably occur upon putidaredoxin (Pdx) binding, electron transfer, and/or O_2 binding, and crystallization of the oxy-P450cam-Pdx complex would test the simulated model's validity. However, due to the photoreduction of the complex by the X-ray beam and radiation-induced substrate turnover, cyanide was utilized as an O_2 mimic. The crystal structure of the CN-P450cam-Pdx structure validated many of the subtle structural changes predicted by our molecular dynamics simulations, and most importantly, the formation of channel 2. One of the most surprising aspects of this structure was the *cis-trans* isomerization of Pro89 and Pro105, which presumably occurred within the crystal upon CN soaking. These changes allowed the closing of channel 1 and opening of channel 2 supporting the unidirectionality of substrate flow predicted in our MD study. Additionally, this structure corroborated an earlier NMR study that suggested that isomerization of proline residues was essential to the mechanism of P450cam and this is observed here for the first time crystallographically.

While P450cam has served as the model system for structure-function studies of P450s, it is one of the most specific P450s for its redox partner, Pdx. The extension of the specificity and conformational regulation of P450cam to other systems is still being investigated. In chapter 4, we examined P450terp (CYP108A1), a homologue of P450cam, in regard to its interactions with

its redox partner, terpredoxin (Tdx). The crystal structure of Tdx was determined and potential P450terp-Tdx complex was compared to P450cam-Pdx. Tdx was also shown to exhibit a similar destabilization of the oxy-complex as seen in P450cam. P450terp demonstrated a less strict requirement for its native redox partner as it was capable of utilizing Arx as an electron donor.

In chapter 5, we stepped outside of Class I systems to look into the structure and potential role of P450s in viruses. Recently, bioinformatics has revealed a number of P450s in giant and non-giant viruses. A new class of CYP102 was discovered to exist in both a virus and its bacterial host. CYP102L1 from *Mycobacterium phage Adler* was crystallized and shown to bind fatty acids. CYP102L1 showed a remarkable structural similarity to CYP102A1 despite a low sequence identity. However, substrate turnover assays with fatty acids failed to yield conclusive NAD(P)H consumption with a number of redox partners including BM3 reductase, the native electron transfer partner of 102A1. Further investigations are required to understand the role of viral P450s and find their natural redox partners.

Future Directions and a possible P450 supercomplex

In closing, I would like to suggest an idea and a direction for future work that the P450cam system forms a four- component supercomplex: PdR-Pdx-Pdx-P450cam (Fig 6-1). The idea of a supercomplex would be an adjustment from the traditional shuttling mechanism in Fig 1-7 and Fig 1-8. Support for this prediction of a supercomplex, like the motivation for chapters 2 and 3, stems from a reexamination of a number of experimental results.

First, let's look at how NADH consumption assays are performed. They are always performed with an excess of ferredoxin, are substrate dependent, and P450cam is nearly 100%

coupled.[1-2] As NADH, PdR, and excess Pdx are all present prior to substrate introduction and reduced Pdx rapidly autoxidizes, the system should not be as tightly coupled. This implies some sort of communication between the reductase and the P450. PdR should be able to transfer electrons to the excess Pdx and prime them for ET to P450cam.

Second, a number of studies examining the electron transfer between PdR-Pdx find the semiquinone intermediate formed after a one electron transfers to Pdx is either highly unstable or undetectable.[3-6] However, this is difficult to reconcile under the standard shuttling model as Fe_2S_2-ferredoxins are only capable of undergoing one electron redox chemistry. *In vitro* measurements of steady state and kinetic properties have traditionally used terminal one-electron acceptors such as cytochrome *c* or ferricyanide limiting the interpretability of the second

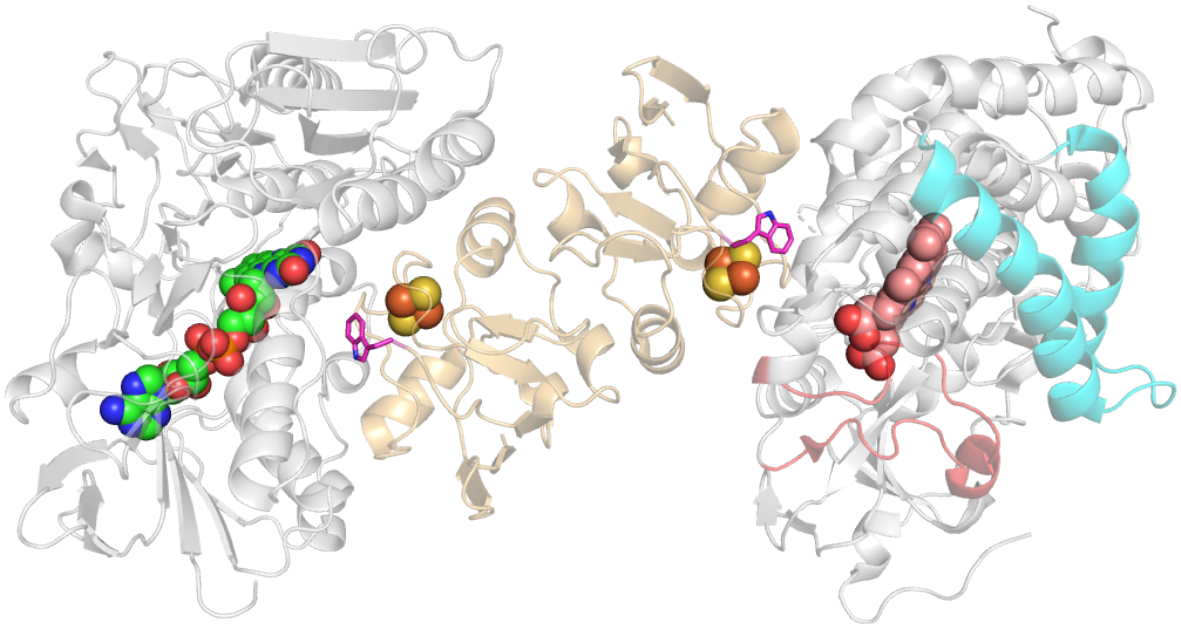

Figure 6-1. Potential supercomplex of PdR-Pdx-Pdx-P450cam. Model was generated by aligning Pdx of PdR-Pdx (3LB8) to a monomer of a dimer within the asymmetric unit of Pdx (1XLQ) and the P450-Pdx complex (4JWU) to the other monomer. FAD – green. W106 – magenta. Pdx – orange. Heme – pink. F/G helices – cyan. B/C loop – red.

ET event as PdR needs to provide both electrons to the P450 and the semiquinone intermediate is especially unstable. Related to this is the effect of nucleotide binding on the ET rate of PdR to Pdx as binding of NAD^+ strongly influences the PdR's redox potential and thus increases the rate by orders of magnitude.[5-6] It is known that Apoptosis Reducing Factor, a bifunctional mitochondrial flavoprotein that plays an important role in energy metabolism undergoes an NADH induced dimerization.[7] It is possible that NADH binding to PdR induces a similar complex formation that is then capable of substrate dependent ET.

The third piece of evidence is the oligomerization of Pdx. As discussed in chapter 4, one obstacle to the crystallization of Pdx was the non-ligating cysteines forming intermolecular disulfide bonds.[8] The activity of these mutants was measured and a marked decrease turnover rate is observed. It is possible that these oligomers form *in vivo* and facilitate the complex formation and these non-ligating cysteines may be involved in electron transfer.

Fourth is the interfaces of Pdx–PdR and Pdx–P450cam. In these two complexes, Pdx presents the same interface to Pdr and P450cam, which supports the shuttling mechanism of the ferredoxin.[9-10] However, if we look at these results all together, one can imagine that if Pdx dimerizes, then Pdx can present the same interface to both PdR and P450cam. Additionally, if a complex forms, then PdR can transfer two electrons derived from the hydride to the two ferredoxins and with communication from the P450 so it can perform in a substrate dependent manner.

Supporting this is idea of a four component or oligomeric complex is the fifth and final piece of evidence. One of the initial studies by Lipscomb[11] found the formation of half of an

equivalent of product after incubation of the oxy complex with oxidized Pdx. Normally, the oxycomplex would require one more electron to drive turnover and oxidized Pdx should not drive this chemistry. These results are from the same oxycomplex decay experiment described in chapter 4, but the formation of product result was unexplainable. However, these stopped-flow experiments were done with wt-Pdx, which oligomerizes and then is mixed with oxy-P450cam. Pdx presents the same interface to PdR and P450cam. If Pdx forms a dimer and naturally forms the complex, then P450cam-Pdx-Pdx-P450cam complex is possible, which allows for back electron transfer from one oxy-P450, directly to the other, releasing O_2 in one P450 unit and forming product in the other. Turnover and release of O_2 returns both molecules of P450cam back to ferric high-spin in the presence of excess substrate, one through uncoupling and one through productive turnover.

Formation of a supercomplex would prevent the need for dissociation and supports rapid turnover. Looking to nature, we can find many similar examples of this type of co-factor alignment (especially when O_2 is involved) in systems like nitrate reductase or the respiratory complexes. (Fig 6-2).[12-14]

Whatever the case may be, cytochromes P450 are one of the most complex and fasinating aspects of nature with much left to discover. The efforts to understand cytochrome P450 are highly interdisciplinary in the truest sense and the field is filled with a rich past and a bright future.

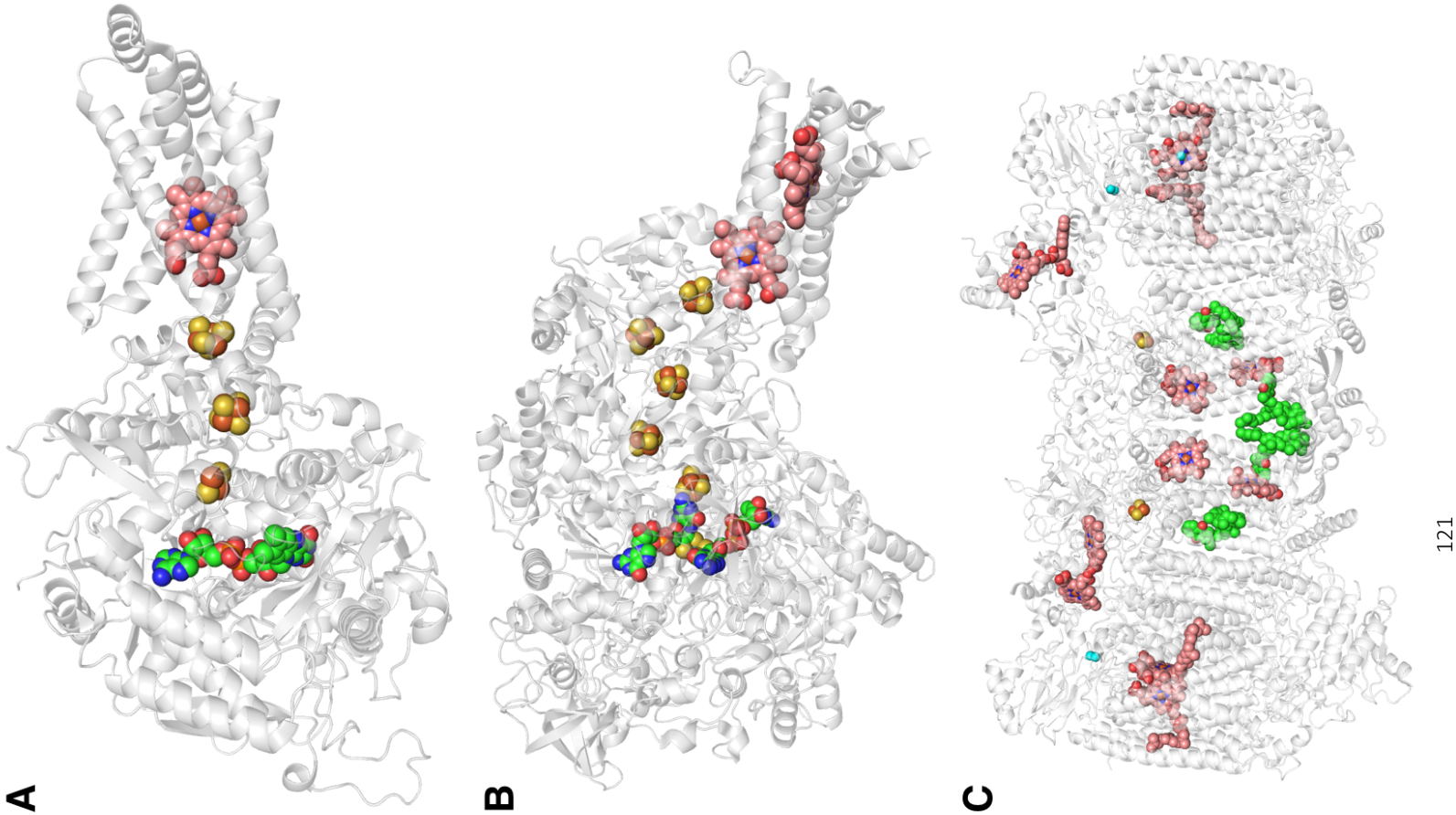

Figure 6-2. (A) Avian Mitochondrial Respiratory Complex II (2H88) with FAD (green), Fe-S clusters (orange, yellow), heme (pink). **(B)** Nitrate Reductase A, NarGHI, from Escherichia coli (1Q16) with molybdo-bis(molybdopterin guanine dinucleotide) (Mo-bisMGD) (green), Fe-S clusters, and heme. **(C)** Obligate respiratory supercomplex from Mycobacterium smegmatis (6HWH) with menaquinone-9 (green), copper (cyan), Fe-S clusters and heme.

References

1. Yang, W.; Bell, S. G.; Wang, H.; Zhou, W.; Hoskins, N.; Dale, A.; Bartlam, M.; Wong, L. L.; Rao, Z., Molecular characterization of a class I P450 electron transfer system from Novosphingobium aromaticivorans DSM12444. *J Biol Chem* **2010,** *285* (35), 27372-84.
2. Ortiz de Montellano, P. R., *Cytochrome P450: Structure, Mechanism, and Biochemistry*. 2015.
3. Reipa, V.; Holden, M. J.; Vilker, V. L., Association and redox properties of the putidaredoxin reductase-nicotinamide adenine dinucleotide complex. *Biochemistry* **2007,** *46* (45), 13235-44.
4. Sevrioukova, I. F.; Poulos, T. L., Putidaredoxin reductase, a new function for an old protein. *J Biol Chem* **2002,** *277* (28), 25831-9.
5. Roome, P. W.; Peterson, J. A., The reduction of putidaredoxin reductase by reduced pyridine nucleotides. *Arch Biochem Biophys* **1988,** *266* (1), 32-40.
6. Roome, P. W.; Peterson, J. A., The oxidation of reduced putidaredoxin reductase by oxidized putidaredoxin. *Arch Biochem Biophys* **1988,** *266* (1), 41-50.
7. Sevrioukova, I. F., Redox-linked conformational dynamics in apoptosis-inducing factor. *J Mol Biol* **2009,** *390* (5), 924-38.
8. Sevrioukova, I. F.; Garcia, C.; Li, H.; Bhaskar, B.; Poulos, T. L., Crystal structure of putidaredoxin, the [2Fe-2S] component of the P450cam monooxygenase system from Pseudomonas putida. *J Mol Biol* **2003,** *333* (2), 377-92.
9. Sevrioukova, I. F.; Poulos, T. L.; Churbanova, I. Y., Crystal structure of the putidaredoxin reductase x putidaredoxin electron transfer complex. *J Biol Chem* **2010,** *285* (18), 13616-20.
10. Tripathi, S.; Li, H.; Poulos, T. L., Structural basis for effector control and redox partner recognition in cytochrome P450. *Science* **2013,** *340* (6137), 1227.
11. Lipscomb, J. D.; Sligar, S. G.; Namtvedt, M. J.; Gunsalus, I. C., Autooxidation and hydroxylation reactions of oxygenated cytochrome P-450cam. *J Biol Chem* **1976,** *251* (4), 1116-24.
12. Wiseman, B.; Nitharwal, R. G.; Fedotovskaya, O.; Schafer, J.; Guo, H.; Kuang, Q.; Benlekbir, S.; Sjostrand, D.; Adelroth, P.; Rubinstein, J. L.; Brzezinski, P.; Hogbom, M., Structure of a functional obligate complex III2IV2 respiratory supercomplex from Mycobacterium smegmatis. *Nat Struct Mol Biol* **2018,** *25* (12), 1128-1136.
13. Huang, L. S.; Shen, J. T.; Wang, A. C.; Berry, E. A., Crystallographic studies of the binding of ligands to the dicarboxylate site of Complex II, and the identity of the ligand in the "oxaloacetate-inhibited" state. *Biochim Biophys Acta* **2006,** *1757* (9-10), 1073-83.
14. Bertero, M. G.; Rothery, R. A.; Palak, M.; Hou, C.; Lim, D.; Blasco, F.; Weiner, J. H.; Strynadka, N. C., Insights into the respiratory electron transfer pathway from the structure of nitrate reductase A. *Nat Struct Biol* **2003,** *10* (9), 681-7.

Appendix A

Comparison of *in vitro* rates to *in vivo* requirements for P450cam

The use of glucose vs camphor as a carbon source to produce acetyl-CoA are quite different net reactions. Utilizing a molecule of glucose, 2 molecules acetyl-CoA are produced and during their production is the net gain of 2 NADH and 2 ATP. While in the case of camphor, a net loss of a molecule of NADH and NADPH to produce only one molecule of acetyl-CoA and isobutyryl-CoA.[1]

The question I posed to myself was, how much camphor would it take to power a cell for an hour? And can the *in vitro* rates we measure sustain this level of consumption?

I need to first clarify that most of the numbers utilized below come from *E.coli* as it is the most well-documented systems for bacterial growth and metabolic function. First, what is the power consumption of a bacterial cell? This is a challenging question and the definition of this is dependent on how you measure power. The most useful definition for our purposes a measurable quantity is the O_2 consumption by the cell. With glucose, the oxygen uptake rate of E.coli was 30 mmol/g (CDW)/ hour where CDW is cell dry weight.[2] And per molecule of O_2, 3-5 molecules of ATP are produced or about 100mM ATP/g(CDW)/hour.[3-5] Assuming a single bacterial cell weighs about $1x10^{-12}$ g,[6] then this translates to ~10^9 ATP/s/cell or ~10^{10}-10^{11} ATP/hour/cell.

Ok, now we have an idea of power consumption by a bacterial cell. Can P450cam support this ATP requirement? One assumption here is that camphor hydroxylation is the rate determining step of ATP production. About 30 molecules of ATP can be produced from a

molecule of glucose.[7] However, we only get one molecule of acetyl-CoA per camphor,[1] which cuts ATP production in half to ~15 ATP per camphor. NADH consumption in a perfectly coupled P450cam system is 1:1 with product formation, so we can estimate that per NADH, 15 ATP are produced. The fastest reported rates for turnover rates by P450cam are ~2400 nmol/min/nmol of P450[8] or 36000 nmol ATP/min/nm P450. Or ~3.6 x 10^{17} ATP/hour/6x10^{14} molecules of P450.

Now the question is, how much protein is in a bacterial cell? It is estimated that there are between 3-4 x 10^6 proteins/μm^3 of bacterial cell.[9] So, we can ask, on average, what is the volume of a Pseudomonad? With a size of 1-5 µm long and 0.5 to 1 µm wide, a small cell would be on the order of 1 μm^3.[10]

If a cell contained 3.6 x 10^6 proteins in a 1 μm^3 cell and we assume that EVERY SINGLE PROTEIN in the cell was a P450, then 3.6 x 10^9 ATP are produced per hour. Within an order of magnitude, this could meet the requirement of ~10^{10}-10^{11} ATP/hour/cell. However, this assumes that EVERY SINGLE PROTEIN in the cell is a P450 and camphor hydroxylation is the rate determining step. P450cam alone requires 2 additional component proteins to function and this calculation doesn't include the downstream proteins that would be required to turn hydroxycamphor to acetyl-CoA and ATP.

While this estimate is entirely crude, it illustrated to me that there were worthwhile mechanistic issues worth revisiting in P450cam. Additionally, it began to chang the way I think about biology *in vitro* vs *in vivo* and keeping the biological context in mind when thinking about our chemistry (e.g. demands for survival about rates and function and efficiency).

References

1. Iwaki, H.; Grosse, S.; Bergeron, H.; Leisch, H.; Morley, K.; Hasegawa, Y.; Lau, P. C., Camphor pathway redux: functional recombinant expression of 2,5- and 3,6-diketocamphane monooxygenases of Pseudomonas putida ATCC 17453 with their cognate flavin reductase catalyzing Baeyer-Villiger reactions. *Appl Environ Microbiol* **2013,** *79* (10), 3282-93.
2. Jain, R.; Srivastava, R., Metabolic investigation of host/pathogen interaction using MS2-infected Escherichia coli. *BMC Syst Biol* **2009,** *3*, 121.
3. Ferrier, D. R., *Biochemistry*. Wolters Kluwer Health/Lippincott Williams & Wilkins: Philadelphia, 2014.
4. Rigoulet, M.; Ouhabi, R.; Leverve, X.; Putod-Paramelle, F.; Guerin, B., Almitrine, a new kind of energy-transduction inhibitor acting on mitochondrial ATP synthase. *Biochim Biophys Acta* **1989,** *975* (3), 325-9.
5. Taymaz-Nikerel, H.; Borujeni, A. E.; Verheijen, P. J.; Heijnen, J. J.; van Gulik, W. M., Genome-derived minimal metabolic models for Escherichia coli MG1655 with estimated in vivo respiratory ATP stoichiometry. *Biotechnol Bioeng* **2010,** *107* (2), 369-81.
6. Neidhardt, F. C.; Curtiss, R., *Escherichia coli and Salmonella : cellular and molecular biology*. ASM Press: Washington, D.C., 1996.
7. Berg, J. M.; Tymoczko, J. L.; Stryer, L.; Stryer, L.; National Center for Biotechnology, I., Biochemistry. **2002**.
8. Kadkhodayan, S.; Coulter, E. D.; Maryniak, D. M.; Bryson, T. A.; Dawson, J. H., Uncoupling oxygen transfer and electron transfer in the oxygenation of camphor analogues by cytochrome P450-CAM. Direct observation of an intermolecular isotope effect for substrate C-H activation. *J Biol Chem* **1995,** *270* (47), 28042-8.
9. Milo, R., What is the total number of protein molecules per cell volume? A call to rethink some published values. *Bioessays* **2013,** *35* (12), 1050-5.
10. Pseudomonas aeruginosa - microbewiki. https://microbewiki.kenyon.edu/index.php/Pseudomonas_aeruginosa.